THESIS FOR THE DEGREE OF MASTER OF PHILOSOPHY

Modelling and Control of Multi-Terminal HVDC Networks for Offshore Wind Power Generation

SHU ZHOU

Institute of Energy

Department of Engineering School

CARDIFF UNIVERSITY

Cardiff, Wales, UK, 2011

Abstract

Due to the recent developments in semiconductors and control equipment, Voltage Source Converter based High Voltage Direct Current (VSC-HVDC) becomes a promising technology for grid connection of large offshore wind farms. The VSC-HVDC provides a number of potential advantages over the conventional HVDC, such as rapid and independent control of reactive and active power, black-start capability and no restriction on multiple infeeds. Therefore, VSC-HVDC will likely to be widely used in the future transmission networks and for offshore wind power connections.

Multi-terminal VSC-HVDC (VSC-MTDC) system, which consists of more than two voltage source converter stations connecting together through a DC link, is able to increase the flexibility and reliability of transmission systems. It allows connection of multiple offshore wind farms to the AC grid.

In this thesis, a three-terminal MTDC system was investigated using simulations and experiments. MTDC system with its control was implemented in PSCAD/EMTDC. The control strategy developed through simulation was verified using experiments. The results of PSCAD/EMTDC simulation and laboratory demonstration were then compared. Additionally, a scenario of four-terminal MTDC transmission system for

offshore wind power generation was investigated. A control system was designed considering the operating characteristics of VSCs and wind farms. An open loop control method was used for the wind farm side VSCs to establish a constant AC voltage and frequency. Droop control was used for the grid side VSCs to generate DC voltage reference by measuring the DC current. When the system was under fault operation condition, the output power of wind farm was reduced by reducing the DC voltage reference. Simulation results show that good coordination was achieved among VSCs for voltage control and power sharing. The system is able to recover to the normal operation status automatically when subjected to AC balanced fault (three phase fault) and unbalanced fault (single phase fault) on the grid.

Keywords: control system, modelling, MTDC, Multi-terminal, offshore, VSC-HVDC, wind power generation

Acknowledgements

The research work is carried out at the Institute of Energy, Department of Engineering School at Cardiff University. The project was sponsored by the UK-EPSRC SUPERGEN-FLEXNET. This is gratefully acknowledged.

First I would like to thank my supervisors Dr. Jun Liang and Dr. Janaka B Ekanayake for their help, guidance, patience and encouragement, without which this thesis would not be possible to finish. I would also like to thank Prof. Nick Jenkins for many enlightening discussions at the key stage of my M.Phil. study.

Many thanks to Prof. Tim Green from Imperial College and Dr. Stephen J Finney from University of Strathclyde. With the Work-stream of Power System Electronics, I really enjoy the interesting discussions at every Work-streams meeting and acquire many useful information.

Last but not the least, I want to thank my girl friend Yanting for her love, understanding and support all the time. I need to say thanks to my parents, my family and my friends for their encouragement. I should thank all the persons who love me and give me supports all the time.

Nomenclature and Abbreviation

AC : Alternating Current

CB : Circuit Breaker

CO_2 : Carbon Dioxide

CSC : Current Source Converter

DC : Direct Current

Fig. : Figure

GSVSC : Grid Side VSC

GTO : Gate Turn-Off Thyristor

HVAC : High Voltage Alternating Current

HVDC : High Voltage Direct Current

IGBT : Insulated Gate Bipolar Transistor

LCC : Line Commutated Converter

MI : Mass Impregnated

MMC : Modular Multilevel Converter

MTDC : Mutli-terminl HVDC

PLL : Phase Lock Loop

PM : Power Modular

PMSG : Permanent Magnetic Synchronous Generator

pu : per unit

PWM : Pulse Width Modulation

REC : Receiving Converter

SCC : Self Commutated Converter

SEC : Sending Converter

SVC : Static Var Compensator

TBC : Tran Bay Cable

UHVDC : Ultra HVDC

USD : United States Dollar

VSC : Voltage Source Converter

WF : Wind Farm

WFVSC : Wind Farm side VSC

Contents

Chapter 1

Introduction

1.1 Background

High voltage direct current (HVDC) transmission is a technology based on high power electronics and used in electric power systems for long distances power transmission, connection of non-synchronized grids and long submarine cable transmission [1, 2]. HVDC based on thyristor commutated converters was used for many years [3, 4]. With the development of semiconductors and control equipment, HVDC transmission with voltage source converters (VSC-HVDC) based on IGBTs is possible today and several commercial projects are already in operation [5–8]. The use of such DC links provides possible new solution to the transmission system of wind power generation, especially in offshore wind power transmission.

A multi-terminal HVDC (MTDC) system consists of three or more AC/DC converters and interconnected by a DC transmission network. Delivery of electrical energy across long distances between nodes of an interconnected network is considered to accomplish by an MTDC network. An MTDC system embedded in a large AC grid can offer more economical utilization of DC transmission lines as well as greater

flexibility in power dispatch and stabilization of AC transmission systems [9].

1.2 Objects of the thesis and achievements

The main objective of the thesis is to build a model of voltage source converter multi-terminal HVDC transmission system (VSC-MTDC) for the connection of large offshore wind farms to the terrestrial grid. Furthermore, a control system of the VSC-MTDC will be designed and the dynamics of the system will be analyzed.

The main achievements are described as follows:

- The three-terminal VSC-MTDC model has been developed by PSCAD/EMTDC according to the configuration of laboratory devices.
- The results of laboratory experiment have been obtained. The comparison of the simulation of software by PSACD/EMTDC and laboratory experiment has been achieved. The control system has been verified.
- A four-terminal VSC-MTDC model has been established by PSCAD/EMTDC.
- The control system for the model has been designed according to the coordinated control scheme. In this particular case, the droop-control is applied.
- The dynamic performance of the four-terminal VSC-MTDC has been obtained in terms of the variation of input active power.
- Investigation of the four-terminal VSC-MTDC operation under abnormal operation conditions has been achieved. The dynamic performance of the four-terminal VSC-MTDC under balanced and unbalanced faults in the supplying grid AC system is investigated.

1.3 Outline of the thesis

Chapter 2 introduced the characteristics of HVDC transmission system systematically in terms of development, advantages and system configuration. Then, LCC-HVDC and VSC-HVDC were discussed, the comparison of which was processed. Some fundamentals of LCC-HVDC and VSC-HVDC were introduced. Furthermore, different topologies of VSC and related manufacturers were presented. The applications of VSC-HVDC were illustrated at the end of chapter 2.

Chapter 3 presented the fundamentals, opportunities, development and challenges of MTDC. The opportunities of MTDC for offshore wind energy and offshore wind farms in the UK were introduced. Advantages of multi-terminal HVDC networks were also introduced. Then the control strategy for MTDC was discussed. The challenges of MTDC were also introduced at the end of this chapter.

Chapter 4 focused on the laboratory experiment demonstration. The design of control system was illustrated. Then the design of control systems for wind farm side and grid side converters was introduced separately. The simulation results using PSCAD/EMTDC and laboratory experimental results were obtained and compared. The control strategy was verified.

Chapter 5 gave the simulation results for a four terminal VSC-MTDC transmission system for offshore wind power transmission network. A control system was designed

considering operating characteristics of voltage source converters and wind farms. The droop control approaches were applied for considering automatic coordinating when the system operated under abnormal operation condition. PSCAD/EMTDC was also chosen as the simulation tool. The simulation model was built and simulated under varies of conditions, such as normal condition and abnormal condition. The simulation results showed that the system reached good dynamic response under different types of conditions.

Finally, the conclusions of the work and some suggestions for future research were pointed out in Chapter 6.

Chapter 2

High Voltage Direct Current System

2.1 Introduction

High Voltage Direct Current (HVDC) transmission systems have been researched and developed for many years, and it was based initially on thyristors and more recently on fully controlled semiconductors such as Gate Turn-Off Thyristors (GTO) and Insulated Gate Bipolar Transistors (IGBT) [10, 11-35]. In 1930s, mercury arc rectifiers were invented, which was a milestone of HVDC transmission systems. In 1941, the first HVDC transmission project of the world was constructed to supply power to Berlin with an underground cable of 115 km. However, due to the World War Ⅱ, this HVDC link had never been used. In 1954, the first commercial HVDC transmission project was commissioned in Gotland, Sweden by ABB. HVDC transmission system is now a mature technology and has been playing a vital role in both long distance transmission and in the interconnection systems [10].

HVDC transmission is widely recognized as being advantageous for long-distance-bulk-power delivery, asynchronous interconnections and long submarine cable crossings [9, 10, 36]. Advantages of HVDC links include:

- The power flow on an HVDC link is fully controllable – fast and accurate.

  The operator or automatic controller could set the magnitude and direction of the power flow in the link irrespective of the interconnected AC system conditions.

- An HVDC link is asynchronous.

  The two AC voltages that linked with HVDC system can be controlled independently. Also it is no need for common frequency to the AC systems.

- Faults and oscillations don't transfer across HVDC interconnected systems.
- HVDC can transport energy economically and efficiently over longer distances than AC lines or cables.

Conventional HVDC transmission is based on Line-Commutated current source Converters (LCC) with thyristor valves, which can only operate with the AC current lagging the voltage so the conversion demands reactive power [36]. Recently, Voltage Source Converter (VSC) based HVDC systems have been developed. The VSC technology has been used for low power driver applications. With the development of semiconductor switches, the VSC technology has been used in higher power transmission projects, up to 1200 MW and ±500 kV [37]. The main highlight of the VSC technology is that it can rapidly control both active and reactive power independently [36]. Many manufactures are developing their own products such as ABB's HVDC *Light*, Siemens' HVDC *Plus* and Alstom Grid's HVDC *Extra* [9]. Nevertheless, there are still some issues to overcome such as high switching losses.

2.2 Advantages and applications of HVDC System

The conventional application of HVDC systems are transmission of bulk power over long distance because the overall cost for the transmission system is less and the losses are lower than AC transmission [9]. It is feasible for HVDC to interconnect two asynchronous networks and multi-terminal systems. HVDC also provides AC system support, voltage control and system reserve. The significant advantage of DC interconnection is that there is no limit in transmission distance. Fig. 2.1 shows the ± 500 kV HVDC transmission line for the 2000 MW Intermountain Power Project between Utah and California [36].

Fig. 2.1 ±500 kV HVDC transmission line [36].

2.2.1 Advantages of HVDC system

- *Long Distance Bulk Power Transmission*

HVDC transmission systems often provide a more economical alternative to AC transmission for long-distance, bulk-power delivery from remote resources such as hydro-electric power station, coal-base power plants or large-scale wind farms [36]. HVDC transmission for higher power delivery over longer distances uses fewer lines than AC transmission. The typical HVDC configuration is bipolar with two independent poles. The HVDC transmission offers the following advantages:

- Compared to double circuit AC lines with three conductors, a DC system only requires two conductors.
- The power transfer capacity of DC system is up to three times of an AC system.
- Insulation requirement for a DC system is only one-third for an AC system.
- In terms of tower construction, a DC system is also more economical than an AC system.

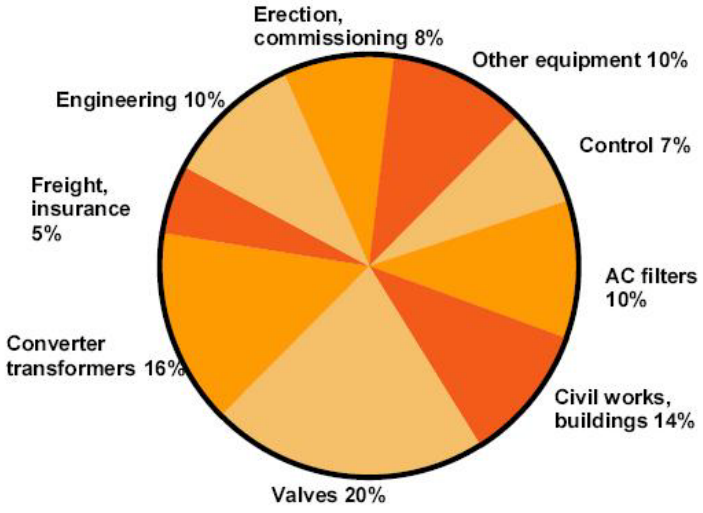

Fig. 2.2 Cost structure for the converter stations [38].

The typical cost structure for the converter stations could be as shown in Fig. 2.2. The main cost inured is valves for converters, which is up to 20%.

An HVDC transmission system has smaller losses than AC transmission if the same amount of electric power is delivered. Normally, the HVDC transmission system is more beneficial if the distance is at least more than 450 km [9]. The main reason is the cost of transmission line. The cost of DC converter station is more than AC substation. However, the cost of AC line is much more than DC line. An approximation of savings in line construction is 30% [36]. Besides, AC lines for long distance transmission are subjected to the intermediate switching stations and reactive power compensation, which increases the substation cost.

The Fig. 2.3 shows an example of cost comparison of HVDC and High Voltage Alternating Current (HVAC) with variation of length. For the AC transmission a double circuit is assumed with a price per km of 250 kUSD/km (each), AC substations and series compensation (equal and above 700 km) are estimated to 80 MUSD. For the HVDC transmission a bipolar overhead line was assumed with a price per km of 250 kUSD/km, converter stations are estimated to 250 MUSD.

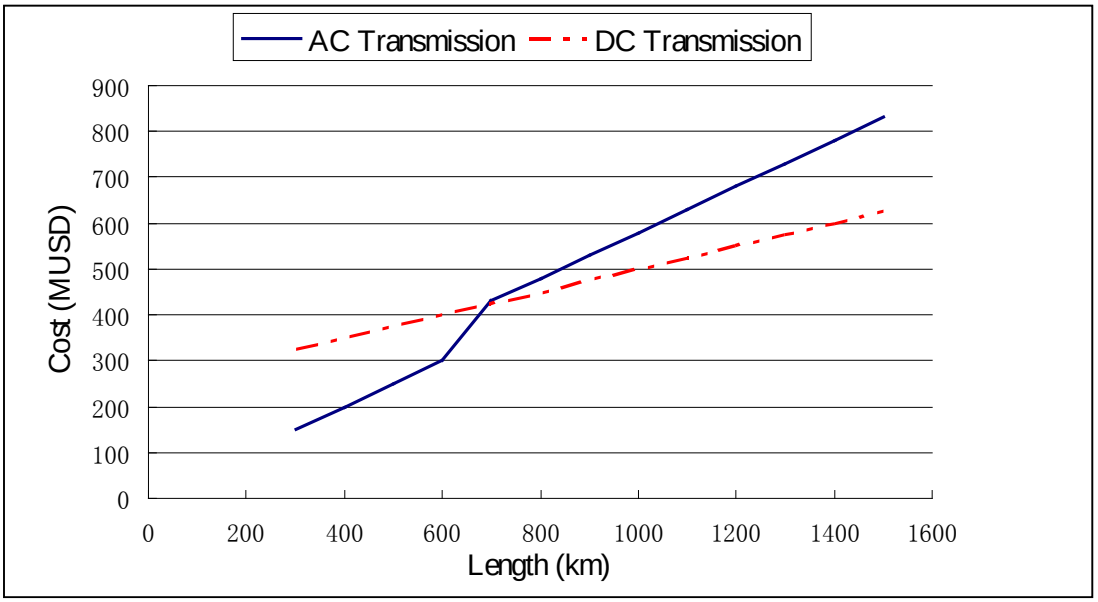

Fig. 2.3 Cost of HVDC and HVAC systems by length (2000 MW) [9].

The cost associated with HVDC transmission lines for a power flow of 2000 MW compared with the AC transmission is shown in Fig. 2.3. Initially, the DC cost is higher than AC cost. However, the AC cost is equal to DC cost at the length of around 700 km. After this crossing point, both of AC and DC cost increase with the AC cost rises faster. Therefore, the gap between AC and DC cost is increasing. So that, at 1500 km AC cost is 200 MUSD more expensive than DC cost.

- *Asynchronous Interconnection*

An HVDC transmission network links with two AC systems which can be totally different frequency. The asynchronous interconnection with HVDC transmission networks allows many benefits, such as more economical and reliable system operation. Typically, the back-to-back converters with no transmission line are used for interconnecting two asynchronous systems. The link acts as effective “firewall”

against propagation of cascading outages in one network to another [36].

- *Offshore Transmission*

For large offshore wind farms with cable route lengths of over 50 km, HVDC transmission should be considered. Between 60 and 80 km, HVAC and HVDC are expected to be similar in cost. It depends on the difference of specific project. Furthermore, while the cable length is around 100 km, HVDC is a better option due to the HVAC transmission system is limited by the loss of the power and the compensation of large amount of reactive power [9]. Otherwise, the HVDC option will have the least amount of cables connecting the wind farm to shore than HVAC. The Fig. 2.4 shows the cost comparison of HVDC and HVAC with variation of length for offshore connection.

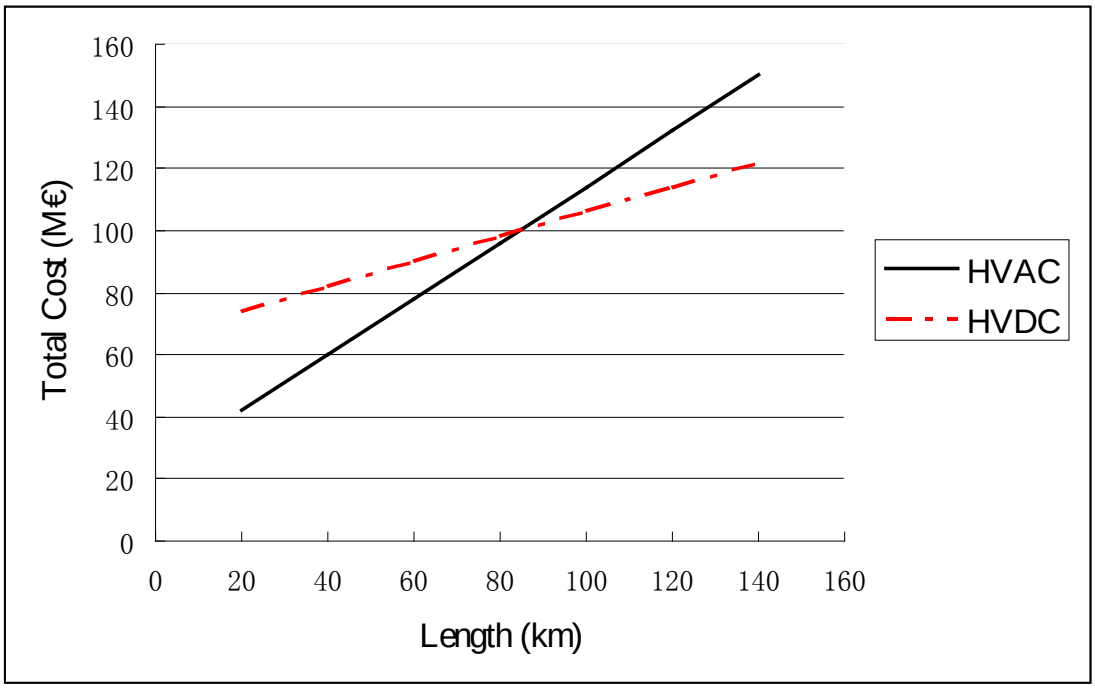

Fig. 2.4 Cost of HVDC and HVAC systems for offshore connection [9].

2.2.2 Applications of HVDC System

Due to a large number of advantages of HVDC transmission system, the application of HVDC has been spread over the world the last decades. Fig. 2.5 shows HVDC projects around the world by power capacity and frequency.

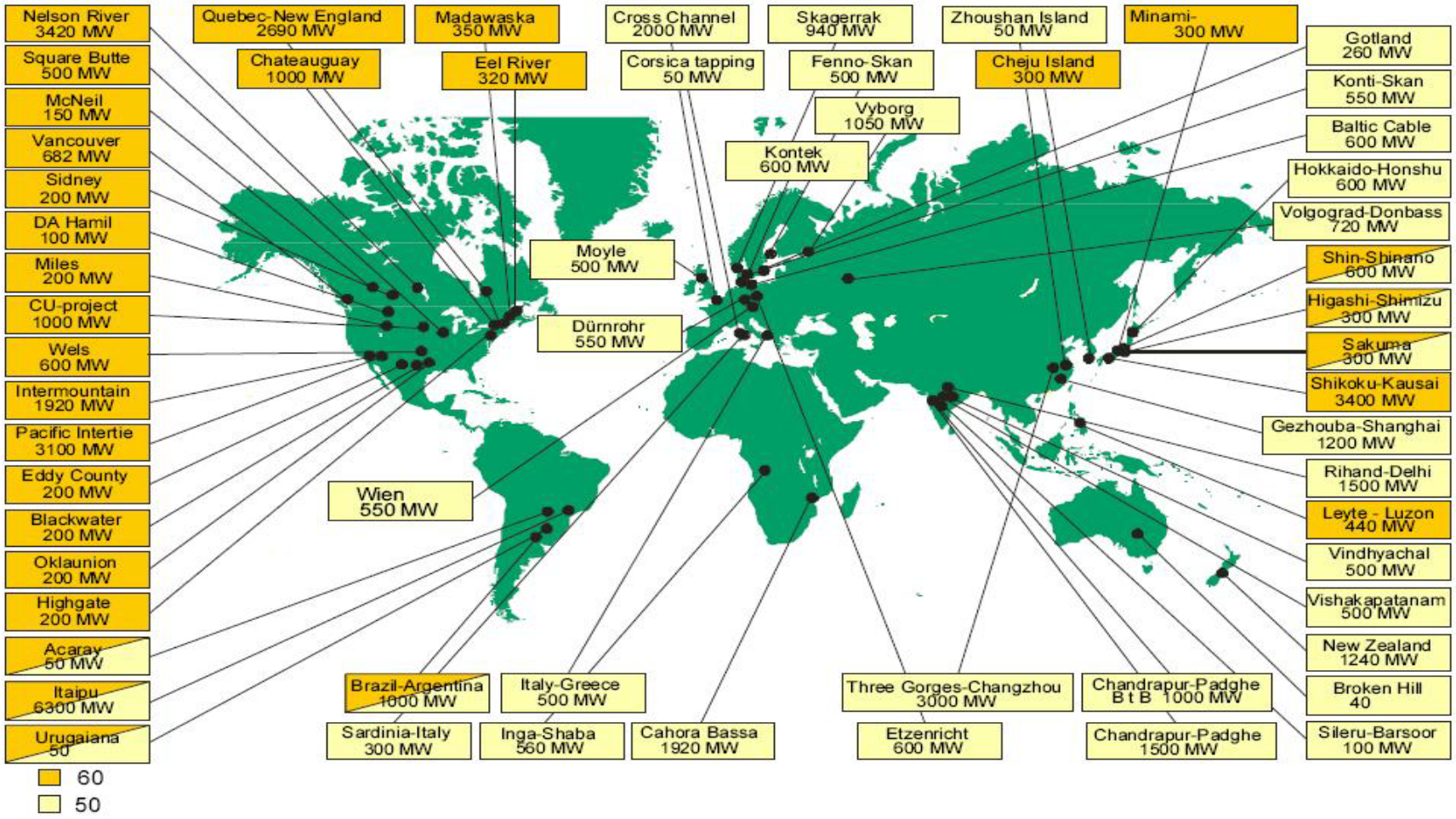

Fig. 2.5 HVDC applications in the world [38].

2.3 Configurations of HVDC system

Many different types of HVDC configurations are exist. Some of them are introduced here.

I. Back-to-back HVDC system

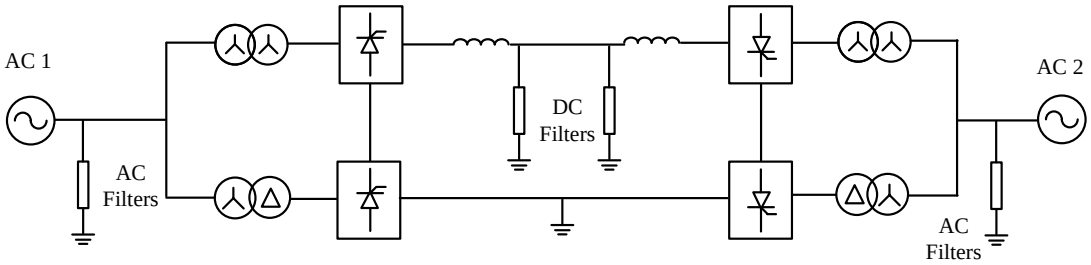

Fig. 2.6 Back-to-back HVDC system.

Fig. 2.6 shows the back-to-back HVDC system. In this configuration, two converter stations are built at the same place, and there is no long-distance power transmission in the DC link. It is the common configuration for connecting two adjacent asynchronous AC systems. The two AC systems interconnected may have the same or different nominal frequencies, i.e. 50 Hz and 60 Hz.

II. Monopolar HVDC system

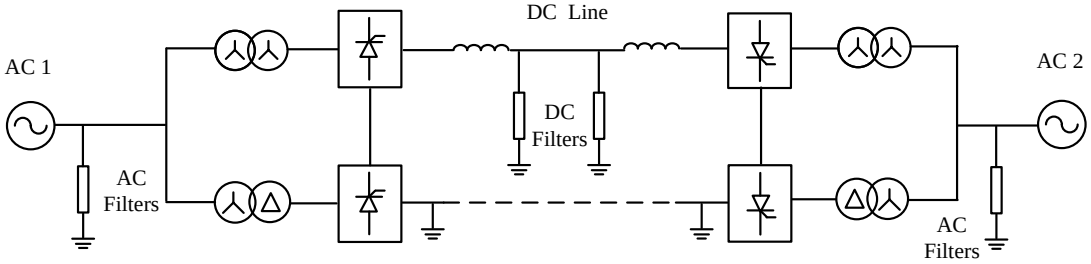

Fig. 2.7 Monopolar HVDC system.

Fig. 2.7 illustrates a monopolar HVDC system. In this case, the two converter stations are separated by a single pole line with a positive or a negative DC voltage. The ground is used to return current. Furthermore, submarine connections for many transmission systems used monopolar configuration.

III. Bipolar HVDC system

Fig. 2.8 shows Bipolar HVDC system, which is the most commonly used configuration. Most overhead line HVDC transmission systems use the bipolar configuration [9].

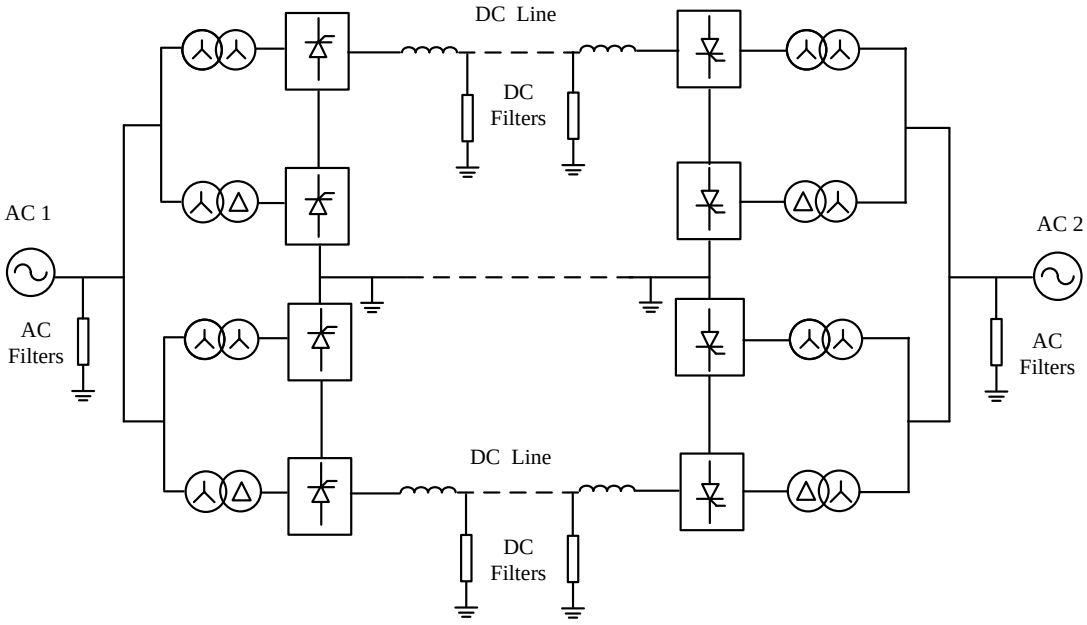

Fig. 2.8 Bipolar HVDC system.

As shown in the figure the bipolar system is essentially two monopolar systems connected in parallel. The advantage of such system is that one pole can continue to transmit power in the case of a fault on other one. Each system can operate separately

as an independent system with the earth return. Both poles have equal currents since one is positive and one is negative, so the ground current is theoretically zero, or in practice, the ground current is within a difference of 1% [9].

IV. Multi-terminal HVDC system

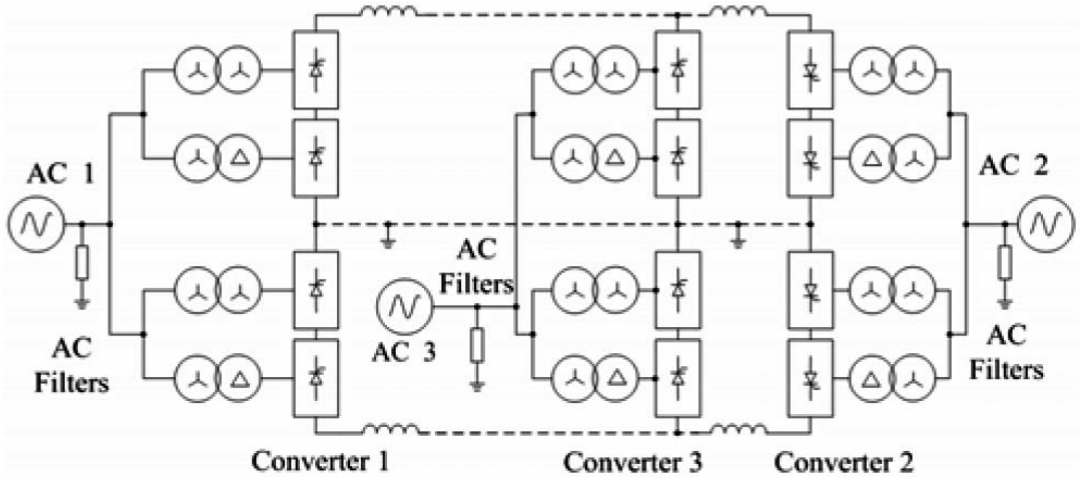

Fig. 2.9 Multi-terminal HVDC system [10].

Fig. 2.9 illustrates a multi-terminal HVDC system, which is more than two sets of converter stations. The three or more HVDC converter stations are separated by location and interconnected through transmission lines or cables. In the example shown in Fig. 2.9, converter stations 1 and 3 operate as rectifiers and converter 2 operate as an inverter.

2.4 LCC-HVDC

Line Commutated Converters-HVDC transmission is also called conventional HVDC. Typically, it is suitable for high power applications. The world's highest HVDC transmission voltage rating project is Xiangjiaba - Shanghai ±800 kV UHVDC transmission in China. Also it is one of the longest overhead line transmission projects in the world, the length of which is 2071 km [39].

2.4.1 Line commutated converter

The Fig. 2.10 shows a LCC-HVDC with the components of LCC converter. Converter station and thyristor valve are included. Also, the transformers, reactive equipment, AC filters and smoothing reactor are shown in this figure.

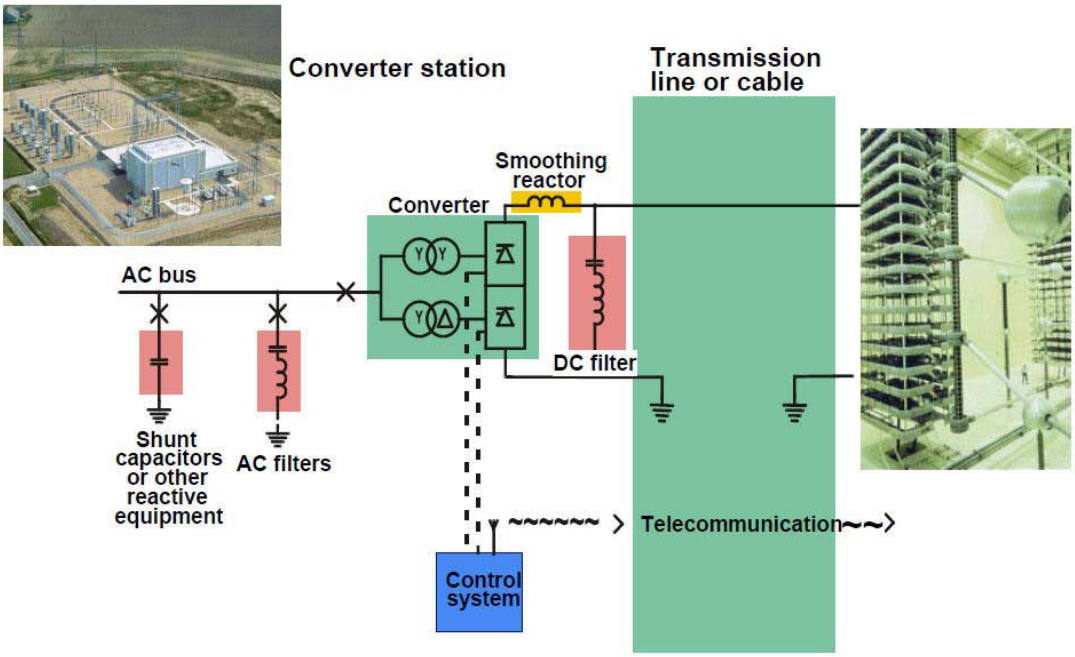

Fig. 2.10 LCC-HVDC (converter station and thyristor valve) [37].

2.4.2 Components of LCC-HVDC

LCC-HVDC transmission system consists of converter, transformer, AC breaker, AC filter, capacitor bank, smoothing reactor and DC filter. The various basic components are described as follows,

a) Line-Commutated Current Source Converter

Converter is an essential component of HVDC power transmission system. It uses power electronic converters to achieve the power conversion from AC to DC (rectifier) at the sending end and from DC to AC (inverter) at the receiving end. The conventional HVDC system technology is based on the current source converters (CSCs) with line-commutated thyristor switches. LCC operates at a lagging power factor for the firing of the converter. Therefore it requires a large amount of reactive power compensation.

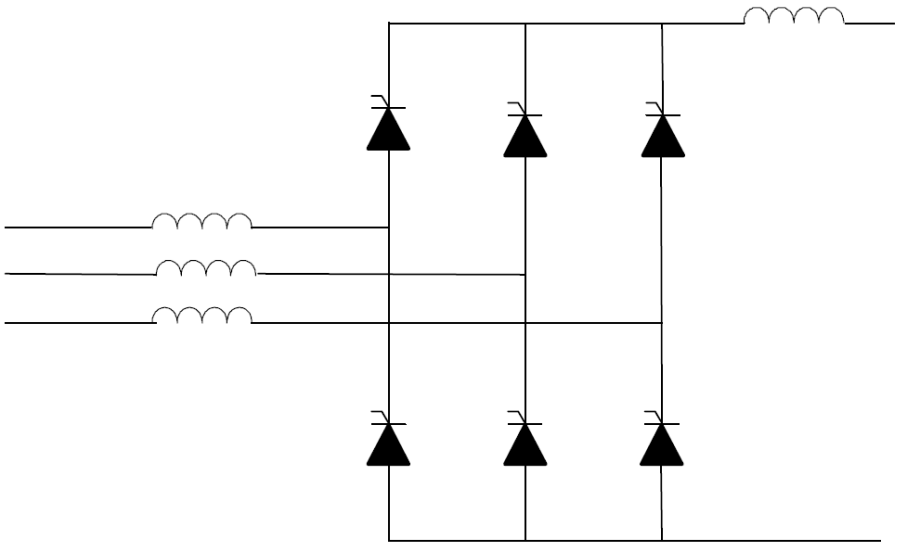

Fig. 2.11 Configuration of a basic 6 pulse thyristor valves.

The basic converter unit of conventional HVDC is a six pulse valves, shown in Fig. 2.11. It is for both conversions, i.e. rectification and inversion. Even though one thyristor is shown in the figure, in real applications a number of thyristors are connected in series and parallel to form a valve as shown in Fig. 2.12.

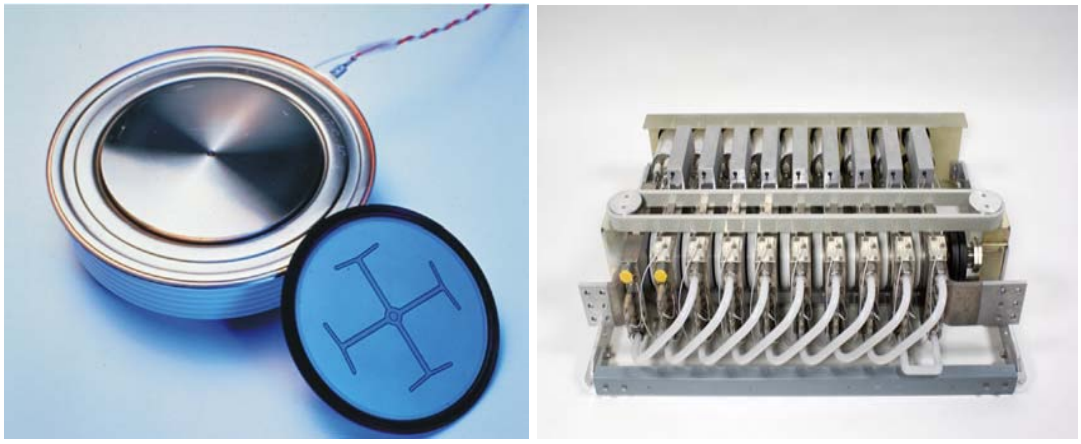

Fig. 2.12 Modern thyristor and front view of HVDC thyristor module [40].

Thyristors are switched on by a pulse. The thyristors cease to conduct when the current flowing through them reduces to zero. Therefore the converters have a requirement to be connected to a reliable AC system, since the AC system voltage forces the current to commutate from one phase to another. Furthermore, LCC-HVDC system requires reactive power in order to operate. The amount of reactive power required varies according to the amount of active power transferred. Therefore, additional components such as switched capacitor banks or Static Var Compensator (SVC) are generally employed to supply the reactive power [9, 10, 36].

As the current only follows from anode to cathode through a thyristor shown in Fig. 2.11, in order to reverse the power flow, the voltage polarity of the converters must

be reversed. Due to switching the voltage polarity, the transient phenomenon appears in the cable. Therefore, the cables used in LCC-HVDC transmission system require a higher insulation capability than VSC cables [41].

b) AC Breaker

AC breaker is used to isolate the HVDC system from AC system whenever there is a fault on the HVDC system. AC breaker must be rated to carry full load current and interrupt the fault current. The expected location of AC breaker is for the interface between AC busbar and HVDC system.

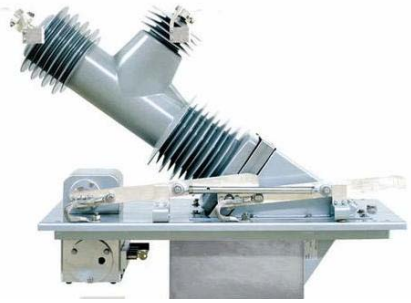

Fig. 2.13 AC breaker [42].

c) AC Filters and Capacitor Bank

The converter generates voltage and current harmonics at both the AC and DC sides. Such harmonic overheat the generator and disturb the communication system. On the AC side a double tuned AC filter is used to remove these two types of harmonics. In addition, the reactive power sources such as a capacitor bank or synchronous compensator are installed to provide the reactive power to power conversation.

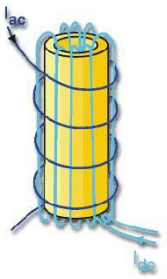

Fig. 2.14 AC filter [42].

d) Converter Transformer

The voltage of AC system to be supplied to the DC system is by converter transformer. It also provides a separation between AC and DC system.

e) Smoothing Reactor and DC Filters

The smoothing reactor forms an integral component, together with the DC filter, to protect the converter valve during a commutation failure by limiting the rapid rise of current flowing into the converter.

Fig. 2.15 HVDC Smoothing Reactor and DC-filter with capacitor [42].

2.5 VSC-HVDC

VSC-HVDC systems represent recent developments in the area of DC power transmission technology [41]. The experience with VSC-HVDC at commercial level developed over the last 13 years [1-8]. The breakthrough was made when the world's first VSC-based PWM-controlled HVDC system using IGBTs was installed in March 1997 (Hällsjön on project, Sweden, 3 MW, 10 km distance, ±10 kV) [1, 2]. Since then, more VSC-HVDC systems have been installed worldwide [3-8, 42]. In addition, there are a lot of advantages of VSC-HVDC than LCC-HVDC transmission systems for offshore wind power generation [43-51].

2.5.1 Voltage source converter

Forced-commutated VSC uses gate turn-off thyristors (GTOs) or in most industrial cases insulated gate bipolar transistors (IGBTs). It is well-established technology for medium power levels, thus far, with recent projects ranging around 300–400MW power level [1-8, 42]. The simple configuration is shown in Fig. 2.16.

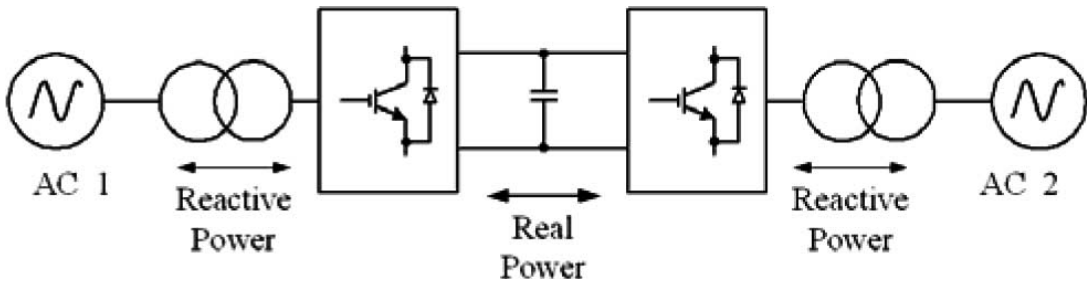

Fig. 2.16 HVDC system based on VSC built with IGBTs [10].

The following list shows many advantages for using Voltage Source Converter (VSC) compared to the LCC [9],

- Independent control of reactive and active power
- Provides continuous AC voltage regulation
- No restriction on multiple infeeds
- No polarity reversal needed to reverse power
- Black-start capability

For the above advantages, the VSC-HVDC can be used for conventional network interconnections, back-to-back AC system linking, voltage or stability support, and integration of large-scale renewable energy sources with the gird and most recently large onshore or offshore wind farms [10, 36, 41].

Particularly, there are many advantages by using VSC-HVDC in multi-terminal system. Within the use of IGBT or GTO, the commutation failure is eliminated because these new semi-conductor components not only have the ability of turn-on, but also turn-off. Also, VSC technology offers the ability of absorb and generate the active and reactive power independently. Therefore, it is not necessary to make the reactive power compensation by adding the expensive reactive power compensators (SVC or capacitor bank) as with LCC-CSC technology. Furthermore, the number of filters is minimised as less harmonics are generated. Additionally, the system has the ability of “black start”. It means restoring a power station to operation without relying on external energy sources. Although the VSC technology in HVDC transmission is

not fully mature, the capacity of these transmission projects has already reached 2 GW in 2010.

2.5.2 Topologies and manufacturers

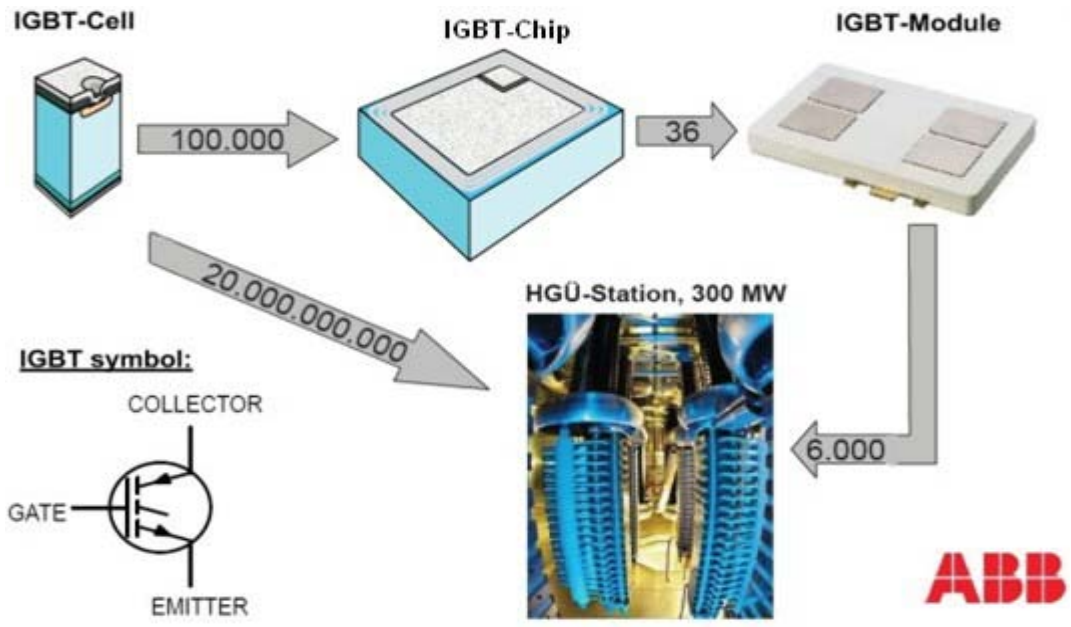

Fig. 2.17 IGBT symbol and representation of a valve from IGBT cells [52].

A VSC-HVDC transmission system uses self-commutated semiconductor component for commutation. The Insulated-Gate Bipolar Transistor (IGBT) is the typical semiconductor used for VSC. The first-generation of IGBT was applied in industry in 1980s. However, due to the slow speed of switching on and off, they have been gradually replaced by the second-generation IGBT in 1990s. The second-generation IGBT shows the very good performance for the high voltage and current. With the small size of the IGBT-Cell (around 1 cm^2), many of them are connected in parallel to

form IGBT chips. Then a number of IGBT-Chip are connected to form IGBT-Module, which is able to withstand current up to 2.4 kA with blocking voltage up to 6.5 kV. In Fig. 2.17, it shows the valve consists of 20 billion IGBT-Cells.

A conventional two-level three-phase topology is shown in Fig. 2.18. Even though one IGBT with anti-parallel diodes is shown in each box, in real applications, a number of IGBTs are connected in series to form a valve. Therefore, the DC bus voltage level is increased.

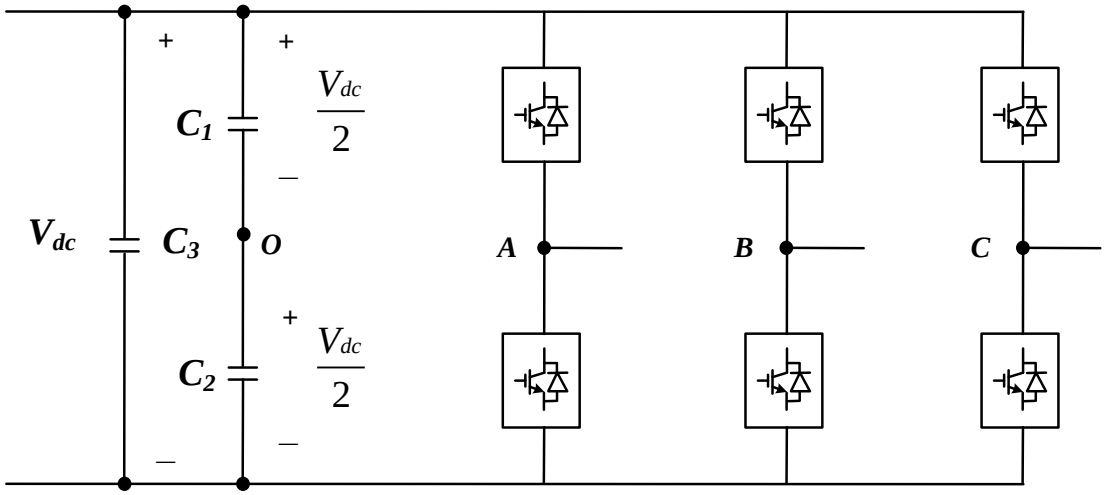

Fig. 2.18 Conventional two-level three-phase VSC topology.

HVDC Light® was introduced by ABB in 1997 at first. It first implemented to the project in Gotland, Sweden in 1999. HVDC Light® is based on the topology shown in Fig. 2.18 [41, 52]. It uses a carrier-based PWM (sinusoidal) control method to control the gate switching frequency of IGBT. Due to the requirement of reducing harmonics, the special PWM control methods named optimum frequency-PWM was developed. Within this method, the switching frequency is not fixed, however, it is varied (from 1

kHz to 2 kHz) with the current. For instance, the switching frequency reduces while the current increases. It is to reduce the losses across the converter valves while eliminating the harmonics. Because the series connected IGBTs need to be switched at the same moment accurately, it is required to measure the voltage over each IGBT. Based on the measured voltage, a control signal is provided to the gate of each IGBT in converter valve to decide the working state of IGBT. It is for controlling the IGBT switch-on or switch-off. Due to the above reasons, ABB developed a patented control system for monitoring the states of IGBTs.

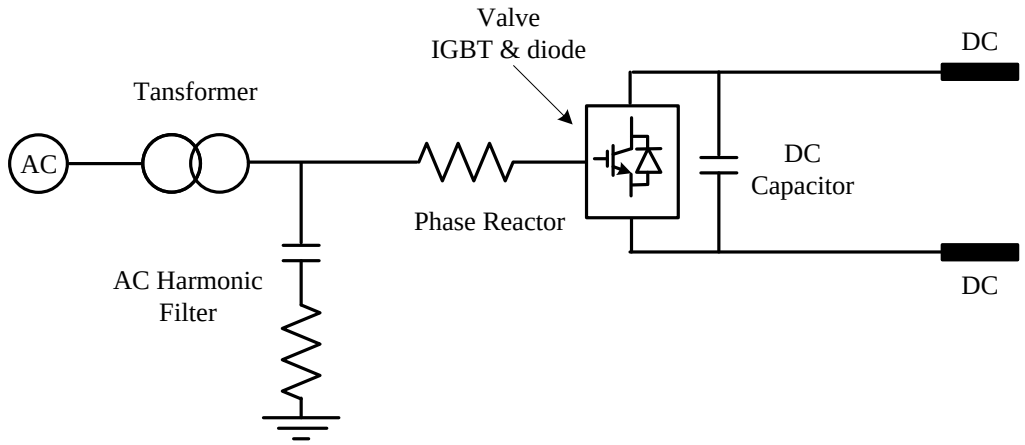

Fig. 2.19 Scheme of typical configuration of VSC terminal.

The Fig. 2.19 shows the typical configuration of VSC terminal, which is also applied in ABB's HVDC Light®. The main component of the VSC converter valve comprises of series-connected IGBTs with anti-parallel diodes. With the snubber capacitors (C_1 and C_2 in Fig. 2.18) connected in parallel each IGBT, the overvoltage in IGBT valves is able to avoid effectively. The phase reactors, which connected with converter valve, are one of the important components in a VSC-based transmission system. They allow continuous and independent control of active and reactive power. They reduce the

harmonic current generated by the converter. Also, the phase reactors are able to limit the short circuit current of the IGBT valves. Therefore, the AC system connected with valves is separated by the phase reactors. AC harmonic filters between the phase reactor and the transformer are designed to reduce the harmonics. It avoids the DC voltage stresses and damaging harmonics generated by converter valves affecting the transformers operation.

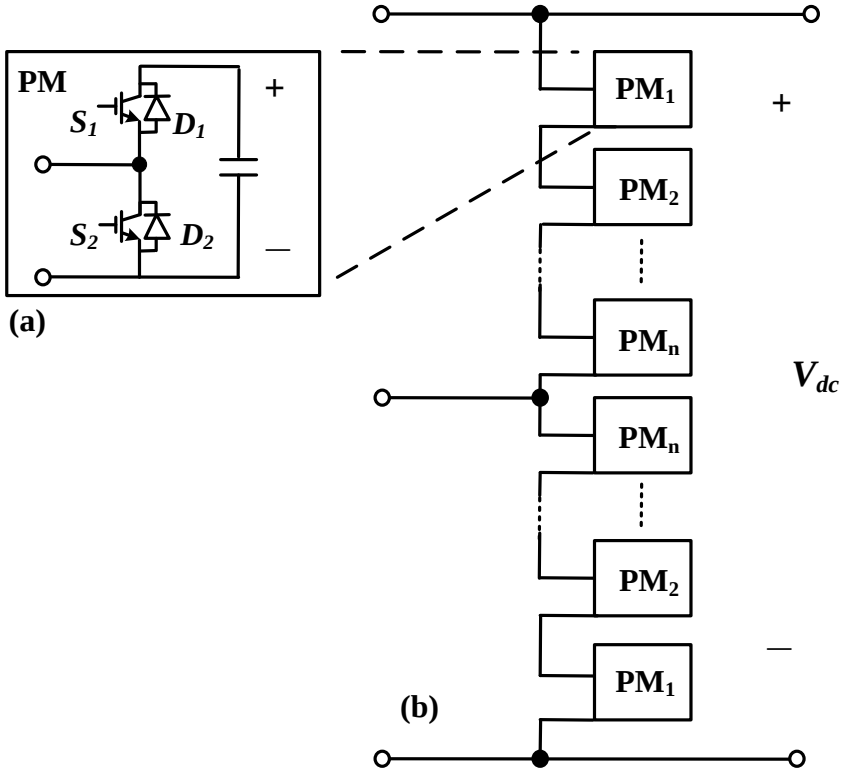

Fig. 2.20 MMC topology (a) structure of power module (b) Phase unit [53].

In recent years, Siemens developed HVDC Plus® technology including the advanced multilevel approach [53]. The basic design of the technology is based on the Modular Multilevel Converter (MMC). The topology is shown in Fig. 2.20. It uses the half-bridge cascaded connections for each power modular (PM). There is a separate

small capacitor of each PM, which forms a half bridge rectifier. The converter output voltage has been maximized by many modules connected in series. By controlling turn-on or turn-off of each PM at given instant, many small voltage steps are formed, which then built the step-wise AC waveform. Due to modular nature of this converter topology, it is suitable for applications operating on different voltage level. In [54], different power level projects have been introduced and the relevant control schemes have been proposed based on this topology. In comparison of conventional 2-level or 3-level converter technology, HVDC Plus® based on MMC shows the advantages including low switching losses and low level of HF-noise because of low switching frequency. The first project based HVDC Plus® technology has been commissioned in 2010. The 400 MW, 88 kilometers project is called Trans Bay Cable and links San Francisco and Pittsburg. The other projects named HelWin1, BorWin2, SylWin1 and INELFE which are also based on HVDC plus® technology will be commissioned in Germany and France-Spain respectively from 2013 to 2014.

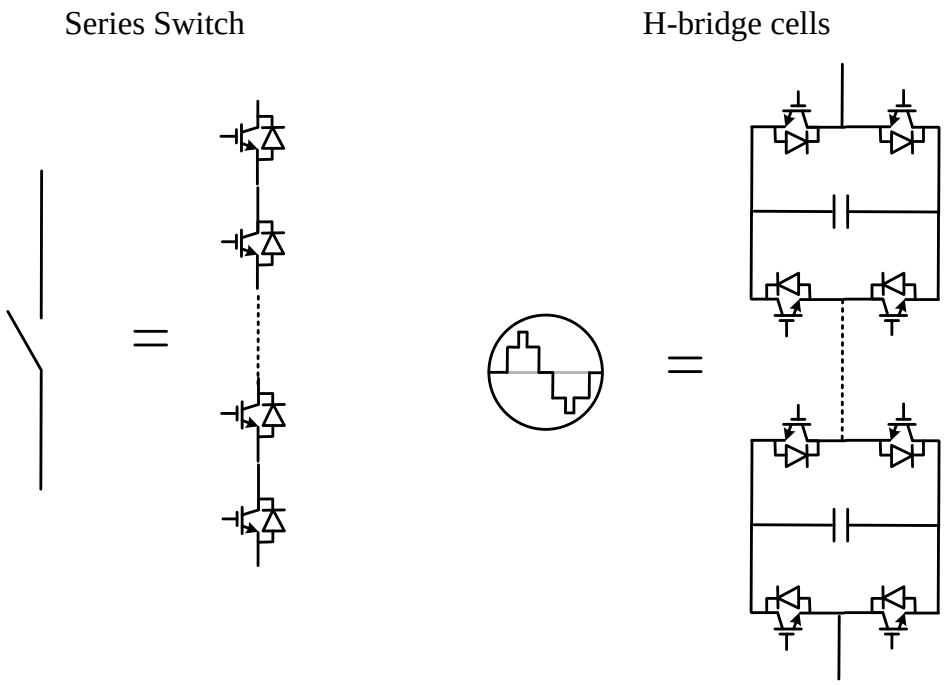

Fig. 2.21 Blocks of hybrid converters [55].

Besides ABB and Siemens, Alstom Grid is also a strong manufacture in this area. Their own HVDC solution - HVDC extra is being developed for a long time [9]. Last year, Alstom Grid introduced their latest converter structure called New Hybrid Multi-Level Voltage Source Converter. Based on the specific topology, the system is able to operate within lower losses and also maintains the ability to deal with DC-side faults [56]. As shown in Fig. 2.21, the fundamental blocks of the new topology are series switch and H-bridge cells. In Fig. 2.22, it shows the topology consists of series switch and H-bridge cells. It reserves the advantage of 2-level converter, which minimizes the total number of semiconductors. A lot of H-bridge cells series connected for constructing the requested converter voltage. It works similar to a LCC-CSC because of the series of IGBTs, called series switch. In each phase, the soft series switch direct the current to the upper or lower. For instance, while the series switch is closed, the converter voltage was constructed by its H-bridges cells and

adding or subtracting several small voltage leads to the DC-bus voltage. The AC phase current passes into either the positive or negative DC terminal and, together with the two other phase currents, create a DC current with a 6-pulse ripple [56]. Moreover, based on this topology, the system is able to operate within very high efficiency. The simulation results shows the Semiconductor losses is only 1.02% in 20 MW power simulation case [56]. Besides the advantage of high efficiency, it is able to control current flow into faults on the DC side of the circuit because the converter based on H-bridge cells, which is full-bridge cell. And also it has the potential to provide reactive power to the AC network during this type of the fault [55].

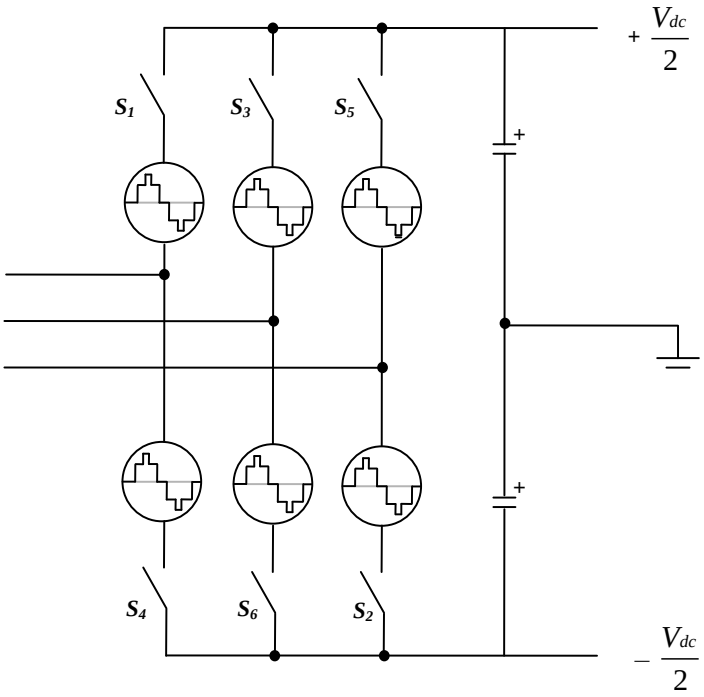

Fig. 2.22 Representation of a single phase converter [55].

2.5.3 Pulse width modulation

There are a variety of switching techniques that can be used for VSC-HVDC

operation. The switching technique to be used is usually determined by the requirement for reduced harmonics at the output and low losses in the converter. The simplest form of Pulse Width Modulation used in this technology is sine-triangular Pulse Width Modulation. This involves very fast switching between two fixed voltage signals to create an AC voltage. The PWM method used as an operational algorithm for the VSC has an advantage of instantaneously controlling the phase and magnitude of the voltage.

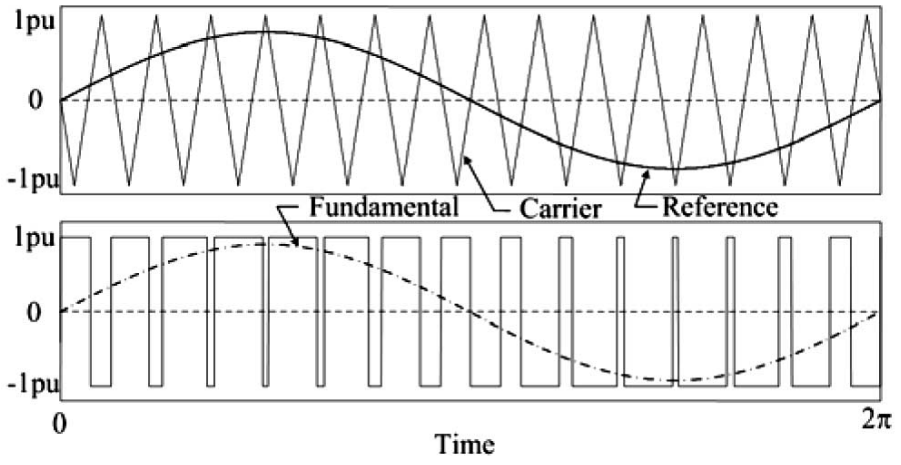

Fig. 2.23 Two-level sinusoidal PWM method: reference (sinusoidal) and carrier (triangular) signals and line-to-neutral voltage waveform [10].

In order to create this AC voltage, a (sinusoidal) reference control signal at the desired frequency is compared with a (triangular) carrier waveform, as shown in Fig. 2.23. The carrier waveform determines the switching frequency of the devices and its amplitude and frequency are generally kept constant. PWM enables wide range of phase angle or amplitude to be created. The reference signal is used to modulate the switch duty ratio. The amplitude modulation ratio m_a is defined as [40]:

$$m_a = \frac{V_{ref}}{V_{ca}}$$

where V_{ref} is the peak amplitude of the reference signal and V_{ca} is the amplitude of the carrier signal.

The frequency modulation ratio m_f is defined as:

$$m_f = \frac{f_{ca}}{f_{ref}}$$

where f_{ca} is the carrier frequency and f_{ref} is the reference signal frequency.

Harmonics produced by the converter are mainly determined by the width and position of the converter output pulse. The switching losses are determined by the switching frequency and the number of switches used in the converter.

2.5.4 VSC-HVDC power capacity

Fig. 2.24 shows the power capability curve for VSC-HVDC transmission system. There are three factors that limit the power capability [1]. The first is the current rating of the IGBTs which gives rise to a maximum MVA circle in the power plane where the maximum current and nominal AC voltage is multiplied. If the AC voltage decreases, the MVA capability will also be affected.

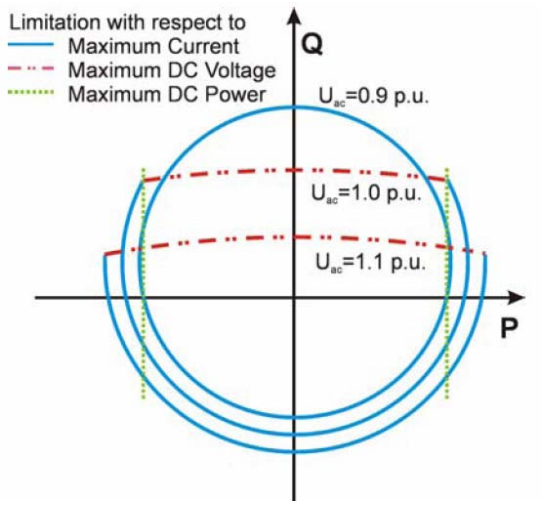

Fig. 2.24 Capability curve for VSC-HVDC [57].

The second limit is the maximum DC voltage level. Reactive power transmission is mainly dependent on the difference between the AC voltage generated by the VSC DC voltage and the grid AC voltage. In the event of high grid AC voltages, the difference between the AC and DC voltages will be low and so the reactive power capability will be reduced. The third limit is the maximum DC current through the cable [57].

2.5.5 Fault ride - through strategies

As we know, the LCC have the natural ability to withstand short circuits as the DC inductors can assist the limiting of the currents during faulty operating conditions. In contrast, the VSC is more vulnerable to DC faults [58-62]. Faults on the DC side of VSC-HVDC systems can also be addressed through the use of DC circuit breakers (CBs) [63-69].

When a DC fault occurs, the fault current is fed through to the anti-parallel diodes. The converter is not able of extinguishing the fault current. The fault current is only limited by the impedance of the reactance, causing high currents that can destroy the semiconductor devices. The current withstand of the IGBT is typically twice of the nominal rated current [60]. It is the main limitations of present day VSCs. The fault current withstand of VSCs is much lower than thyristor based converters, typically twice of the nominal current rating of the converter [70, 71].

Basically, there are two solutions for dealing with DC over voltage when the system is subjected to a fault [58, 59]. The first method is to consume the redundant energy by a resistor of DC chopper. The diagram is shown in Fig. 2.25. The second method is fast power reduction.

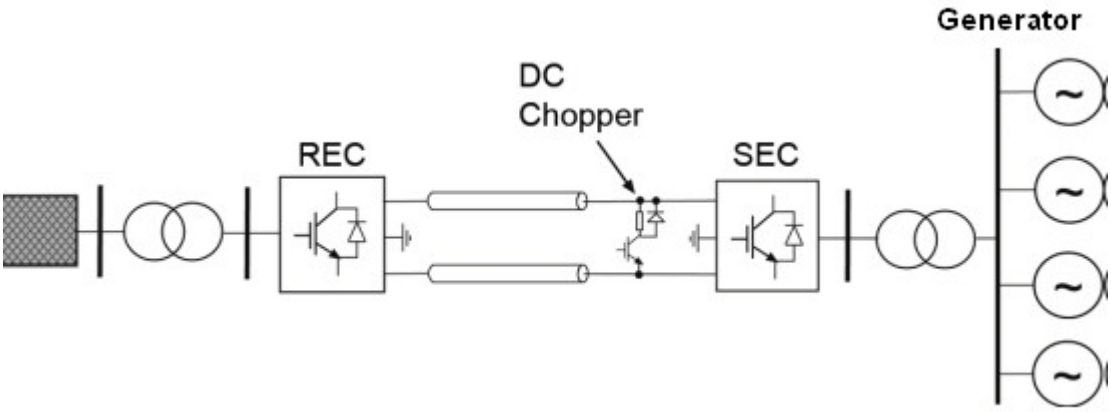

Fig. 2.25 VSC-HVDC system with DC chopper [58].

- DC chopper

This method requires only a very simple control and can directly be triggered using a hysteretic function based on DC voltage measurement [58, 59].The main advantage of

this technique is that the wind farm stays completely unaffected by the fault. In this case, the output power of the wind turbines remains a constant during the fault. Therefore, it is no impact on the mechanical operation [58].

- Fast power reduction

The other solution is based on a fast reduction of the generated power in the wind park. If the power fed into the DC link can be reduced fast enough, the excessive energy that is stored in the DC capacitors can be limited and the DC voltage remains controllable. In [59], the specific methods regarding “direct communication”, “voltage reduction” and “frequency droop” have been discussed.

2.5.6 Applications for VSC-HVDC systems

Self-commutation, dynamic voltage control and black-start capability allow the VSC-HVDC transmission system to serve isolated loads on islands or offshore production platforms over long distance submarine cables [36]. A collector system, reactive power support and long distance transmission are the most basic features of large remote offshore wind power generation. Not only VSC based HVDC transmission system provides higher efficiency for long distance land or submarine cables transmission, but also offers active power control and reactive power compensation for wind power generation. Therefore, VSC-HVDC projects have been developed gradually in recent years.

So far, there are 13 VSC-HVDC projects, which are commissioned. Table 1 shows the projects with fundamental characteristics.

Project name	Year of Commission	Power rating	NO. of circuits	AC voltage	DC voltage	Length of DC cables	Comments and reasons for choosing VSC-HVDC	Topology	Semi-contactors
Hällsjön, Sweden	1997	3 MW ± 3 MVAr	1	10 kV (both side)	± 10 kV	10 km Overhead lines	Test transmission. Synchronous AC grid.	2-level	IGBTs (series connected)
Gotland HVDC Light, Sweden	1999	50 MW -55 to +50 MVAr	1	80 kV (both side)	± 80 kV	2 × 70 km Submarine cables	Wind power (voltage support). Easy to get permission for underground cables.	2-level	IGBTs (series connected)
Eagle Pass, USA	2000	36 MW ±36 MVAr	1	138 kV (both side)	± 15.9 kV	Back-to-back HVDC Light station	Controlled asynchronous connection for trading. Voltage control .Power exchange.	3-level NPC	IGBTs (series connected)
Tjæreborg, DENMARK	2000	8 MVA 7.2 MVA -3 to +4 MVAr	1	10.5 kV (both side)	± 9 kV	2 × 4.3 km Submarine	Wind power. Demonstration project. Normally synchronous AC grid with variable frequency control.	2-level	IGBTs (series connected)
Directlink, Australia	2002	180 MW -165 to +90 MVAr	3	110 kV- Bungalora 132 kV- Mullumbimby	± 80 kV	6 × 59 km Underground cable	Energy trade. Asynchronous AC grid. Easy to get permission for underground cables.	2-level	IGBTs (series connected)
Murray link, Australia	2002	220 MW -150 to +140 MVAr	1	132 kV – Berri 220 kV – Red Cliffs	± 150 kV	2 × 180 km Underground cable	Controlled asynchronous connection for trading. Easy to get permission for underground cables.	3-level ANPC	IGBTs (series connected)
Cross Sound, USA	2005	330 MW ±150 MVAr	1	345 kV – New-Heaven 138 kV Shoreham	± 150 kV	2 × 40 km Submarine cables	Controlled asynchronous connection for exchange. Submarine cables	3-level ANPC	IGBTs (series connected)
Troll A, Norway	2006	84 MW -20 to +24 MVAr	2	132 kV – Kollsnes 56 kV - Troll	± 60 kV	2 × 70 km Submarine cables	Environment, CO_2 tax. Long submarine cable distance. Compactness of converter on platform electrification.	2-level	IGBTs (series connected)
Estlink, Estonia-Finland	2009	350 MW ±125 MVAr	1	330 kV – Estonia 400 kV - Finland	± 150 kV	2 × 31 km, Underground 2 × 70 km, Submarine	Length of land cable, sea crossing and non-synchronous AC system..	2-level	IGBTs (series connected)
NordE.ON 1, Germany	2009	400 MW	1	380 kV – Deile 170 kV – Borkum 2	± 150 kV	2 × 75 km, Underground 2 × 128 km, Submarine	Offshore wind farm to shore. Length of land and sea cables. Asynchronous system.	-----	IGBTs (series connected)
Caprivi Link, Namibia	2009	300 MW	1	330 kV – Zambezi 400 kV - Gerus	± 350 kV	970 km Overhead lines	Synchronous Ac grids. Long distance, weak networks.	-----	IGBTs (series connected)
Vallhall offshore, Norway	2009	78 MW	1	300 kV – Lista 11 kV - Valhall	± 150 kV	292 km Submarine coaxial cable	Reduce cost and improve operation efficiency of the field. Minimize emission of green house gases.	2-level	IGBTs (series connected)
Tran Bay Cable (TBC), USA	2010	400 MW	1	115 kV – San Francisco 230 kV - Pittsurg	± 200 kV	85 km Submarine cable	Increased network security and reliability due to network upgrades and reduced system losses.	Multi-level	IGBTs (series connected)

Table 1. Summary of worldwide VSC-HVDC project and their basic parameter [10, 72].

2.6 Summary

In this chapter an overview of the HVDC system was presented. Advantages and applications of HVDC were described. Configurations of HVDC system were presented. It can be summarised that the bipolar HVDC link is the most common HVDC configuration so far. The function of each component of the conventional HVDC was presented in detail. Additionally, different topologies of VSC and related manufacturers were presented. Moreover, the basic aspects of the VSC-HVDC system, which are PWM, power capacity and fault ride through strategies, were discussed. Due to the flexible controllability of the VSC-HVDC, many new advantages and applications were focused gradually. Therefore, it makes VSC-HVDC more attractive for the future.

Chapter 3

Multi-terminal HVDC Networks

3.1 Introduction of Multi-terminal HVDC networks

Transmitting electrical energy across long distances between nodes of an interconnected network or between islanded networks is considered to accomplish by a number of point-to-point HVDC, as well as by a multi-terminal HVDC (MTDC) networks. Compared with conventional point-to-point HVDC networks, a MTDC network consists of three or more DC converters and interconnected by a DC transmission network. Fig. 3.1 shows a typical MTDC system (3-terminal).

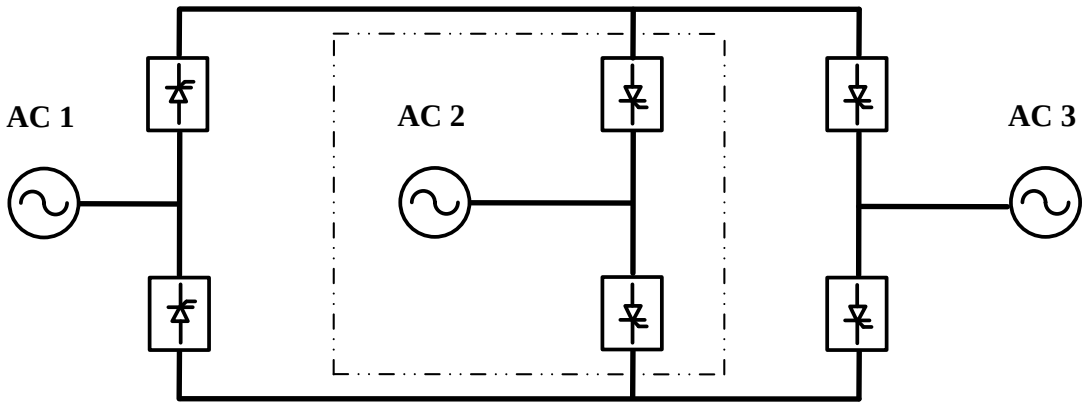

Fig. 3.1 MTDC system.

There has been an interest for the extension of point-to-point HVDC system based on line commutated current source converter (LCC-CSC) technology to multi-terminal HVDC since 1980s. The only one multi-terminal scheme was constructed. Its

objective was to convert the Hydro Quebec-New England link into a five-terminal scheme with the additional of three further terminals [73]. However, the original two-terminal link of Hydro-Quebec-New England project (between Des Cantons and Comerford) was never integrated into multi-terminal DC network due to the unsatisfied performances.

Although there are a number of challenges for the development of multi-terminal HVDC based on LCC-CSC technology, the operating experience of the above 2000 MW project proved that from the technical point of view there are no problems to interconnect several converter stations to the same HVDC transmission line. Furthermore, the successful application of the project suggests that more economical and technical advantages might be realized by a multi-terminal HVDC system.

With the development of fully controlled semiconductor, IGBT-based (Insulated-gate bipolar transistor) VSC technology is now considered for medium power HVDC schemes. The VSC-based HVDC is better suitable for MTDC networks than LCC-CSC-based HVDC, especially for interconnecting different energy sources, such as wind, solar and oil/gas platforms. Fig. 3.2 shows an MTDC network for the connection of wind farms and oil/gas platforms. Moreover, the VSC are well-established technology for medium-voltage level applications with recent projects ranging around 300-400 MW [10].

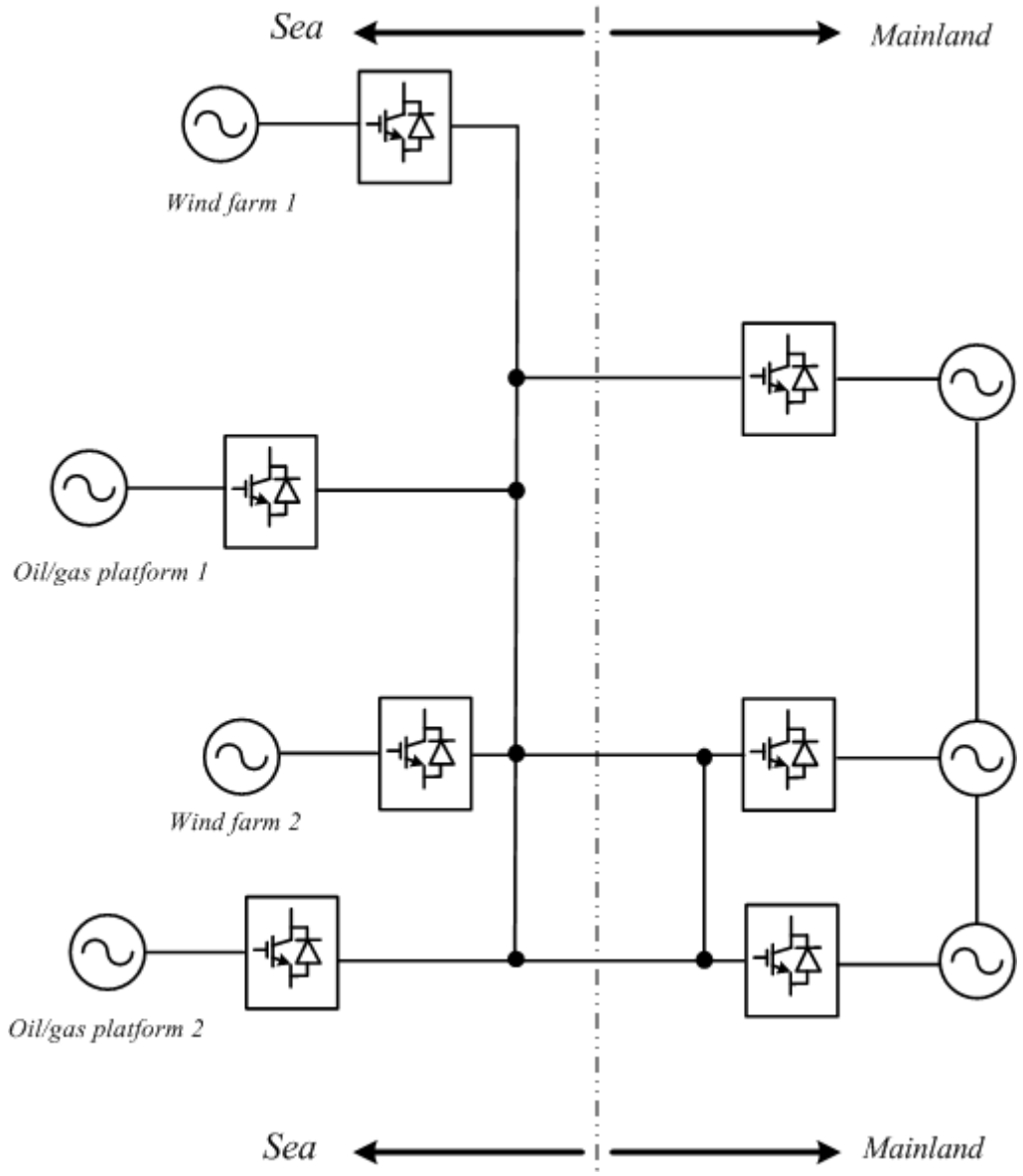

Fig. 3.2 Example of MTDC networks.

3.2 Opportunities of MTDC on offshore wind energy

3.2.1 Background of offshore wind energy

Renewable energy showed the economical and environmental advantages. For instance, wind power and hydropower are considered as a possible option to reduce the emission of greenhouse gases (carbon dioxide) [74, 75]. Compared with onshore wind farms, offshore wind farms are more attractive due to the wind speeds of offshore are higher than that on onshore (except for in elevated onshore sites) and larger wind turbines can be installed. Many offshore wind farms are being proposed and developed today close to densely populated areas where there is limited space on land but relatively large offshore areas with shallow water.

The UK has potentially the largest offshore wind resource in the world, with relatively shallow waters and a strong wind resource extending far into the North Sea. Moreover, the UK has been estimated to have over 33% of the total European potential offshore wind resource. As a result of the vast wind resource, the offshore wind farms were being developed in recent years.

It is anticipated that up to 33 GW of offshore wind power will be installed in the UK by 2020. More and more wind farms will be built along the northern, western and eastern coast of the UK, where there is vast wind resource. The expected solution of connection the wind farms to the mainland of the UK is point-to-point way. However, the MTDC method, which is connecting terminals together and building up a systematic network, shows flexibility and economy.

3.2.2 The status of offshore wind farm in the UK

The first large scale offshore wind farm in the UK is 60 MW - North Hoyle project, which commenced operation in December 2003. North Hoyle project covers an area of 10 km², and is located approximately 7.5 kilometres (4.7 miles) off the coast of North Wales. The second one is also 60 MW - Scroby Sands project, which was commissioned in December 2004. After that, the 90 MW-Kentish Flats project was commenced and in operationa in August 2005. Together with these projects, the capacity of offshore wind farms in the UK is standing at 1341.2 MW in 2010 [76]. Furthermore, 4 projects with total power 1154.4 MW are under construction and 7 projects with total power 2591.7 MW are approved. Tables 2, 3 and 4 show the details of operational, under construction and approved offshore wind farms in the UK respectively.

Wind farm	**Location**	**Region**	**Turbines**	**Power**	**MW**	**Developer**
Barrow	7km Walney Island	North West	30	3	90	Warwick Energy
Beatrice	Beatrice Oilfield, Moray Firth	Scotland	2	5	10	Scottish & Southern
Blyth Offshore	1km Blyth Harbour	North East	2	2	4	E.ON UK Renewables
Burbo Bank	5.2km Crosby	North West	25	3.6	90	DONG Energy
Gunfleet Sands I	7km Clacton-on-Sea	East of England	30	3.6	108	DONG Energy
Gunfleet Sands II	8.5km off Clacton-On-Sea	East of England	18	3.6	64.8	DONG Energy
Kentish Flats	8.5 km offshore from	South East	30	3	90	Vattenfall
Lynn & Inner Dowsing	5KM Skegness	East Midlands	54	3.6	194.4	Centrica Renewable Energy Ltd
North Hoyle	7.5km Prestatyn & Rhyl	North Wales	30	2	60	RWE Npower Renewables
Rhyl Flats	8km Abergele	North Wales	25	3.6	90	RWE Npower Renewables
Robin Rigg	9.5km Maryport/8.5km off Rock Cliffe	North West	60	3	180	E.ON UK Renewables
Scroby Sands	2.5 km NE Great Yarmouth	East of England	30	2	60	E.ON UK Renewables
Thanet	11-13km Foreness Point, Margate	Thames Estuary	100	3	300	Vattenfall
Totals			**436**		**1,341.2**	

Table 2. Operational offshore wind farms in the UK [76].

Wind farm	Location	Region	Turbines	Power	MW	Developer
Greater Gabbard	26km off Orford, Norfolk	Thames Estuary	140	3.6	504	Scottish & Southern
Ormonde	off Walney Island	North West	30	5	150	Vattenfall
Sheringham Shoal	Sheringham, Greater Wash	East of England	88	3.6	316.8	Scira Offshore Energy Ltd
Walney I	14km Walney Island, Irish Sea	North West	51	3.6	183.6	DONG Energy & SSE Renewables
Totals			**309**		**1,154.4**	

Table 3. Under construction offshore wind farms in the UK [76].

Wind farm	Location	Region	Turbines	Power	MW	Developer
Gwynt y Mor	13km off the North Wales coast	North Wales	160	3.6	576	RWE Npower Renewables
Lincs	8km off Skegness	East of England	75	3.6	270	Centrica/ DONG & Siemens Project Ventures
London Array I	24km off Clacton-on-Sea	Thames Estuary	175	3.6	630	DONG Energy / E.On Renewables / Masdar
London Array II	24km off Clacton-on-Sea	Thames Estuary	166	2.3*	370	DONG Energy / E.On Renewables / Masdar
Teesside	1.5km NE Teesmouth	North East	27	2.3	62.1	EdF
Walney II	14km Walney Island, Irish Sea	North West	51	3.6	183.6	DONG Energy & SSE Renewables
West of Duddon Sands	N. Irish Sea	North West	160	3.6	500	Scottish Power/DONG Energy
Totals			**814**		**2,591.7**	

Table 4. Approved offshore wind farms in the UK [76].

*The data is unknown. Calculation by 370/166.

Offshore wind energy is expected to be a major contributor towards the Government's 2020 target for renewable generation, and is being taken increasingly seriously by the UK energy sector. Round 2 of offshore tenders from the Crown Estate with a total of 7.2 GW applications, equivalent to 7% of UK supply [76]. With the high-speed development of offshore wind projects, the total power of Round 3 will reach to 32.2 GW. Also the round 1, 2 and 3 offshore wind project sites are shown in Appendix.

3.2.3 Advantages of MTDC

"An MTDC network embedded in a large AC grid can offer more economical utilization of DC transmission lines as well as greater flexibility in power dispatch and stabilisation of AC transmission system" [9]. In comparison with conventional point-to-point HVDC systems, a MTDC network for offshore system offers the following advantages,

- The flexible power flow control - Increased availabilities of the network [1, 10]
- Fewer negative effects than point-to-point HVDC to the entire system when one terminal lost [10, 11]
- MTDC required a less number of converter units than that of point-to-point HVDC [9]
- Easy connection of a new offshore load/generation terminal [12, 14]

3.3 Control strategy of Multi-terminal HVDC networks

Although the development of MTDC transmission is only at the starting stage, the control method of MTDC has been discussed widely by many researchers. Basically, there are two different control methods, “Master-Slave” and “Coordinated control”, which have been proposed for MTDC.

a) Master-slave

The control principles of two-terminal was extended to multi-terminal initially. The obvious difference between two-terminal and multi-terminal is that the master controller was added based on the previous control scheme. The main purpose of adding master controller was to set a major control such as start or stop and deciding power flow direction. Then the local control variables were controlled by each terminal. It means that the active and reactive power, DC and AC voltage were controlled respectively by each terminal. Fig. 3.3 shows the control scheme of Master-slave. Particularly, the ‘voltage margin method’ has been developed in [77]. Within the specific control system, one of VSCs controlled the DC bus voltage by providing a V_{dc} reference. The other VSCs controlled the active power by giving power reference point which can be constant or assigned by the master controller [78]. In [79, 80], a specific modified approach which mixed voltage margin method and DC voltage droop control has been used for reliable operation of MTDC to reduce the requirement of communication.

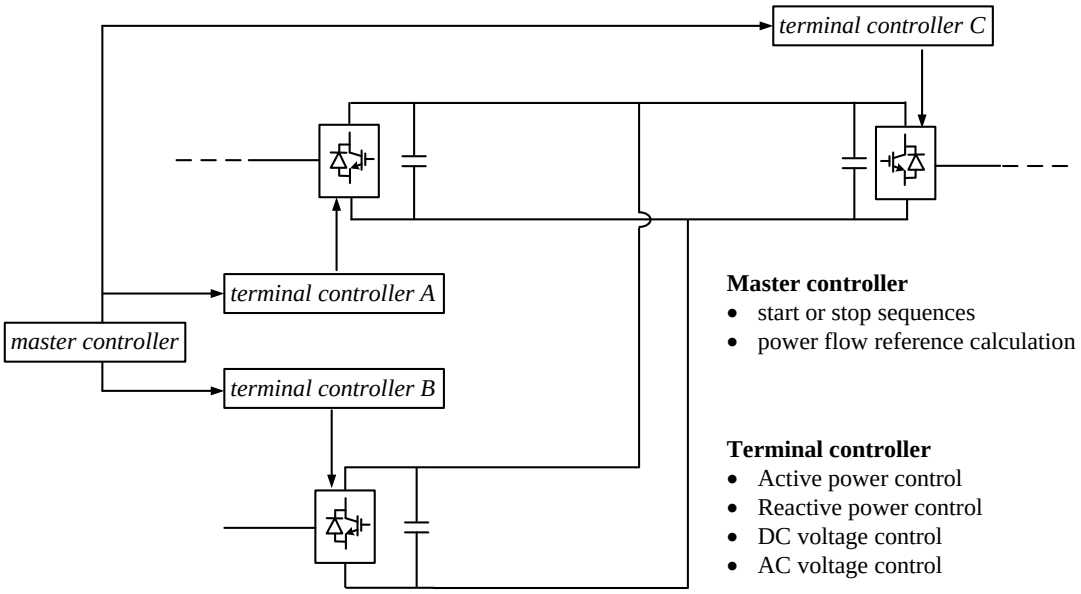

Fig. 3.3 Master-slave control scheme [77].

b) Coordinated control

More recently a coordinated approach between all terminals of MTDC has been developed [81]. DC bus voltage and power delivery were controlled by VSCs within a coordinated way. Initially, the coordinated control often employed one specific terminal to control DC voltage and the other VSCs controlled active power individually. In [82], this approach has been verified. Also the system with this approach was able to keep the steady state voltage even after one certain terminal was disconnected with suitable limit by simulation. Gradually, more and more researchers focused on droop-based technology with coordinated control [83, 84]. The typical characteristic of droop-based technology is that each VSC was given a linear relationship between DC voltage and income power. For instance, the Fig. 3.4 shows the droop control scheme. The DC voltage reference V_{ref}* was generated by the sum of initial voltage V_0, which is 95% of V_{ref}* value, and the coefficient K times DC current I_{dc}. With the droop-based technology, it is unnecessary to add communication system. However, due to the different voltages and currents in the MTDC and also the

requirement of the optimum operation point of the overall system [78], communication is needed for coordinated control of highly complex MTDC system.

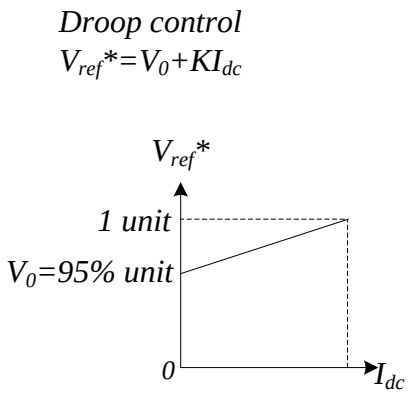

Fig. 3.4 Droop control scheme [83].

The overview of control strategy has been discussed in [85, 86]. Moreover, other control methods and related optimization such as optimal coordinated control, design of H∞ controller, parameters optimization and adaptive control design for MTDC were introduced in [87,88-90].

3.4 Challenges

3.4.1 Voltage/power rating and power loss

Due to the rating limits of converters and cables, the voltage rating and power rating of present VSC transmission network are not more than ±350 kV and 1000 MW respectively. The voltage rating of LCC-CSC system is higher than VSC system. Although the present limits of LCC-CSC technology is ±800 kV, the maximum voltage rating is only ±500 kV. The main reason is present cable constraints. Within the continued development of material technology, the cable constrain is going to be reduced. Therefore, the voltage rating of the VSC technology is able to rise in the future. However, it is still not able to reach to the level of the LCC-CSC converters. It is expected that the Modular Multilevel Converter (MMC) developed by Siemens and other technology such as series connected modular converter are able to increase the voltage rating level. Additionally, "the continued development of MI (mass impregnated) and extruded cable types is needed to improve the capacity of cables in line with converter ratings" [81].

Regarding losses of MTDC transmission system, converter losses are been highly focused because the losses in over head line or cable are much less than the losses of converters. In VSC-MTDC transmission system, IGBTs are core semiconductors of converters which mainly decide the losses of converter. The losses of IGBTs consist of three parts, which are conduction loss, switching loss and blocking loss. The blocking loss is only a very small part which is been neglected normally. Conduction losses is the main part of losses, however, the conduction loss for LCC-CSC and

SCC-VSC (Self Commutated Converter) transmission system is almost the same. Therefore, the comparison of switching loss for LCC-CSC and VSC is the key part. In VSC transmission system, the two level PWM with high frequency leads to high associated switching loss whose typical value is 3% [91]. Therefore, compared with switching loss of classic LCC-CSC transmission system, the power losses of VSC system are much higher. Recently, multi-level topologies have been developed. The new topologies are able to minimize the switching loss by stepping through multiple voltage levels and relative low switching frequency. Although the multi-level topologies have been developed for VSC transmission system, it is not able to reduce the losses of VSC transmission system to 1% which is the typical value of LCC-CSC transmission system [91]. The potential opportunities of reducing loss for VSC-MTDC are using new semiconductor materials and improvement of converter topologies [81].

3.4.2 Control design and coordination

In MTDC network, control system design should follow the requirements of entire network. Normally, controlling of voltage and power (active & reactive) are considered first in control design. Moreover, the control system is been required to control the network when the fault occurred and also recover the network automatically after the fault cleared. In different MTDC, different control strategy need be considered to achieve the above requirements. Additionally, in future large scale MTDC, the mix control strategy is to be more considered because single control method can not achieve the complex control task simply. The communication between each terminal is considered to use in future large scale MTDC even if coordination

control involved such as droop control. Therefore, the control scheme needs to be defined.

3.4.3 Protection and circuit breakers

The direct method to protect the MTDC transmission system when faults occur is to use direct current circuit breaker (DCCB) to isolate the faults. However, the technology of DCCB for high voltage system is not very mature. Based on the view of development of DCCB, it was at first designed for traction applications which operate at low voltage. Compared with AC circuit breakers, DCCBs are lack of a definitive point where the current falls to zero. It is the natural weakness of DC system which leads to hardly extinguish the arcs. In [66-68], electromechanical devices and solid state devices for DC fault have been discussed. With superimposing current zeros, electromechanical devices overcome the inherent weakness of DC system, but the cleaning times are not small enough. Solid state devices are excellent on very fast cleaning time by applying power electronics to block current [68].

In a large scale multi-terminal VSC-HVDC system, it is very difficult to protect the system and clear faults by exist DCCB technology. The main limit of DCCB is lack of very fast cleaning time with low loss and cost. In an MTDC system, the DC fault current increases extremely fast in very small time interval, which requires the DCCB also isolated the faults in extremely small time interval. Although the solid state circuit breaker obtains a very small cleaning time, however, the large loss and expensive cost are still problems which lead them to be abandoned at the design stage. With the development of material technology, the solid state circuit break is a

potential candidate for protection of MTDC transmission system.

3.5 Summary

This chapter focused on the multi-terminal HVDC networks. The definition and historic development of MTDC were presented. The opportunities of MTDC networks on offshore wind energy were discussed. It can be summarised that the MTDC has a bright future due to the huge developmental potential of offshore wind farm in the UK and also the natural advantages of MTDC. Then the control strategy for MTDC was presented. The challenges of MTDC were also discussed in the end of the chapter.

Chapter 4

Simulation and Laboratory Demonstration for a Three Terminal MTDC

4.1 Introduction of system structure

As shown in Fig. 4.1, a three-terminal MTDC system was built for simulation. It consisted of two permanent magnetic synchronous generators (PMSGs), two wind farm side voltage source converters (WFVSCs), one grid side voltage source converter (GSVSC) and grid connection. Two permanent magnet synchronous generators (PMSGs) were used to emulate two wind turbines; WFVSCs were simulated as offshore converters and GSVSC was simulated as onshore converter. All parameters of the system were shown in Fig. 4.1.

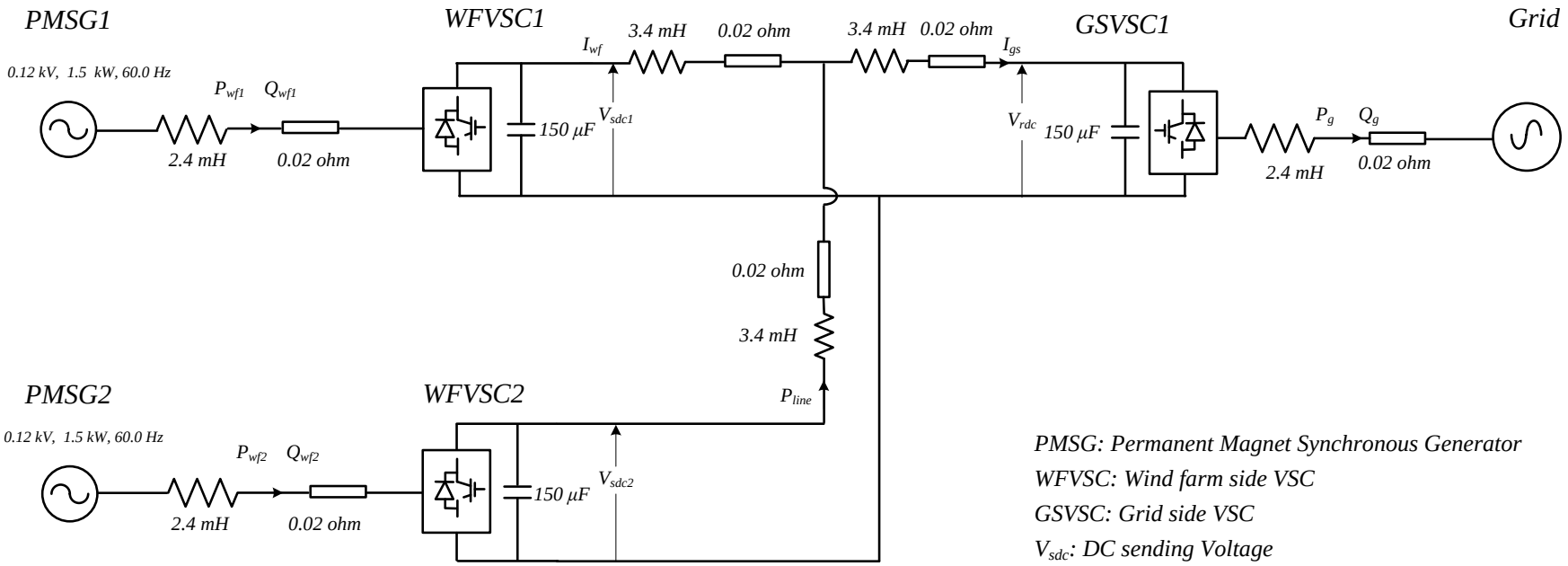

PMSG: Permanent Magnet Synchronous Generator
WFVSC: Wind farm side VSC
GSVSC: Grid side VSC
V_{sdc}*: DC sending Voltage*
V_{rdc}*: DC receiving Voltage*
P_{wf}*: Active Power of wind farm side*
Q_{wf}*: Reactive Power of wind farm side*
P_g*: Active Power of grid side*
Q_g*: Reactive Power of grid side*
P_{line}*: Active Power of line*
I_{wf}*: Wind farm side DC current*
I_{gs}*: Grid side DC current*

Fig. 4.1 System structure of a three-terminal VSC-HVDC system

4.2 Control system design

In a MTDC network for grid-connection of offshore wind power generation systems, different controllers must be designed for wind farm converters (offshore converters) and terrestrial grid converters (onshore converters). In this section, a control scheme based on three-terminal VSC-HVDC system was designed. The control scheme was introduced briefly first. Then the details of control method for each part were presented.

In Fig. 4.2, the control system consisted of two parts. The wind farm side VSCs were designed to maintain the voltage and frequency of the wind farm network at its reference values. It was designed to deliver all power from the wind turbines to the HVDC network. The grid side VSC was controlled to regulate the DC link voltage (V_{sdc} and V_{rdc}) of HVDC network. It ensured that the power collected from the wind farm VSC was transmitted to the grid side VSC, then to the grid AC network. The grid side VSC also supplied reactive power to the AC grid.

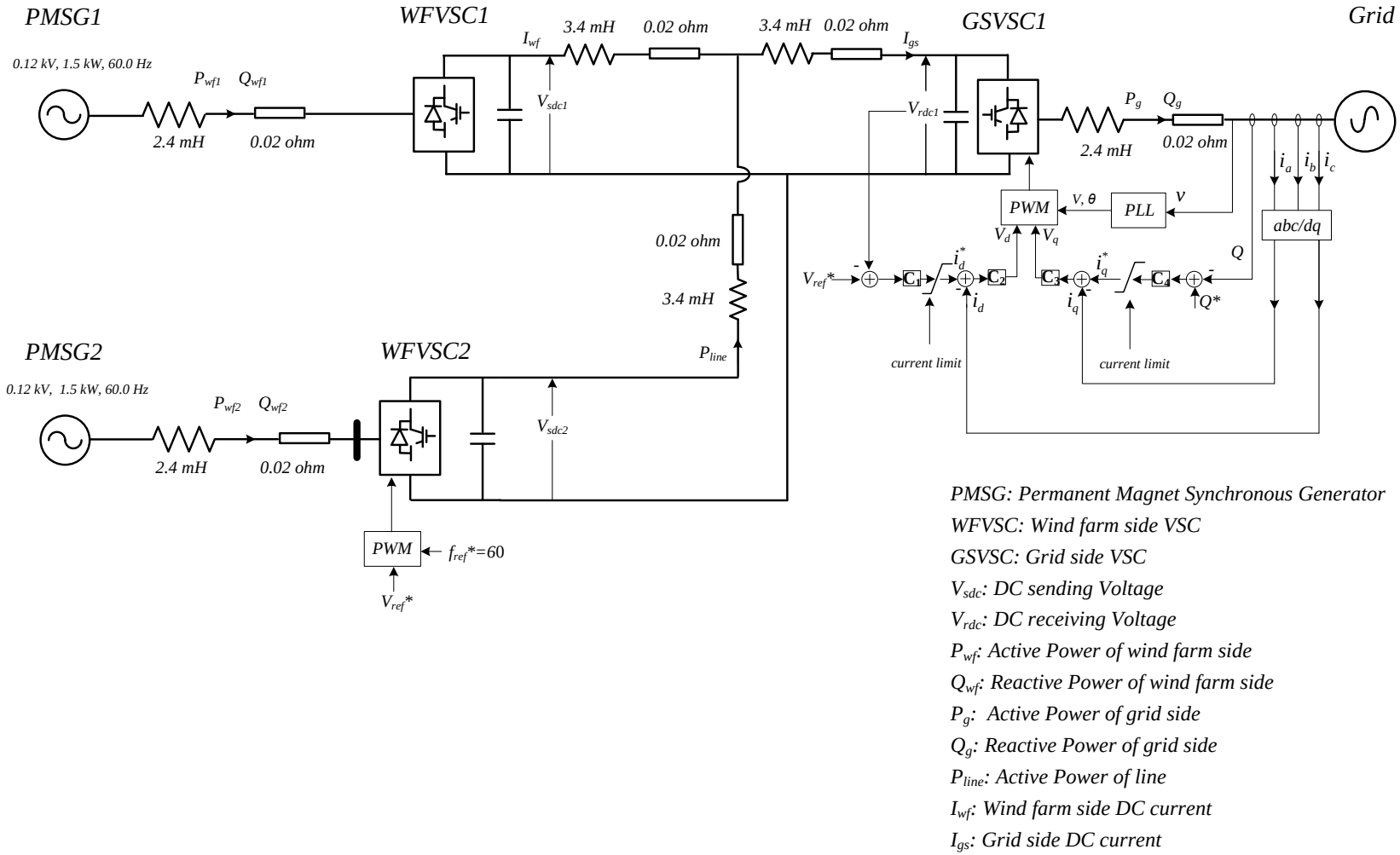

PMSG: Permanent Magnet Synchronous Generator
WFVSC: Wind farm side VSC
GSVSC: Grid side VSC
V_{sdc}: DC sending Voltage
V_{rdc}: DC receiving Voltage
P_{wf}: Active Power of wind farm side
Q_{wf}: Reactive Power of wind farm side
P_g: Active Power of grid side
Q_g: Reactive Power of grid side
P_{line}: Active Power of line
I_{wf}: Wind farm side DC current
I_{gs}: Grid side DC current

Fig. 4.2 Control system of a three-terminal VSC-HVDC system

120

4.2.1 Control system for wind farm side converter

The wind farm side VSC was designed to maintain the voltage and frequency of the wind farm network at its reference values. As shown in Fig. 4.3, by providing the reference voltage amplitude (V_{ref}*) and frequency (f_{ref}*), the VSC terminal was controlled as an infinite busbar for the wind farm network. Therefore, it was used to deliver all power from the wind turbines to the HVDC network.

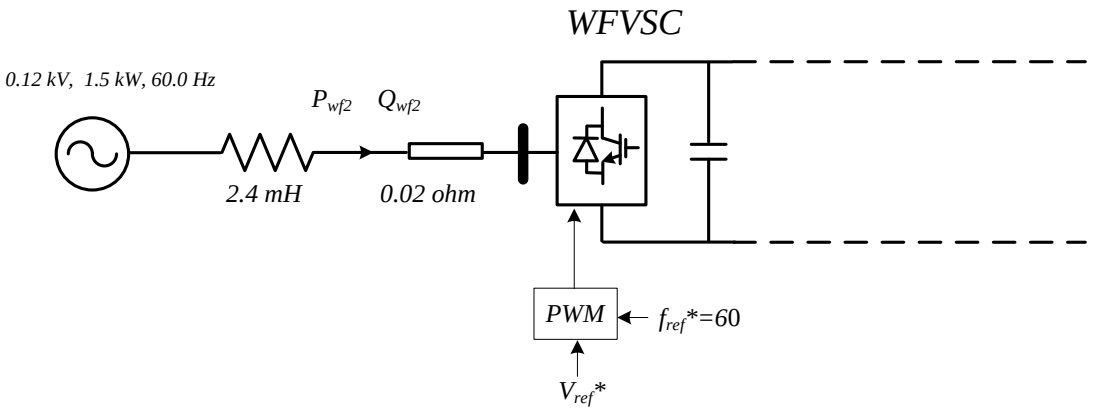

Fig. 4.3 Wind farm side VSC control diagram.

- *Voltage magnitude setting*: The magnitude of the wind farm side VSC voltage was maintained by providing the voltage reference (V_{ref}*), as shown in Fig. 4.4. The open–loop control method was used to maintain the busbar voltage equalled to 0.12 kV.

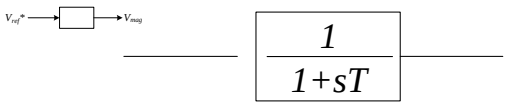

Fig. 4.4 Voltage magnitude setting section.

- *Phase angle setting:* Feeding a signal with 60 Hz to a re-settable integrator, the θ, which is the angle of wind farm side VSC voltage, was determined, as shown in Fig. 4.5. Then the re-settable integrator produced phase angle to a saw-tooth waveform between 0° and 360°.

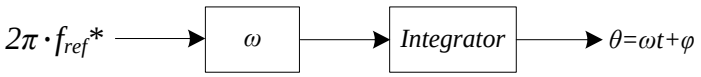

Fig. 4.5 Phase angle setting section.

- *VSC internal voltage calculation:* The wind farm side VSC voltage magnitude and phase angle were used to generate sine-wave signal V_{ins}, as shown in Fig. 4.6. The gate pulses of the wind farm side VSC were generated by feeding the sine-wave signal to a conventional sine-triangular Pulse Width Modulation (PWM) module. Then the WFSVC was controlled by the gate pluses.

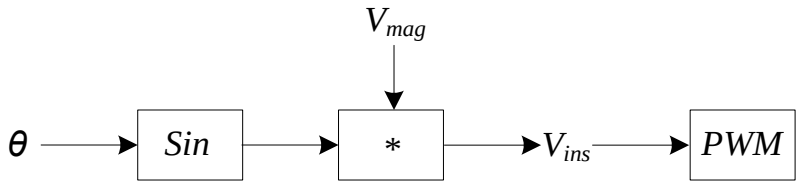

Fig. 4.6 VSC internal voltage calculation section.

4.2.2 Control system for grid side converter

The grid side VSC was controlled to regulate the DC link voltages, V_{sdc} and V_{rdc} of HVDC network, as shown in Fig. 4.7. It ensured that the power collected from the wind farm VSC was transmitted to the grid side VSC, then to AC network. The grid side VSC supplied reactive power injected into grid.

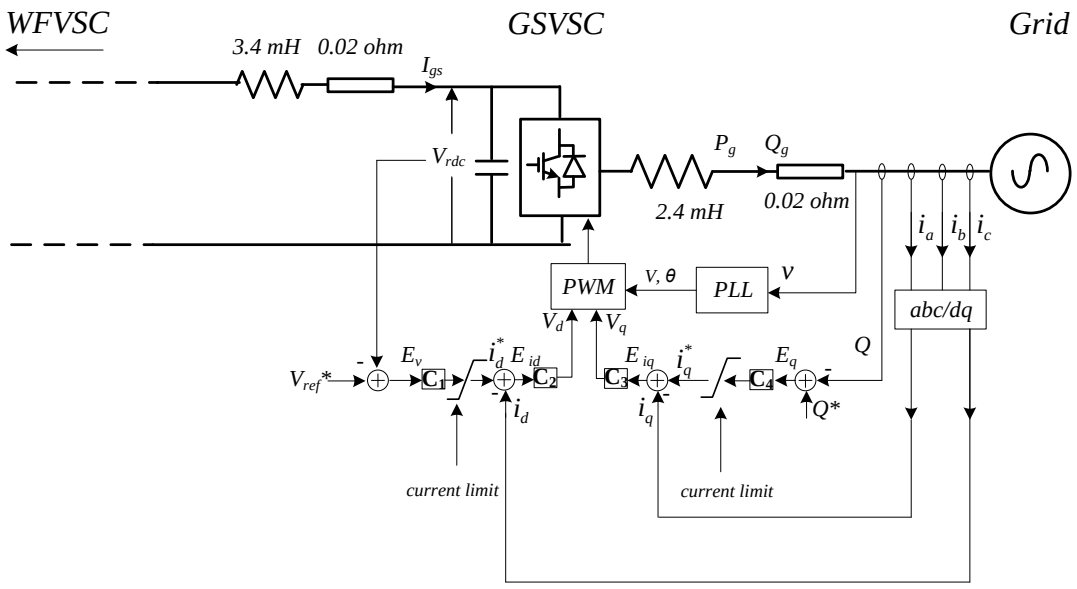

Fig. 4.7 Grid side VSC control diagram.

A Phase Lock Loop (PLL) was used to obtain the phase angle (θ) of the grid side VSC terminal voltage. By sending the phase angle to coordinate transformation of *abc* axis to *dq* axis, the instantaneous reference current i_d and i_q were obtained.

By providing the DC receiving voltage reference V_{ref}^* and compared with DC receiving voltage V_{rdc}, the DC link voltage error E_v was generated. Then the DC link voltage error E_v was regulated through PI controller C_1 to obtain current reference i_d^*. As same as E_v, the reactive power error E_q was obtained by comparing Q with the reactive power reference Q^*. Afterward, current reference i_q^* was obtained by sending E_q to PI controller C_4.

In order to obtain V_d, the current error E_{id}, which is the difference between the current reference i_d^* and instantaneous current i_d, was sent to PI controller C_2. Similarly, V_q was obtained by feeding current error E_{iq} to PI controller C_3. Then the sine-wave

signal for the PWM was created by using V_d, V_q and θ with dq inverse transform. By comparison of the sine-wave signal and triangular carrier signal, the errors were obtained. At last, gate pulses were generated.

4.3 Comparison of simulation and experimental results

4.3.1 Simulation environment and experimental configuration

The three-terminal MTDC system shown in Fig. 4.1 was simulated using PSCAD®/EMTDC. In simulation parameters, there were two turbines, each was of 120 V, 1.5 kW and 60 Hz. The inductance and impedance of each part were shown in Fig. 4.1. The DC receiving voltage reference V_{ref}* was set to 250 V, the reactive power reference Q* was set to 2 k VAr. The project of PSCAD/EMTDC was set to 9 seconds for Duration of Run, 1 μS for Solution Time Step and 100 μS for Channel Plot Step respectively. According to the circuits and control system shown in Fig. 4.2, the simulation was performed. The parameters and circuits of simulations were completely identical to the laboratory experiments.

In experiments, the two permanent magnet synchronous machines (PMSGs) were simulated as two wind turbines; each wind farm side VSC was three-phase, two-level, six-pulse configuration; also grid side VSC was the same configuration as wind farm side; the third PMSG was simulated as grid generator connection. There were two cabinets. Cabinet 1 was converter cabinet and cabinet 2 was machine drive cabinet. The voltage source converters for wind farm side and grid side were in cabinet 1; the circuit of drive modules for PMSGs were in cabinet 2. The system was implemented by MATLAB-Simulink-dSPACE. Therefore, the computer was connected with dSPACE Box. The overview diagram is shown in Fig. 4.8. The procedure of laboratory experiment was presented in Appendix II.

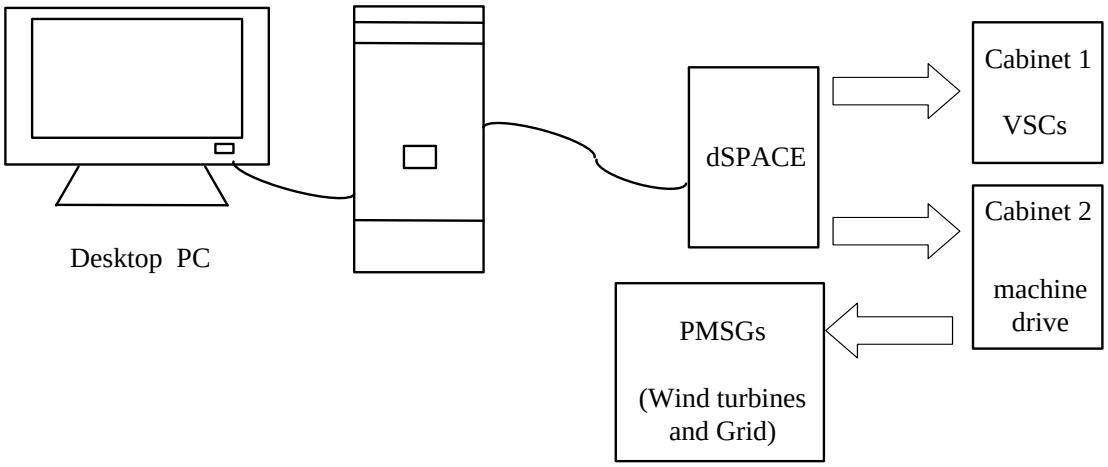

Fig. 4.8 Overview of laboratory configuration.

4.3.2 Comparison of results

The simulation was processed under two different simulation conditions. Case 1 and Case 2 as follows,

Case 1:

The output power of wind turbine 1 varied. It was 50% power (0.75 kW) during 1-3 seconds, and it increased from 50% to 100% power (1.5 kW) during 3-3.7 seconds, then it kept 100% power after 3.7 seconds.

The input power of wind farm 2 kept 100% power (1.5 kW).

Case 2:

The output power of wind farm 1 and wind farm 2 varied perfectively. They were 50% power (0.75 kW) during 1-3 seconds, and they increased from 50% to 100% power (1.5 kW) during 3-3.7 seconds, then they kept 100% power after 3.7 seconds.

The comparison results were shown as follows,

1. Comparison results of Case 1,

I. Comparison of active power

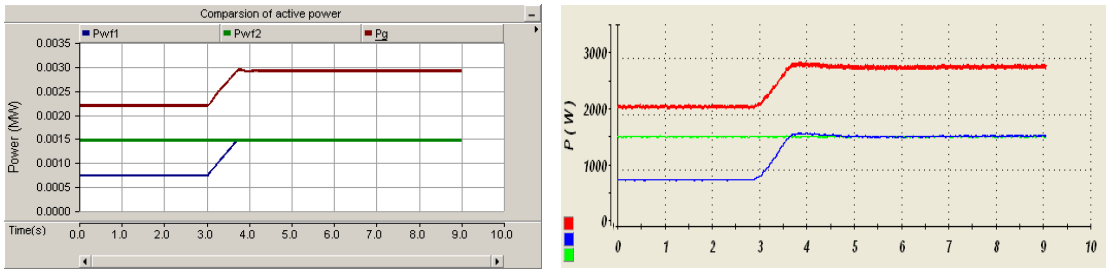

(a) (b)

Fig. 4.9 Active power by PSCAD simulation (a) and laboratory experiments (b).

Blue line - P_{wf1} (power of wind farm 1) - the bottom line
Green line - P_{wf2} (power of wind farm 2) - the mid line
Red line - P_g (power of grid) - the up line

As shown in Fig. 4.9, the results of simulation and laboratory experiment are the same. The three lines moved with the same movement. The power of gird increased from 2.25 kW to 3 kW during 3-3.7 seconds because the power of wind turbine 1 increased from 0.75 kW to 1.5 kW during 3-3.7 seconds. Due to the same output active power for wind turbine 1 and 2 from 3.7 seconds, the green line and blue line were overlap after 3.7 seconds.

II. Comparison of DC voltage

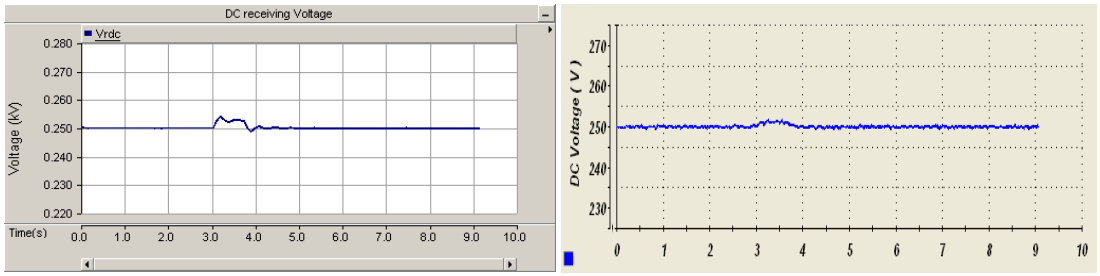

(a) (b)

Fig. 4.10 DC volage by PSCAD simulation (a) and laboratory experiment (b).

V_{rdc} = 250 V

As shown in Fig. 4.10 (a), the DC voltage was controlled at 250 V. Due to the power of wind turbine 1 increased from 0.75 kW to 1.5 kW during 3-3.7 seconds, DC voltage also changed with the same way. The DC voltage increased to 254.7 V at 3.23 seconds, which is 1.88% more than controlled nominal voltage. Then at 3.87 seconds, the DC voltage decreased to 249.2 V, which is 0.32% less than controlled nominal voltage. From the Fig. 4.10 (b), the DC voltage increased to 252.3 at 3.24 seconds, which is 0.92% more than controlled nominal voltage.

2. Comparison results of Case 2,

I. Comparison of active power

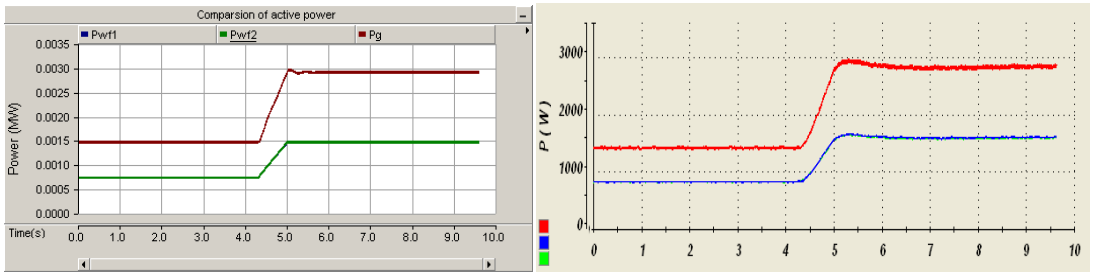

(a) (b)

Fig. 4.11 Active power by PSCAD simulation (a) and laboratory experiments (b).

Blue line - P_{wf1} (power of wind farm 1) - the bottom line

Green line - P_{wf2} (power of wind farm 2) - the mid line

Red line - P_g (power of grid) - the up line

As shown in Fig. 4.11, the results of simulation and laboratory experiment are the same. The three lines moved with the same movement. The power of gird increased from 1.5 kW to 3 kW during 4.3-5 seconds because the power of wind turbine 1 and 2 increased from 0.75 kW to 1.5 kW during 4.3-5 seconds. Due to the same trend for output active power of wind turbine 1 and 2, the green line and blue line were overlap from 0 - 9 seconds completely.

II. Comparison of DC voltage

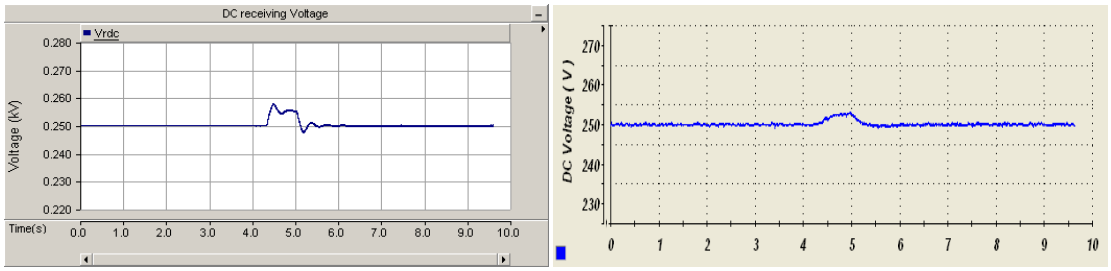

(a) (b)

Fig. 4.12 DC voltage by PSCAD simulation (a) and laboratory experiment (b).

V_{rdc} = 250 V

As shown in Fig. 4.12 (a), the DC voltage was controlled at 250 V. Because the power of wind turbine 1 and 2 increased from 0.75 kW to 1.5 kW during 4.3-5 seconds, DC voltage also changed. The DC voltage increased to 258.2 V at 4.45 seconds, which is 3.28% more than controlled nominal voltage. Then at 5.2 seconds, the DC voltage decreased to 247.8 V, which is 0.88% less than controlled nominal voltage. From the Fig. 4.10 (b), the DC voltage increased to 252.9 at 5 seconds, which is 1.16% more than controlled nominal voltage.

4.4 Summary

In this chapter, a three-terminal VSC-MTDC network has been built for simulation of offshore wind power transmission system. A control scheme was designed considering operating characteristics of voltage source converters and wind turbines. Controllers for wind farms and grid side were introduced respectively. Additionally, the results of simulation and laboratory demonstration were compared. Based on the comparison of results, it can be concluded that the control scheme for the three-terminal VSC-MTDC was effective and the control system worked successfully due to good parameters of controllers.

Chapter 5

Simulation of a Four Terminal MTDC

5.1 Introduction of control system

In a MTDC for grid-connection of offshore wind transmission system, different controllers must be designed for the wind farm converter (rectifier) and terrestrial grid converter (inverter). In addition, coordination among rectifier and inverter must be taken into consideration. In this section, a four-terminal VSC-HVDC system, as shown in Fig. 5.1, was used to demonstrate the control scheme design. The controllers for wind farm side VSCs (WFVSCs) were designed to control wind farm AC voltages to be constant. This allows all the power extracted from wind farm side injected to the HVDC network. The controllers for grid side VSCs (GSVSC) were designed to maintain the DC voltage and inject a certain amount of fixed reactive power to the AC grid. A droop control scheme designed for the DC voltage control was used to obtain coordination among different GSVSCs, in which DC voltage reference values were generated according to the DC current and the proportion coefficient K, as shown in Fig. 5.1. Additionally, coordinated control scheme was also designed at WFVSC. It was for reducing the output power of wind turbines when AC onshore fault occurred. Only one WFVSC controller and one GSVSC controller were given in Fig. 5.1.

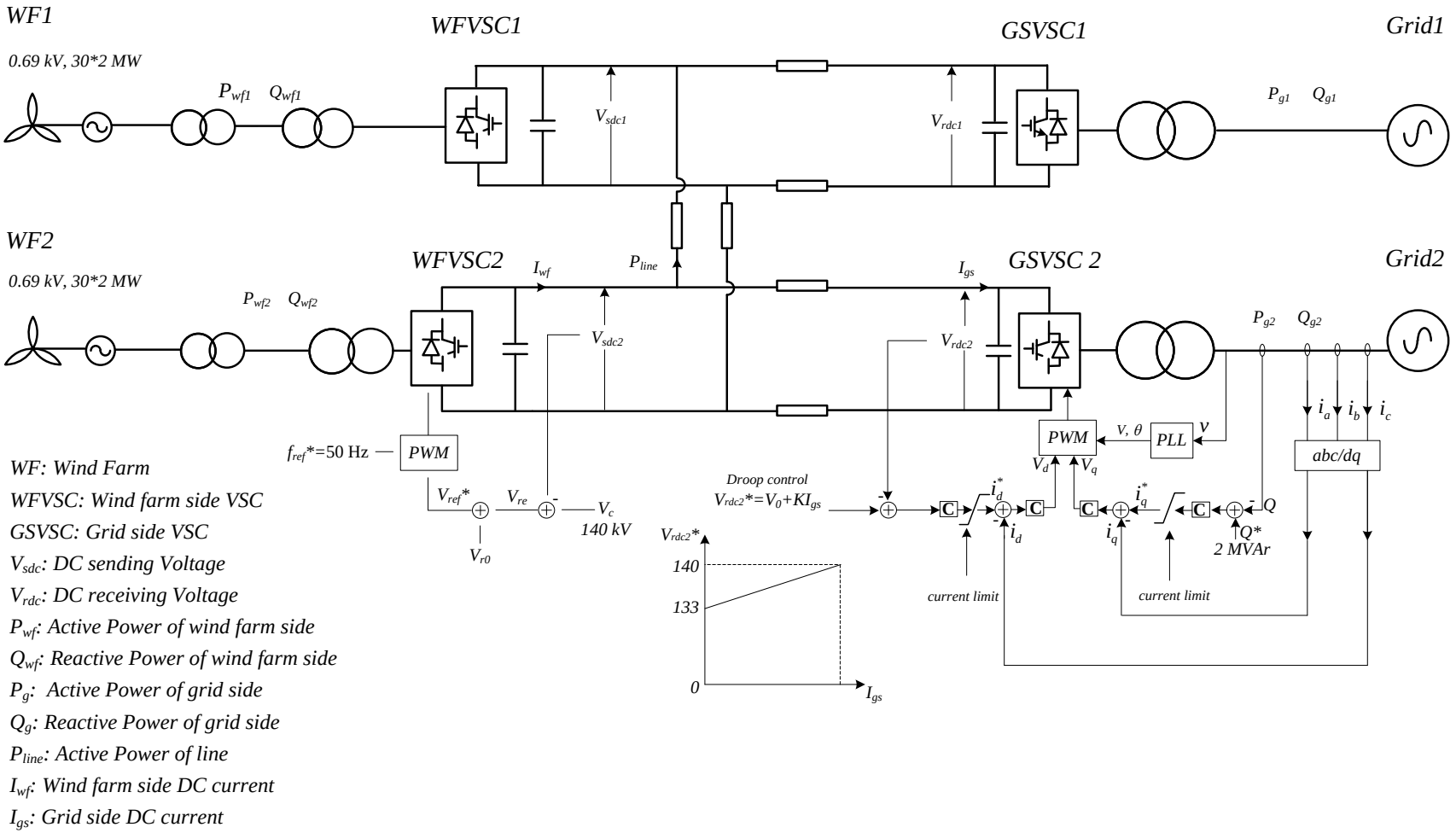

Fig. 5.1 Control system of four-terminal VSC-HVDC system.

5.1.1 Control system for wind farm side converter

The wind farm side VSC was designed to maintain the voltage and frequency of the wind farm network at its reference values. As shown in Fig. 5.2, by providing the reference voltage (V_{ref}*) and reference frequency (f_{ref}*), the VSC terminal was controlled as an infinite busbar (constant voltage and frequency) of the wind farm network. Therefore, it was able to deliver all power from wind turbines to the HVDC network.

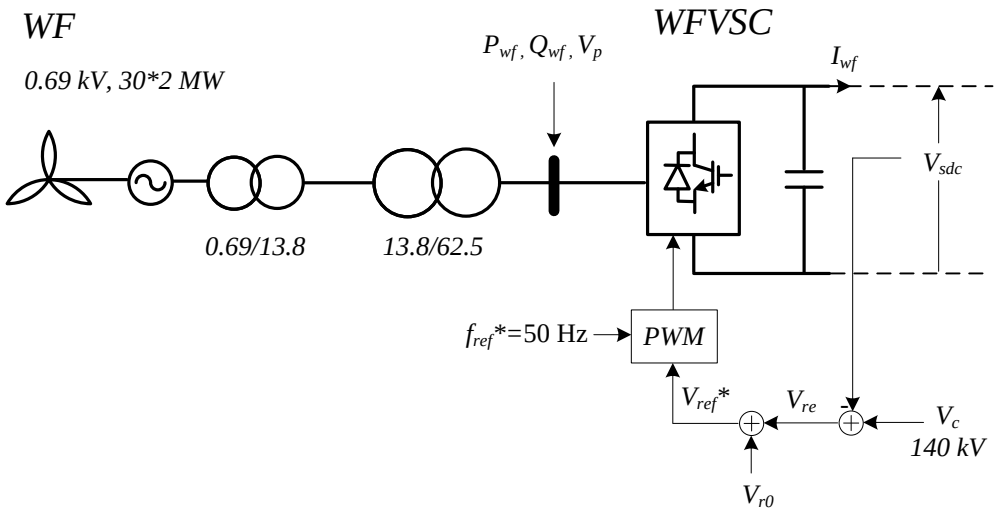

Fig. 5.2 Wind farm side VSC control diagram.

A coordinated control scheme for the entire network was considered by providing the voltage error (V_{re}) and voltage initial value (V_{r0}) to generate reference voltage (V_{ref}*). The loop of voltage error (V_{re}) was designed for fault ride-through strategy. When the system was under normal operation condition, the DC sending voltage (V_{sdc}) equals to the control target voltage (V_c) which made voltage error (V_{re}) equals to zero. Thus the voltage reference (V_{ref}*) equals to V_{r0}. The wind farm busbar voltage was controlled at 62.5 kV under normal operation conditions by setting V_{r0} = 62.5 kV. However, during

abnormal operation conditions (onshore faults occurred at grid side), the reference voltage (V_{ref}*) is influenced by the voltage error (V_{re}) and DC sending voltage (V_{sdc}). The following equations show how the coordinated control scheme works.

$V_{re} = V_{sdc} \times (-1) + V_c$……..Equation 5.1

$V_{ref}^* = V_{r0} + V_{re}$……..Equation 5.2

From the equation 5.1 and 5.2, we have

$V_{ref}^* = V_{r0} + (V_c - V_{sdc})$..……..……Equation 5.3

When the on shore faults occurred at the grid side, the overvoltage will make V_{sdc} equal to a very large value, which leads the ($V_c - V_{sdc}$) equal a minus value. The reference voltage (V_{ref}*) was reduced by summing voltage initial value (V_{r0}) and voltage error (V_{re}). Then the output power of the wind farm has been reduced.

The control signal for PWM was obtained by voltage magnitude and phase angle. This was obtained as follows:

- *Voltage magnitude*: The magnitude of the wind farm side VSC voltage was maintained by providing the voltage reference (V_{ref}*) through a first order lag section as shown in Fig. 5.3.

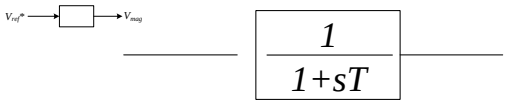

Fig. 5.3 Control signal magnitude setting.

- *Phase angle:* Feeding a signal with 50 Hz to a re-settable integrator, the θ, which is the angle of wind farm side VSC voltage, was determined, as shown in Fig.

5.4. Then the re-settable integrator produced a saw-tooth waveform between 0° and 360°.

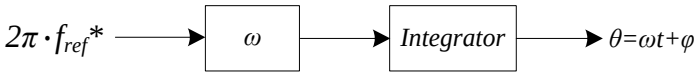

Fig. 5.4 Phase angle setting section.

The control signal was generated using the voltage magnitude and phase angle as shown in Fig. 5.5. The gate pulses of the wind farm side VSC were generated by feeding the control signal to a conventional sine-triangular Pulse Width Modulation (PWM) module. Then the WFSVC was controlled by the gate pluses.

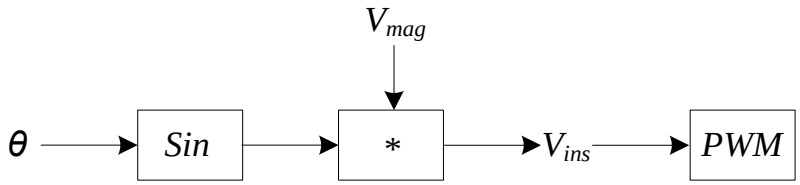

Fig. 5.5 VSC internal voltage calculation section.

5.1.2 Control system for grid side converter

The grid side VSC was controlled to regulate the DC link voltage (V_{sdc} and V_{rdc}) of HVDC network, as shown in Fig. 5.6. It ensured that the power collected from the wind farm side VSC was transmitted to the grid side VSC, then to AC network. The grid side VSC also supplied reactive power injected into grid.

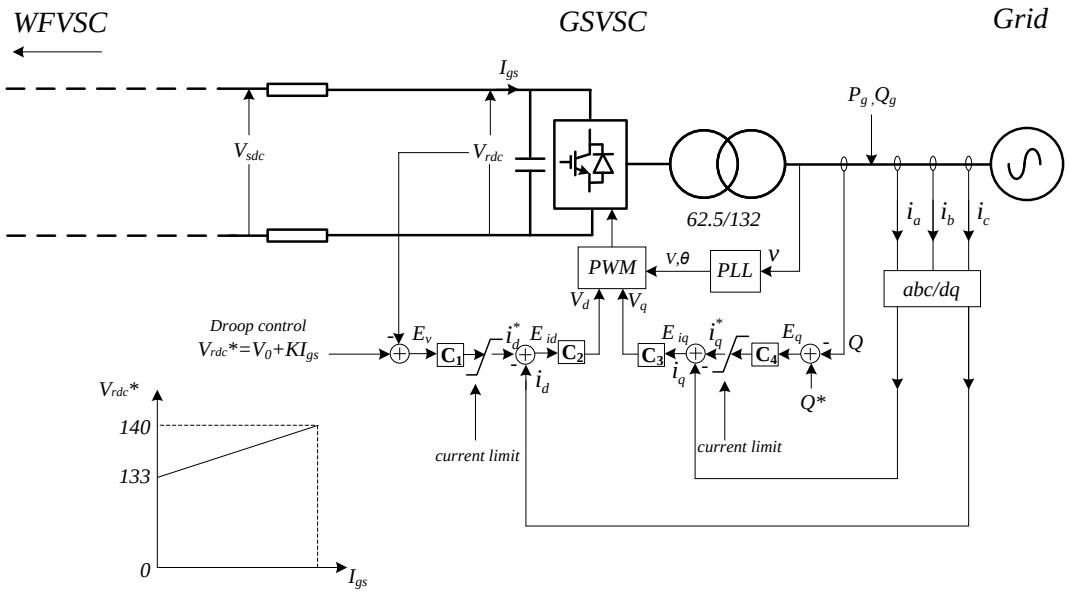

Fig. 5.6 Grid side VSC control diagram.

A Phase Lock Loop (PLL) was used to obtain the phase angle (θ) of the grid side VSC terminal voltage. By sending the phase angle to coordinate transformation of *abc* axis to *dq* axis, instantaneous reference current i_d and i_q were obtained.

With the droop control scheme based on the nominal voltage V_0 and the grid side DC current I_{gs}, the DC receiving voltage reference V_{rdc}^* was obtained. Then, the DC link voltage error E_v, which was generated by V_{rdc} and V_{rdc}^*, was regulated through PI controller C_1 to obtain current reference i_d^*. As same as E_v, the reactive power error E_q was obtained by comparing Q with the reactive power reference Q^*. Afterward, current reference i_q^* was obtained by sending E_q to PI controller C_4.

In order to obtain V_d, the current error E_{id}, which is the difference between the current reference i_d^* and instantaneous current i_d, was sent to PI controller C_2. Similarly, V_q was obtained by feeding current error E_{iq} to PI controller C_3. Then the control reference signal for the PWM was created by using V_d, V_q and θ with *dq* inverse

transform. By comparing the control reference signal and triangular carrier signal, the errors were obtained. Finally, gate pulses were generated.

5.2 Simulations

As shown in Fig. 5.1, the four-terminal VSC-HVDC system was simulated using PSCAD®/EMTDC™. There were two wind farms, each consists of thirty 690 V, 2 MW generators. To generate DC receiving voltage reference V_{rdc}*, V_0 was selected as 133 kV and K was selected as 20, Q* was set to 2 MVAr, the simulation was performed.

The parameters of the system under study were:

Wind turbine generator transformer 0.69/13.8 kV

Wind farm transformer 13.8/62.5 kV

Grid transformer 62.5/132 kV

The configuration of the WFVSC1 and GSVSC1 were identical to WFVSC2 and GSVSC2.

5.3 System performance during normal condition

Fig. 5.7 shows the simulation results for the system under the normal operating condition with 50% power injected from wind farm 1 between 0-5 s, 100% power injected between 5-8 s and 50% power injected between 8-12 s, and the wind farm 2 provided 100% power to the system.

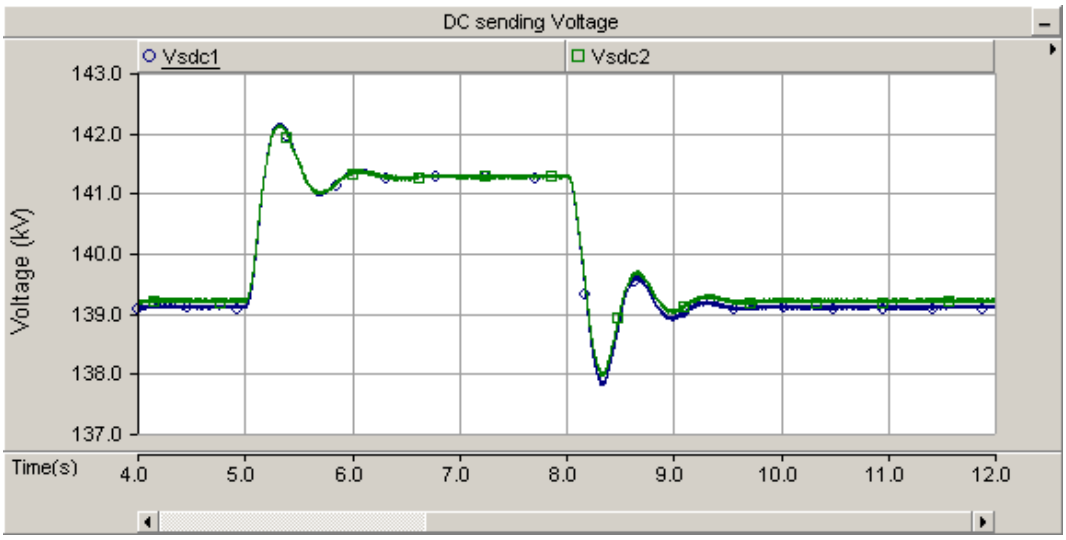

(a) DC sending voltage

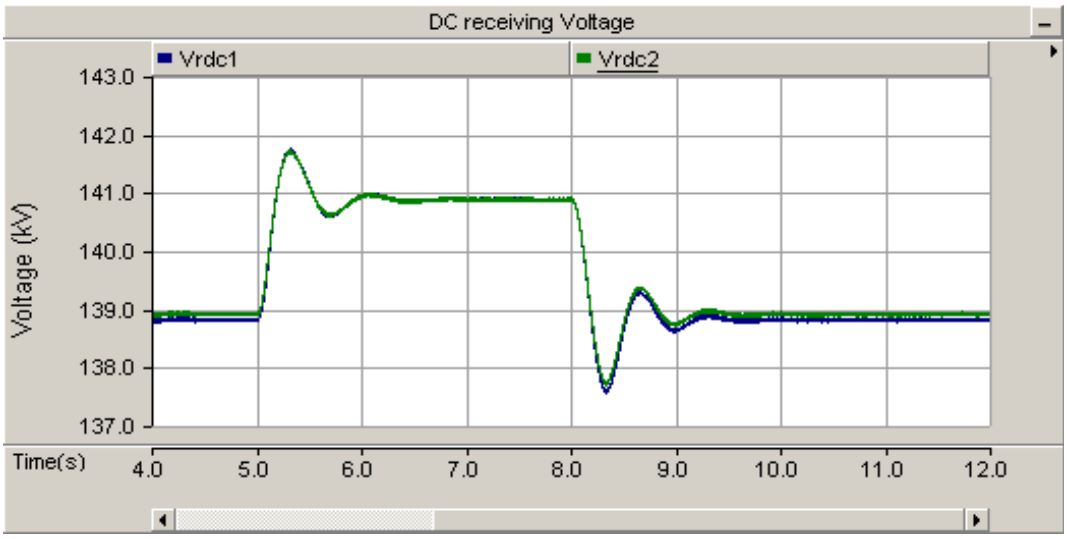

(b) DC receiving voltage

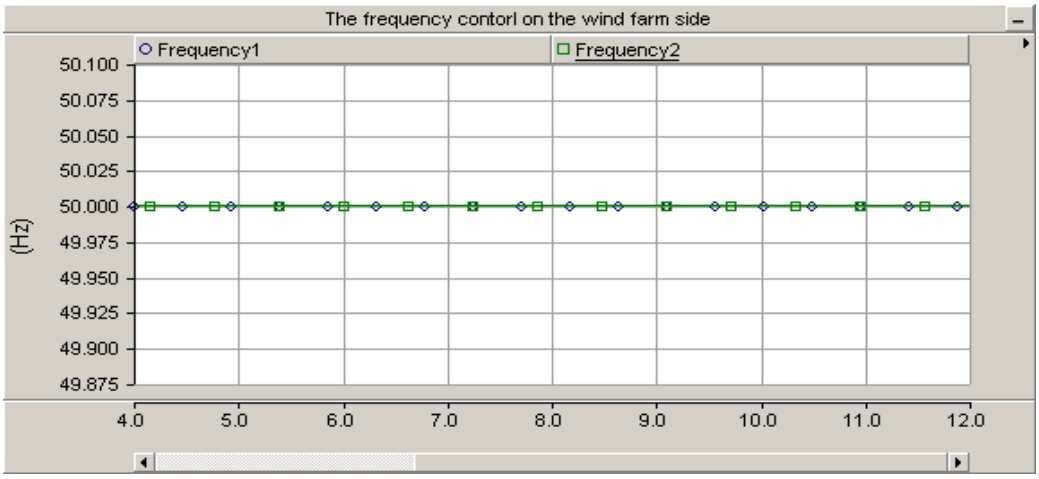

(c) Frequency of the wind farm side

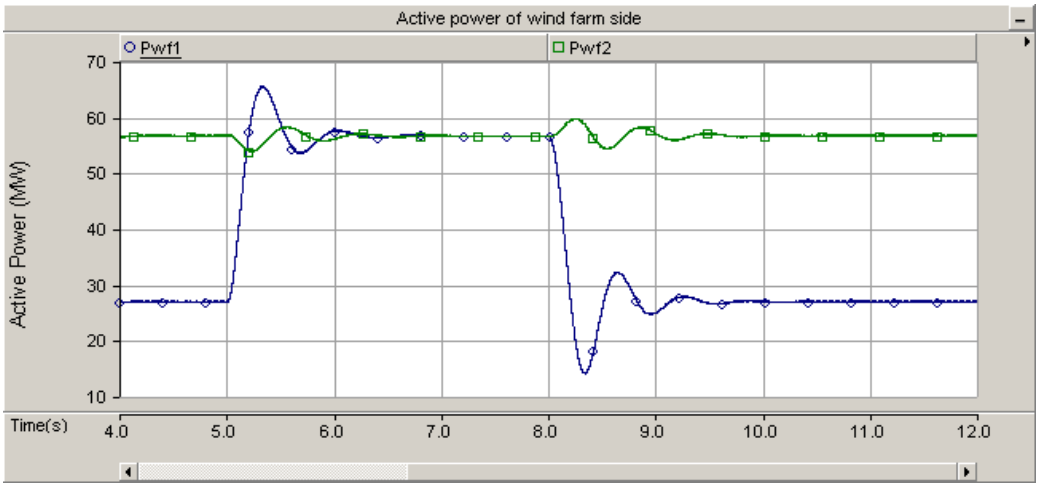

(d) Active power of wind farm side

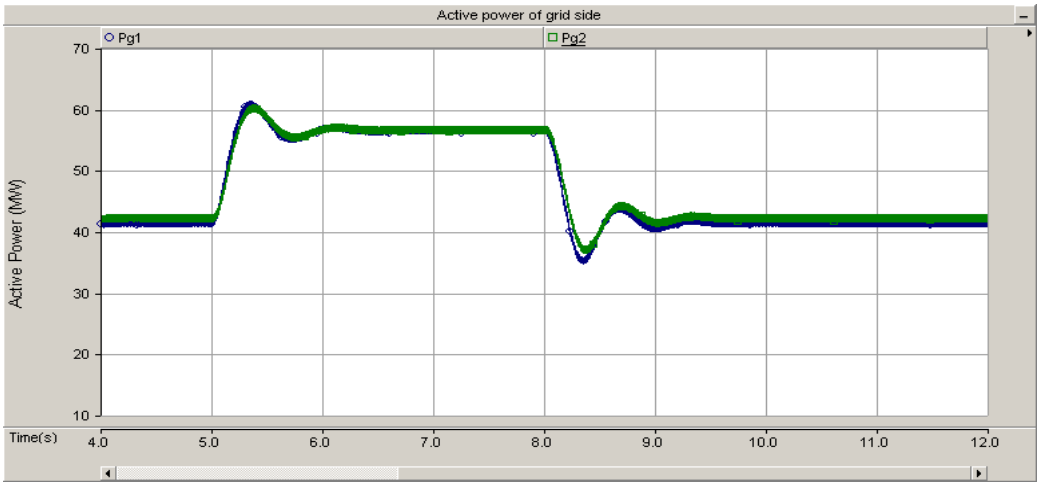

(e) Active power of grid side

Fig. 5.7 Results of normal operation condition.

As illustrated in Fig. 5.7 (a), (b) and (c), the DC sending voltage, DC receiving voltage and frequency of the wind farm network were controlled at set values when the input power varied from 50% to 100% of wind farm 1. With this step change of active power of wind farm 1, the system was showing good dynamic performance. The dynamic response performance indices, which are overshoot, peak time, rise time and settling time, were satisfactory. For instance, the system dynamic response performance indices for power of gird 1 as follows,

σ %= (61.3-56.9)/56.9×100%= 7.73%

T_p= 5.35-5=0.35 s

T_r= 5.19-5.04= 0.15 s (10%-90% standard)

T_s= 6.18-5= 1.08 s ($\pm$5% standard)

As shown in Fig. 5.7 (e), the sum of active power was shared by grid side converters equally (41.5 MW, between 0-5 s and 9-12 s; 57.6 MW between 5-9 s).

5.4 System performance during fault condition

As shown in Fig. 5.8, a fault was applied near the grid side 1. It was assumed that prior to the fault both wind farms provided 100% power (60 MW). In this case, the AC three phase fault and AC single phase fault were discussed.

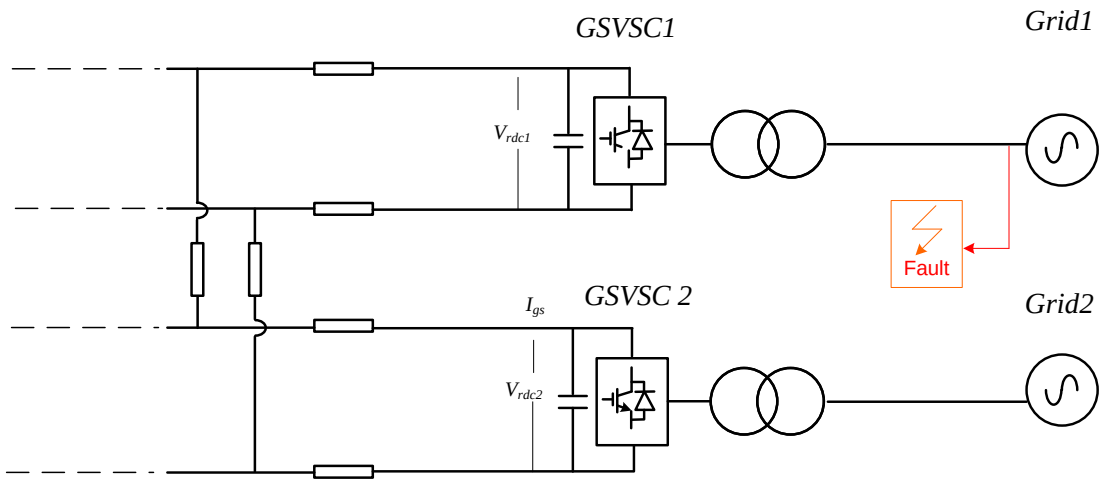

Fig. 5.8 Location of system fault.

5.4.1 Balanced fault - three phase fault

The AC three phase onshore fault was applied at 7 seconds for a duration of 0.2 seconds. As shown in Fig. 5.9, the DC sending and receiving voltages increased to 157 kV at 7 seconds, which was 11.35% more than controlled nominal voltage. After the fault, the DC sending and receiving voltage decreased to 138.5 kV at 7.23 seconds, which was 1.07% less than nominal control voltage. Due to the coordinated control scheme of wind farm side, the active power of wind farm side 1 and 2 reduced when the fault applied. The active power of wind farm 1 and 2 come back to their original values after the fault; the trend of active power of gird side 1 and 2 was completely different. Due to the fault applied near the grid side 1, the active power of the grid

side 1 drooped to 0 MW. However, the active power of wind farm 1 was delivered to the grid side VSC 2 by tie line during the fault. Therefore the active power of grid side 2 increased to 67 MW. The system recovered within 2 seconds. The power of tie line is shown in Fig. 5.9 (e).

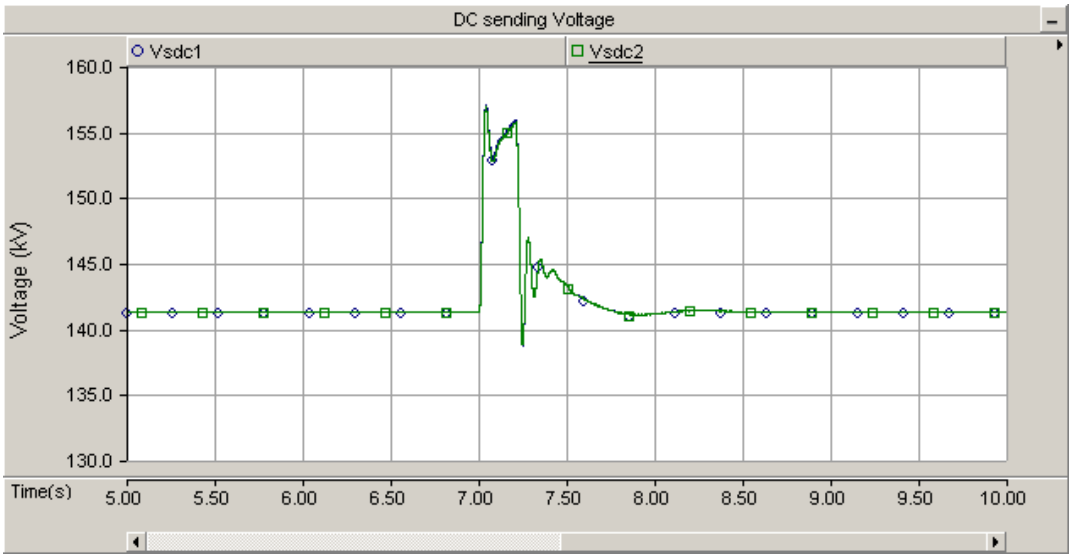

(a) DC sending voltage

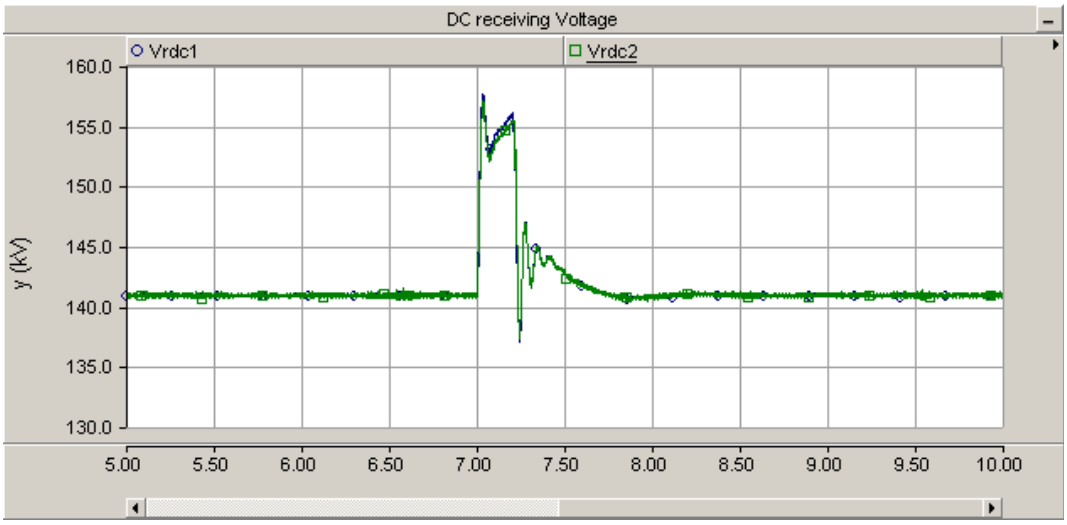

(b) DC receiving voltage

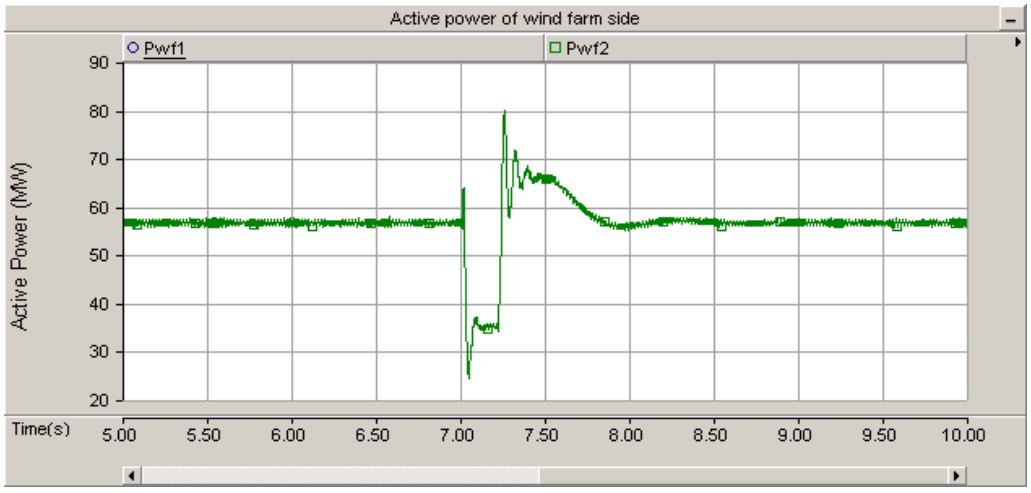

(c) Active power of wind farm side

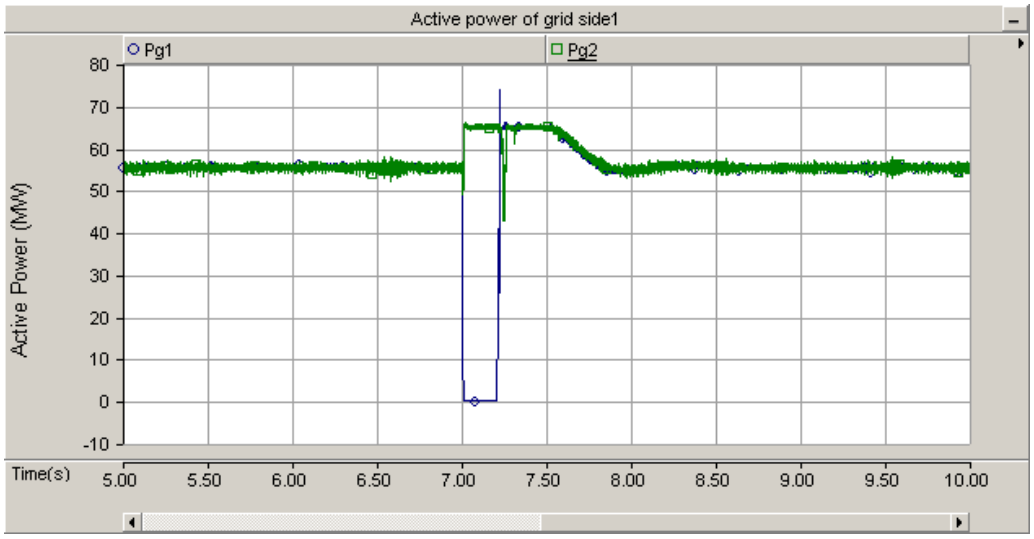

(d) Active power of grid side

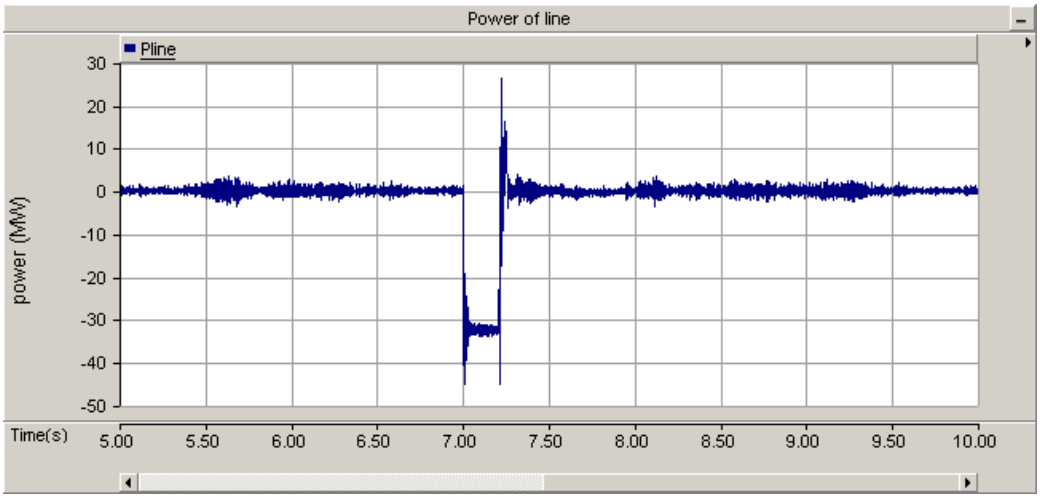

(e) Power of tie line

Fig. 5.9 Results of AC three phase fault.

5.4.2 Unbalanced fault - single phase fault

An AC single phase fault was applied at 7 seconds for a duration of 0.2 seconds. As shown in Fig. 5.10, the DC sending and receiving voltage of both HVDC transmission lines were maintained at 141 kV after the fault was cleared. The active power of wind farms were also maintained a constant value after the fault is cleared. The system recovered within 1 second and the steady-state error is 0.71%. The speed of regulation of all controllers was fast and the precision was acceptable. The power of tie line is shown in Fig. 5.10 (e).

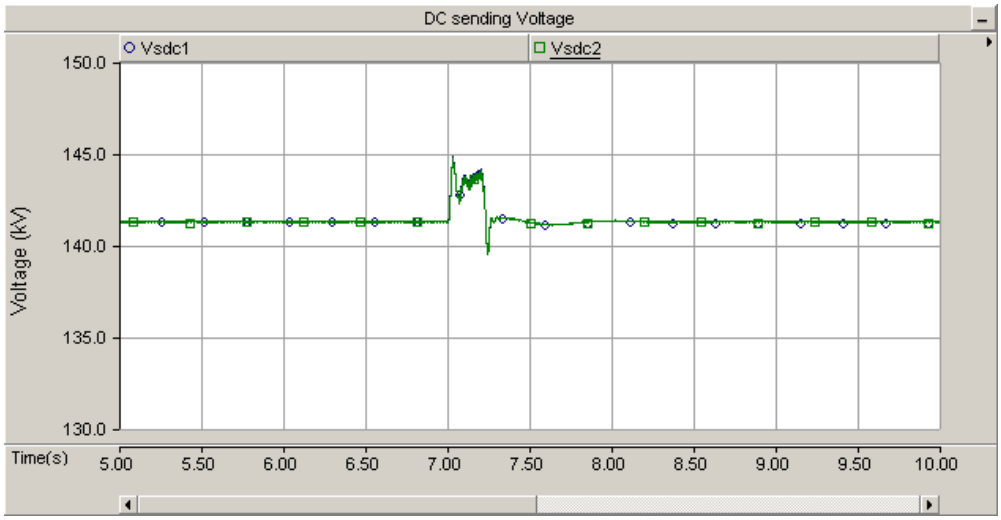

(a) DC sending voltage

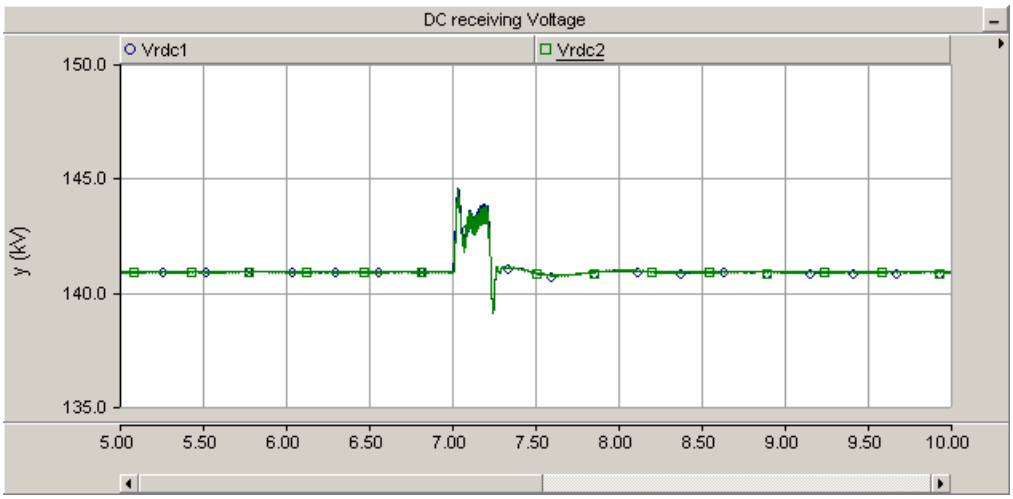

(b) DC receiving voltage

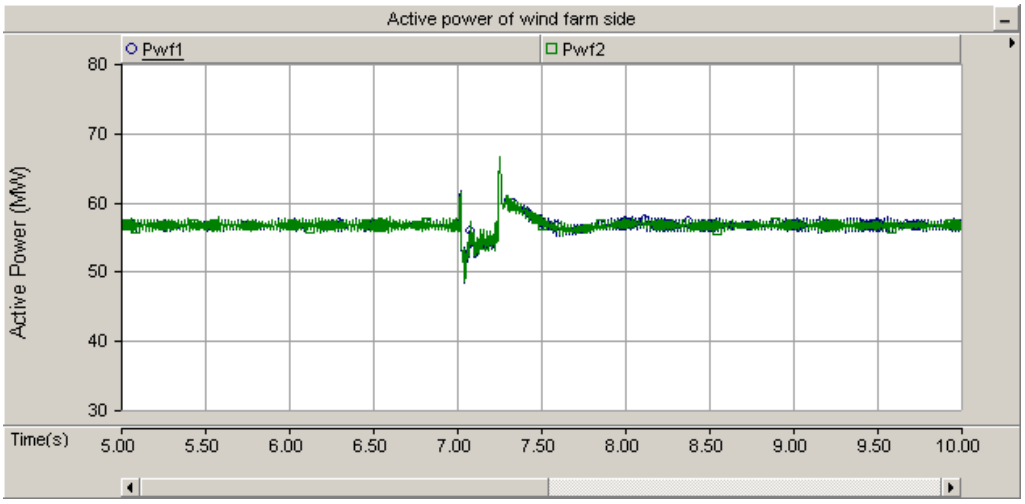

(c) Active power of wind farm side

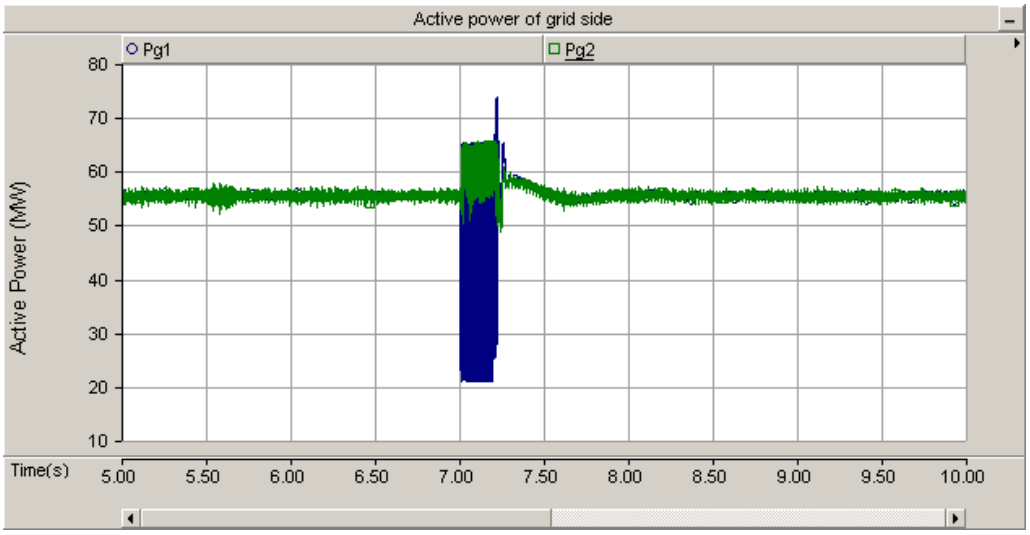

(d) Active power of grid side

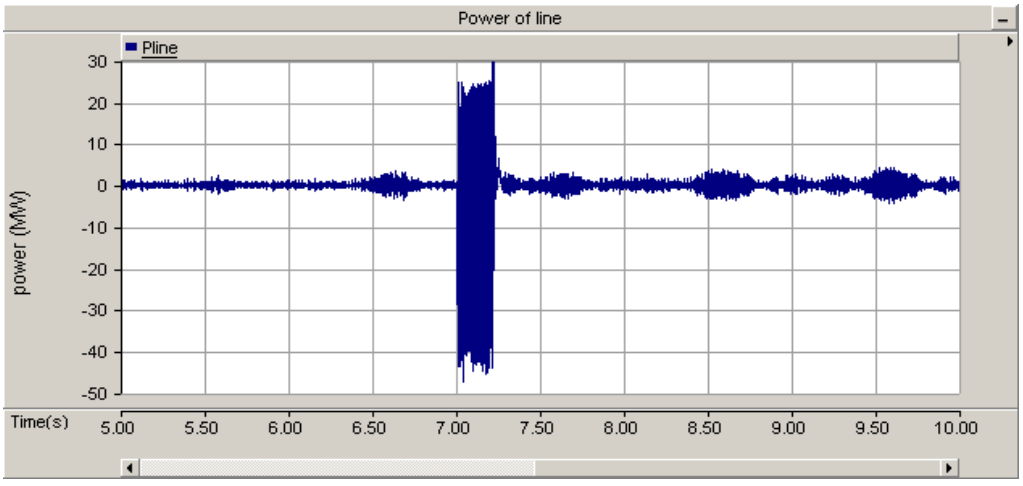

(e) Power of tie line

Fig. 5.10 Results of AC single phase fault.

5.5 Summary

A four-terminal VSC-HVDC transmission system was built for simulation of offshore wind power transmission network. A control system was designed considering operating characteristics of voltage source converters and wind farms. The open loop control method was used for wind farm side to establish a constant AC instantaneous voltage and frequency. A coordinated control scheme was considered. At wind farm side, the output power of wind farm was reduced by reducing reference voltage V_{ref}* when the system was under fault operation condition. At grid side, the droop control scheme was built for grid side VSCs to obtain automatic coordinating. Simulation results showed that good coordination was achieved among VSCs for voltage control and power sharing. The system maintained stability and presented good dynamic performance when subjected to the AC three phase fault and AC single phase fault on the grid.

Chapter 6

Conclusion and future work

6.1 Conclusion

The development and modelling of multi-terminal HVDC system for offshore wind power generation, its control system design and its operation under both normal and abnormal conditions were investigated.

First, a three-terminal MTDC system was investigated using simulations (using PSCAD/EMTDC) and experiments. The control strategy developed through simulation was verified using experiments. The results show the modelling and control strategy is successful.

Second, a four-terminal MTDC transmission system for offshore wind power generation was then simulated. Based on the operating characteristics of voltage source converters and wind farms, a control system was designed. An open loop controller was used at wind farm side. In order to obtain automatic coordination, droop control approach to generate DC voltage reference was used for the grid side VSCs. The good coordination was achieved among VSCs for voltage control and power sharing. The output power of wind farm was reduced by reducing reference voltage V_{ref}* when the system was under fault operation condition. The system was able to recover to the normal operation status automatically after the fault is cleared

when subjected to AC balanced fault (three phase fault) and unbalanced fault (single phase fault) on the grid.

6.2 Future work

Before the multi-terminal HVDC transmission for large offshore wind farms can be fully realised, there are a wide range of issues still remaining. The following are possible areas for further investigation,

- Design the robust control system for MTDC networks: Further studies into control strategies and types of controllers are possible research areas.

- Stability issues of MTDC transmission system: Eigen Value Analysis will be able to use for stability analysis.

- DC faults and protection: The faults in the DC system are serious concern. Fast switching solid-state circuit DC breaker is a possible solution.

- MTDC connecting weak AC systems: Any special requirements for the control system and protection system of MTDC when it is connected to a weak AC system are a possible research aspect in the future.

- Coefficient of determination: In Fig. 5.6, determination of the optimal coefficient K for the droop control to obtain the robust control system is possible research area.

References

[1] G. Asplund, K. Eriksson, and K. Svensson, "HVDC light—DC transmission based on voltage-sourced converters," *ABB Rev.*, vol. 1, pp. 4–9, 1998.

[2] G. Asplund, K. Eriksson, and O. Tollerz, "HVDC light: A tool for electric power transmission to distant load," *in Proc. VI Sepope Conf*., Salvador, Brazil, 1998, pp.1–7.

[3] G. Asplund, "Application of HVDC Light to power system enhancement," *in Proc. IEEE Power Eng*. Soc. Winter Meeting, 2000, pp. 2498–2503.

[4] U. Axelsson, A. Holm, C. Liljegren, M. Aberg, K. Eriksson, and O. Tollerz, "The Gotland HVDC Light Project—Experiences from trial and commercial operation," *in CIRED Conf*., Amsterdam, The Netherlands, 2001, pp. 1–5.

[5] K. Eriksson, "Operational experience of HVDC LIGHT," *in Proc. AC DC Conf. Transmiss.*, London, U.K., 2001, pp. 205–210.

[6] A. Petersson and A. Edris, "Dynamic performance of the Eagle Pass back-to-back HVDC Light tie," *in Proc. 7th Int. Conf. AC-DC Power Transmiss.*, London, U.K., 2001, pp. 220–225, (Conf. Publ. No. 485).

[7] T. F. Nestli, L. Stendius, M. J. Johansson, A. Abrahamsson, and P.C. Kjaer, "Powering Troll with new technology," *ABB Rev*., vol. 2, pp. 15–19, 2003.

[8] S. G. Johansson, L. Carlsson, and G. Russberg, "Explore the power of HVDC LIGHT—A Web based system interaction tutorial," *in Proc. IEEE PES Power Syst. Conf. Expo*., New York, 2004, pp. 839–842.

[9] Chan-Ki Kim, Vijay K. Sood, Gil-Soo Jang, Seong-Joo Lim and Seok-Jin Lee, "HVDC TRANMISSION-Power Conversion Applications in Power Systems."

2009: *IEEE Press*..

[10] N. Flourentzou, V. G. Agelidis and G. D. Demetriades, "VSC-Based HVDC Power Transmission Systems: An Overview," *IEEE Trans. On Power Electronics*, vol. 24, no. 3, pp. 592-602, Mar. 2009.

[11] K.R. Padiyar, "HVDC power transmission systems: technology and system interactions", *John Wiley & Sons Inc.*, ISBN: 0470217065, Sep. 1991.

[12] J. Arrillaga, "High voltage direct current transmission", *Institution of Electrical Engineers*, ISBN: 0852969414, October 1998.

[13] Y.H. Song and A.T Johns, "Flexible AC transmission systems (FACTS)", *Institution of Electrical Engineers*, ISBN: 0852967713, Nov. 1999.

[14] N.G. Hingorani and L. Gyugyi, "Understanding FACTS: concepts and technology of flexible AC transmission systems", *John Wiley & Sons Inc.*, ISBN: 0780334558, Feb. 2000.

[15] E. Acha, V.G. Agelidis, 0. Anaya-Lara and T.J.E. Miller, "Power electronic control in electrical systems", *Butterworth-Heinemann*, ISBN: 0750651261, Jan. 2002.

[16] R.M. Mathur and R.K. Varma, "Thyristor-based FACTS controllers for electrical transmission systems", *John Wiley & Sons Inc.*, ISBN: 0471206431, Feb. 2002.

[17] V.K. Sood, "HVDC and FACTS controllers: applications of static converters in power systems", *Kluwer Academic Publishers*, ISBN: 1402078900, 2004.

[18] L. Gyugyi, "Reactive power generation and control by thyristor circuits", *Industry Applications, IEEE Transactions on Volume:* IA-15, Issue: 5, 521-532.

[19] L. Gyugyi, "Control of shunt compensation with reference to new design concepts", *IEE Proc., Part C*: *Generation, Transmission and Distribution*, v 128, n 6, Nov. 1981, p 374-381. Vol 2, p. 1385-1388.

[20] L. Gyugyi, "Power electronics in electric utilities: static VAR compensators", *Proc. of the IEEE*, v 76, n 4, Apr. 1988, p.483-494.

[21] N.G. Hingorani, "Power electronics in future power systems", *Proc. of the IEEE*, v 76, n 4, Apr. 1988, p. 481-482. Systems, v 25, n 8, Sep. 2005, p 11-17.

[22] N.G. Hingorani, "FACTS-flexible AC transmission system", *IEE Conference Publication*, n 345, 1991, p. 1-7.

[23] L. Gyugyi, "Unified power-flow control concept for flexible AC transmission systems", *IEE Proc., Part C*: *Generation, Transmission and Distribution*, v 139, n 4, Jul. 1992, p. 323-331.

[24] N.G. Hingorani, "Flexible AC transmission", *IEEE Spectrum*, v 30, n 4, April 1993, p. 40-45.

[25] N.G. Hingorani and K.E. Stahlkopf, "High-power electronics", *Scientific American*, v 269, n 5, November 1993, p. 52-59.

[26] N.G. Hingorani, "FACTS technology and opportunities", *IEE Colloquium on "Flexible* AC *Transmission Systems (FACTS)-The Key to Increased Utilisation of Power Systems*" (Digest No.19941005), 1994, p. 4/1-10.

[27] L. Gyugyi, "Dynamic compensation of AC transmission lines by solid-state synchronous voltage sources", *IEEE Trans. on Power Delivery*, v 9, n 2, Apr. 1994, p. 904-911.

[28] N.G. Hingorani, "Future role of power electronics in power systems", *Proc. of IEEE International Symposium on Power Semiconductor Devices & ICs* (ISPSD) 1995, p 13-15.

[29] N.G. Hingorani, "High-voltage DC transmission: a power electronics workhorse", *IEEE Spectrum*, v 33, 4, April 1996, p. 63-72.

[30] R. Grunbaum, M. Noroozian and B. Thorvaldsson, "FACTS–Powerful systems

for flexible power transmission", *ABB Review*, n 5, 1999, p 4-17.

[31] N.G. Hingorani, "Future directions for power electronics", *Proc. Of IEEE PES Transmission and Distribution Conference*, v 2, 2001, p. 1180-1181.

[32] A. A. Edris, S. Zelingher, L. Gyugyi and L.J. Kovalsky, "Squeezing more power from the grid", *IEEE Power Engineering Review*, v 22, n 6, 2002, p 4-6.

[33] D. Povh, "Use of HVDC and FACTS", *Proc. of the IEEE*, v 88, n 2, 2000, p. 235-245.

[34] E.I. Carroll, "Power electronics for very high power applications", *ABB Review*, n 2, 1999, p 4-11.

[35] H. Akagi, "Large static converters for industry and utility applications", *Proceedings of the IEEE*, v 89, n 6, June 2001, p. 976-983.

[36] M. P. Bahrman, P.E., "HVDC Transmission Overview, Transmission and Distribution Conference and Exposition," 2008. *T&D. IEEE/PES*.

[37] "HVDC Light is the most interesting power transmission system developed for several decades", available from ABB, Industries and utilities, Power T&D Solutions, HVDC, HVDC Light *http://www.abb.com/industries/us/9AAC30300394.aspx?country=GB* ,accessed 05/08/2010.

[38] R. Rudervall, J.P. Charpentier, R. Sharma, "High Voltage Direct Current (HVDC)Transmission Systems Technology Review Paper," *Energy Week*, Washington, D.C, USA, March 7-8, 2000.

[39] G. Asplund , "Ultra high voltage transmission," *ABB Rev.*, vol. 2, pp. 22–27, 2007.K. Eriksson, "Operational experience of HVDC LIGHT," *in Proc. AC DC Conf. Transmiss.*, London, U.K., 2001, pp. 205–210.

[40] G. Asplund, K. Eriksson, and K. Svensson, "DC transmission based on voltage

source converters," *in Proc. CIGRE SC14* Colloq. South Africa, 1997, pp. 1–7.

[41] B. Andersen and C. Barker, "A new era in HVDC?" *Inst. Electr. Eng. Rev.*, vol. 46, no. 2, pp. 33–39, 2000.

[42] S L. Stendius and P. Jones, "The challenges of offshore power system construction-bringing power successfully to Troll A, one of the world's largest oil and gas platform," *in Proc. 8th Inst. Electr. Eng. Int. Conf.* AC DC Power Transmiss. (ACDC 2006), pp. 75–78.

[43] Y. H. Liu, L. B. Perera, J. Arrillaga, and N. R. Watson, "A back to back HVDC link with multilevel current reinjection converters," *IEEE Trans. Power Del.*, vol. 22, no. 3, pp. 1904-1909, Jul. 2007.

[44] M. Saeedifard, H. Nikkhajoei, R. Iravani, and A. Bakhshai, "A space vectormodulation approach for a multimodule HVDC converter system," *IEEE Trans. Power Del.*, vol. 22, no. 3, pp. 1643-1654, Jul. 2007.

[45] L. Xu and V. G. Agelidis, "VSC transmission system using flying capacitor multilevel converters and hybrid PWM control," *IEEE Trans. Power Del.*, vol. 22, CHALMERS UNIVERSITY OF TECHNOLOGY no. 1, pp. 693-702, Jan. 2007.

[46] V. G. Agelidis, A. I. Balouktsis, and M. S. A. Dahidah, "A five-level symmetrically defined selective harmonic elimination PWM strategy: Analysis and experimental validation," *IEEE Trans. Power Electron.*, vol. 23, no. 1, pp. 19-26, Jan. 2008.

[47] V. G. Agelidis, A. I. Balouktsis, and C. Cossar, "On attaining the multiple solutions of selective harmonic elimination PWM three-level waveforms through function minimisation," *IEEE Trans. Ind. Electron.*, vol. 55, no. 3, pp. 996-1004, Mar. 2008.

[48] J. L. Thomas, S. Poullain, and A. Benchaib, "Analysis of a robust DC bus voltage

control system for a VSC transmission scheme," *in Proc. 7th Int. Conf. AC-DC Power Transmiss.*, London, U.K., 2001, pp. 119-124, (Conf. Publ. No. 485).

[49] Z. Huang, B. T. Ooi, L. A. Dessaint, and F. D. Galiana, "Exploiting voltage support of voltage-source HVDC," *Proc. Inst. Electr. Eng. Gener., Transmiss. Distrib.*, vol. 150, no. 2, pp. 252-6, 2003.

[50] F. A. R. Al Jowder and B. T. Ooi, "VSC-HVDC station with SSSC characteristics," *IEEE Trans. Power Electron.*, vol. 19, no. 4, pp. 1053-1059, Jul. 2004.

[51] C. Du and M. H. J. Bollen, "Power-frequency control for VSC-HVDC during island operation," *in Proc. 8th Inst. Electr. Eng. Int. Conf. AC DC Power Transmiss.* (ACDC 2006), pp. 177-181.

[52] ABB Power Technologies AB, G.S.-H., *Its time to connect - Technical description of HVDC Light technology*. 2006.

[53] "HVDC PLUS (VSC Technology)" http://www.energy.siemens.com/hq/en/power-transmission/hvdc/hvdc-plus/, accessed 20/06/2011".

[54] A. Lesnicar, and R. Marquardt "An Innovative Modular Multilevel Converter Topology Suitable for a Wide Power Range," *Power Tech Conference Proceedings*, 2003 IEEE Bologna.

[55] C.C. Davidson and D.R.Trainer, "Innovative Concepts for Hybird Multi-Level Converters for HVDC Power Transmission," *IET 9th International Conference on AC and DC Power Transmission*, London, 2010.

[56] M.M.C. Merlin, T.C. Green, P.D. Mitcheson, D.R. Trainer, D.R. Critchley and R.W. Crookes, "A New Hybrid Multi-Level Voltage-Source Converter with DC Fault Blocking Capability," Paper 0017, *IET 9th International Conference on AC and DC Power Transmission*, London, 2010.

[57] C. C. Davidson, G. d. Préville, "The Future of High Power Electronics in Transmission and Distribution Power Systems," *The 13th European Conference on Power Electronic and Applications*, Barcelona, Spain, 2009.

[58] C. Feltes, H. Wrede, F. W. Koch and I. Erlich, "Enhanced Fault Ride-Through Method for Wind Fram," *IEEE Trans. on Power Systems*, vol. 24, no. 3, pp. 1537-1546, Aug. 2009.

[59] Ralph L. Hendriks, R. Völzke and W. L. Kling, "Fault Ride-Through Strategies for VSC-Connected Wind Parks," *Europe's premier wind energy event*, Parc Chanot, Marseille, France 16-19 Mar. 2009.

[60] M. E. Baran and N. R. Mahajan, "Overcurrent Protection on Voltage-Source-Converter- Based Multiterminal DC Distribution Systems," *IEEE Trans. on Power Systems*, Vol.22, No. 1, Jan. 2007.

[61] L. Tang and Boon-Teck Ooi, "Locating and Isolating DC Faults in Connected to the Grid Through VSC-Based HVDC Transmission," *IEEE Trans. on Power Systems*, Vol.24, No. 3, Aug. 2009.

[62] R. L. Hendriks, R. Volzke and W Multi-Terminal DC Systems," *IEEE Trans. on Power Systems*, Vol.22, No. 3, Jul. 2007.

[63] A. M. S. Atmadji and J. G. J. Sloot, "Hybrid switching: A review of current literature," *in Proc. IEEE Conf. Energy Manage. Power Del. (EMPD)*, Singapore, 1998, pp. 683–688.

[64] G. B. D. Lange and A. M. Chol, "Novel application of PWM switching for DC traction circuit breakers," *in Proc. IEEE Int. Conf. Power Syst. Technol. (PowerCon)*, 2006, pp. 1–6.

[65] T. Genji, O. Nakamura, M. Isozaki, M. Yamada, T. Morita, and M. Kaneda, "400 V class high-speed current limiting circuit breaker for electric power system,"

IEEE Trans. Power Del., vol. 9, no. 3, pp. 1428–1435, Jul. 1994.

[66] C. Meyer and R. W. D. Doncker, "LCC analysis of different resonant circuits and solid-state circuit breakers for medium-voltage grids," *IEEE Trans. Power Del.*, vol. 21, no. 3, pp. 1414–1420, Jul. 2006.

[67] C. Meyer and R. W. D. Doncker, "Solid-state circuit breaker based on active thyristor topologies," *IEEE Trans. Power Electron.*, vol. 21, no. 2, pp. 450–458, Mar. 2006.

[68] C. Meyer, S. Schroder, and R.W. D. Doncker, "Solid-state circuit breakers and current limiters for medium-voltage systems having distributed power systems," *IEEE Trans. Power Electron.*, vol. 19, no. 5, pp. 1333–1340, Sep. 2004.

[69] L. Tang and B. T. Ooi, "Protection of VSC-multi-terminal HVDC against DC faults," *in Proc. IEEE Annu. Power Electron. Spec. Conf. (PESC*), 2002, pp. 719–724.

[70] M. Takasaki, N. Gibo, K. Takenaka, T. Hayashi, H. Konishi, S. Tanaka, H. Ito "Control and protection scheme of HVDC system with self-commutated converter in system fault conditions*" IEE* Japan, Vol.118-B No.12, Dec, 1998.

[71] N. Gibo, K. Takenaka, "Protection scheme of Voltage Sourced Converters based HVDC system under DC fault" *Transmission and Distribution Conference and Exhibition 2002, Asia Pacific. IEEE/PES*, 6-10 Oct. 2002.

[72] TBC Trans Bay Cable, Available from *www.transbaycable.com/the-project* Accessed 25/09/09.

[73] J. Arrillaga, Y.H. Liu and N.R. Wsatson, "Flexible Power Transmission-The HVDC Options." 2007: *John Wiley & Sons Ltd Press*.

[74] DTI, "The Energy Challenge," *Energy Review Report 2006*, Presented to Parliament by the Secretary of State for Trade and Industry, 2006.

[75] EU action against climate change; EU emissions trading-an open scheme promoting global innovation. Available from *www.ec.europa.eu/index_en.htm*, Accessed 17/08/09.

[76] BWEA, Offshore Wind Farms, Operational, Available from *www.bwea.com/ukwed/offshore.asp* , Accessed 24/11/09

[77] T. Nakajima, and S. Irokawa "A control system for HVDC transmission by voltage sourced converters," *Power Engineering Society Summer Meeting, 1999*. IEEE Page(s):1113 - 1119.

[78] Olimpo Anaya-Lara, Nick Jenkins, Janaka Ekanayake, Phill Cartwright and Mike Hughes, "WIND ENERGY GENERATION - Modelling and Control" 2009: *John Wiley & Sons Ltd Press.*

[79] T. Haileselassie, M. Molinas and T. Undeland, "Control of Multiterminal HVDC Transmission for Offshore Wind Energy," *Nordic Wind Power Conference*, Bornholm, Danmark, Sept 2009.

[80] K.D. Brabandere, B. Bolsens, J.V.d. Keybus, A. Woyte, J. Driesen, R. Belmans and K.U Leuven, "A Voltage and Frequency Droop Control Method for Parallel Inverters," *IEEE Trans. on Power Electronics*, Vol. 22, Issue 4, Jul. 2007.

[81] L. Livermore, J. Liang and J.B. Ekanayake "MTDC VSC Technology and its applications for Wind Power", *in Proc*. 45th International Universities' Power Engineering Conference, *IEEE Conference*, Cardiff, United Kingdom, Sep. 2010.

[82] T. Haileselassie, M. Molinas and T. Undeland, "Multi-Terminal VSC-HVDC System for Integration of Offshore Wind Farms and Green Electrification of Platforms in the North Sea," *Nordic Workshop on Power and Industrial Electronics*, June 2008.

[83] S. Zhou, J. Liang, J.B. Ekanayake and N. Jenkins, "Control of multi-terminal

VSC-HVDC transmission system for offshore wind power generation", *in Proc*. 44th International Universities' Power Engineering Conference, *IEEE Conference*, Glasgow, United Kingdom, Sep. 2009.

[84] J. Liang, O. Gomis-Bellmunt, J. Ekanayake, and N. Jenkins, Control of multi-terminal VSC-HVDC transmission for offshore wind power," *13th European Conference on Power Electronics and Application*, Barcelona, Spain, September 2009.

[85] C. Du, A. Sannino and M. Bollen, "Analysis of the Control Algorithms of Voltage-Source Converter HVDC," Power Tech, *IEEE Conference*, Russia, Jun. 2005.

[86] Z. Hu, C. Mao, J. Lu and M. Chen "Genetic algorithm based control for VSC HVDC," Transmission and Distribution Conference and Exhibition: *Asia and Pacific*, Dec. 2005 IEEE/PES.

[87] G. Y. Li, M. Yin, M. Zhou and C. Y. Zhao "Decoupling Control for Multi terminal VSC-HVDC Based Wind Farm Interconnection," *Power Engineering Society General Meeting*, *IEEE*, 2007.

[88] S. Wang, G. Li, M. Zhou, Z. Zhang, "Research on Interconnecting Offshore Wind Farms Based on Multi-terminal VSC-HVDC," *Power System Technology (POWERCON)*, 2010 International Conference.

[89] W. Pan, Y. Chang, H. Chen, "Hybrid Multi-terminal HVDC System for Large," *Nordic Wind Power Conference*, Bornholm, Danmark, Sept 2009.

[90] J.M Mauricio and A.G. Exposito, "Modeling and Control of an HVDC-VSC Transmission System," *Transmission & Distribution Conference and Exposition*: Latin America, 2006. TDC '06. *IEEE/PES*

[91] CIGRE-Sc-B4 ed. 2009. "Which role will HVDC technology have in the future?"

Bergen Colloquium.

Appendices

Appendix I

Round 1, 2 and 3 offshore wind farm sites

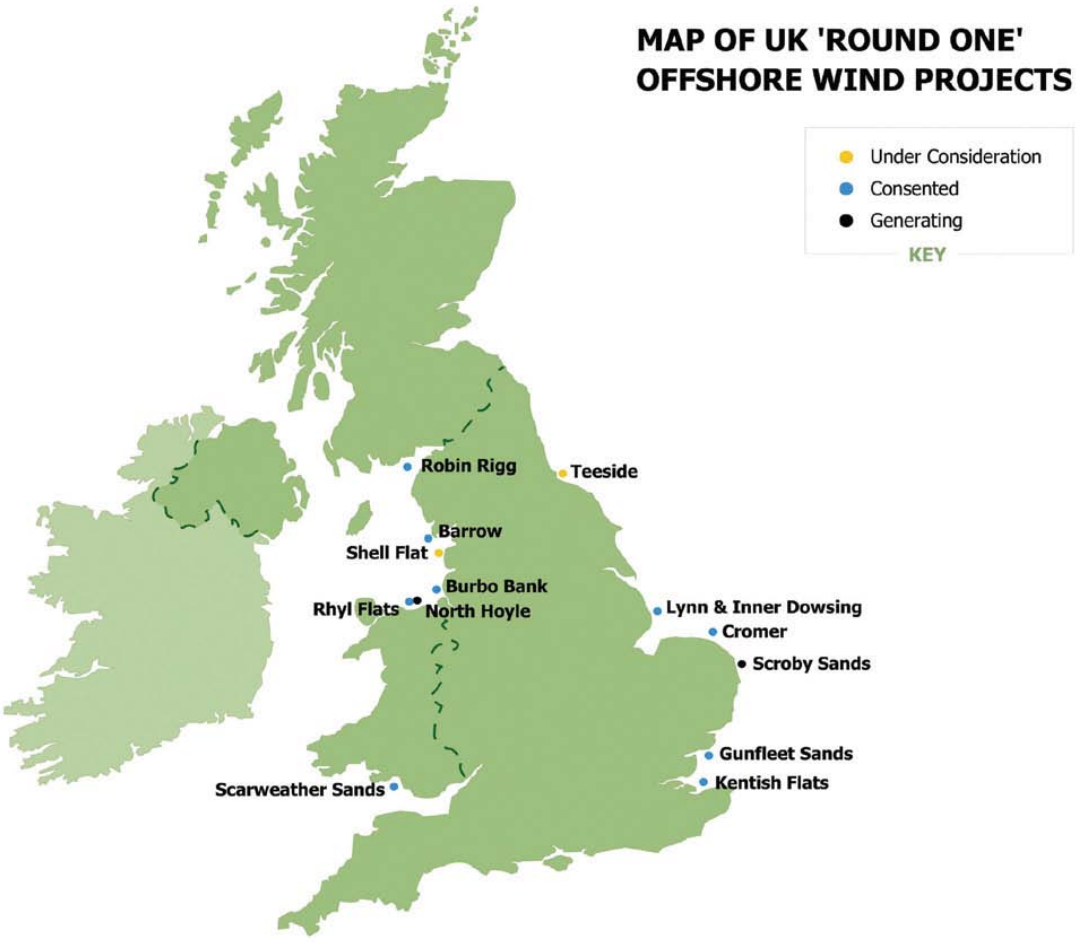

Round 1 offshore wind farm sites [36].

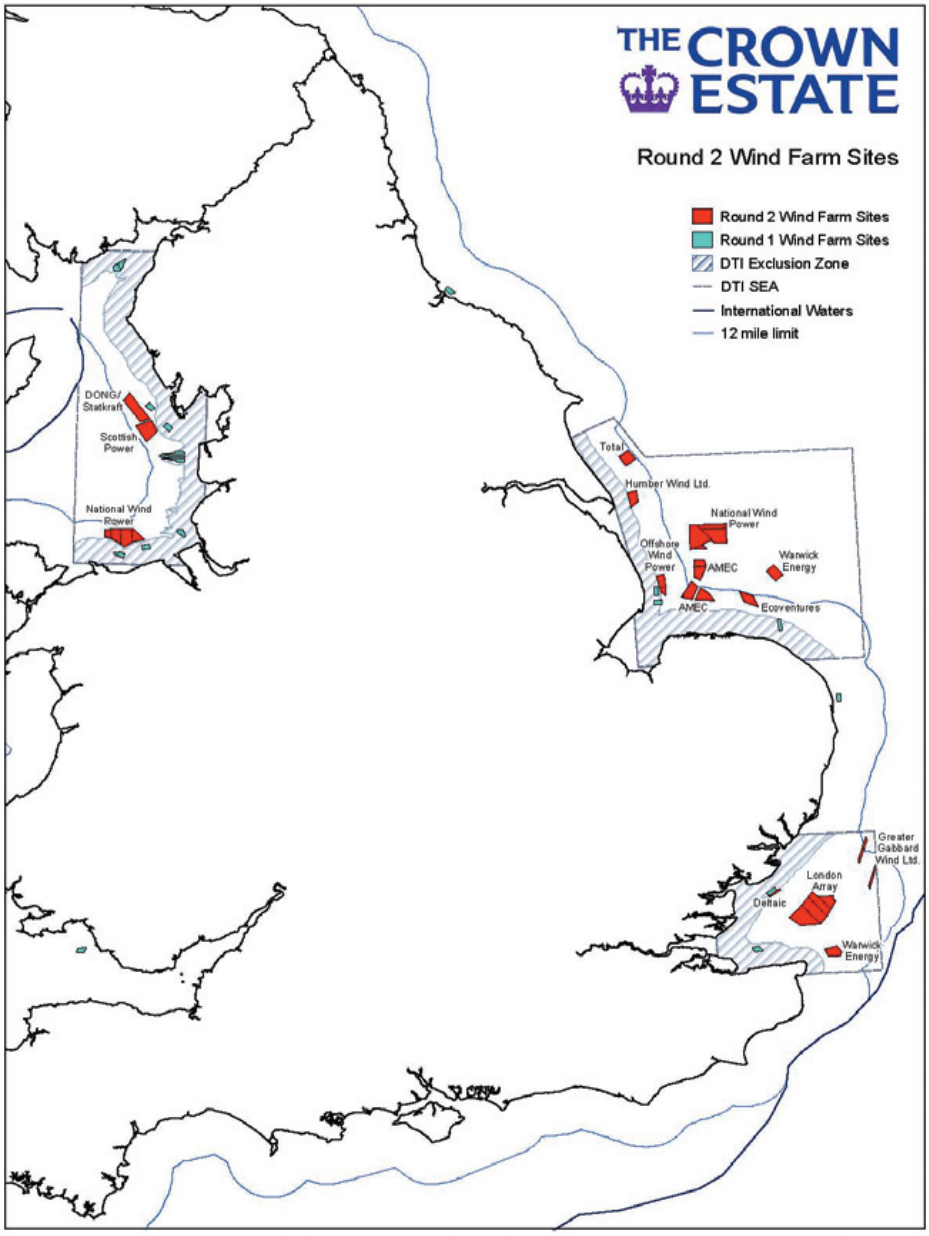

Round 2 offshore wind farm sites [88].

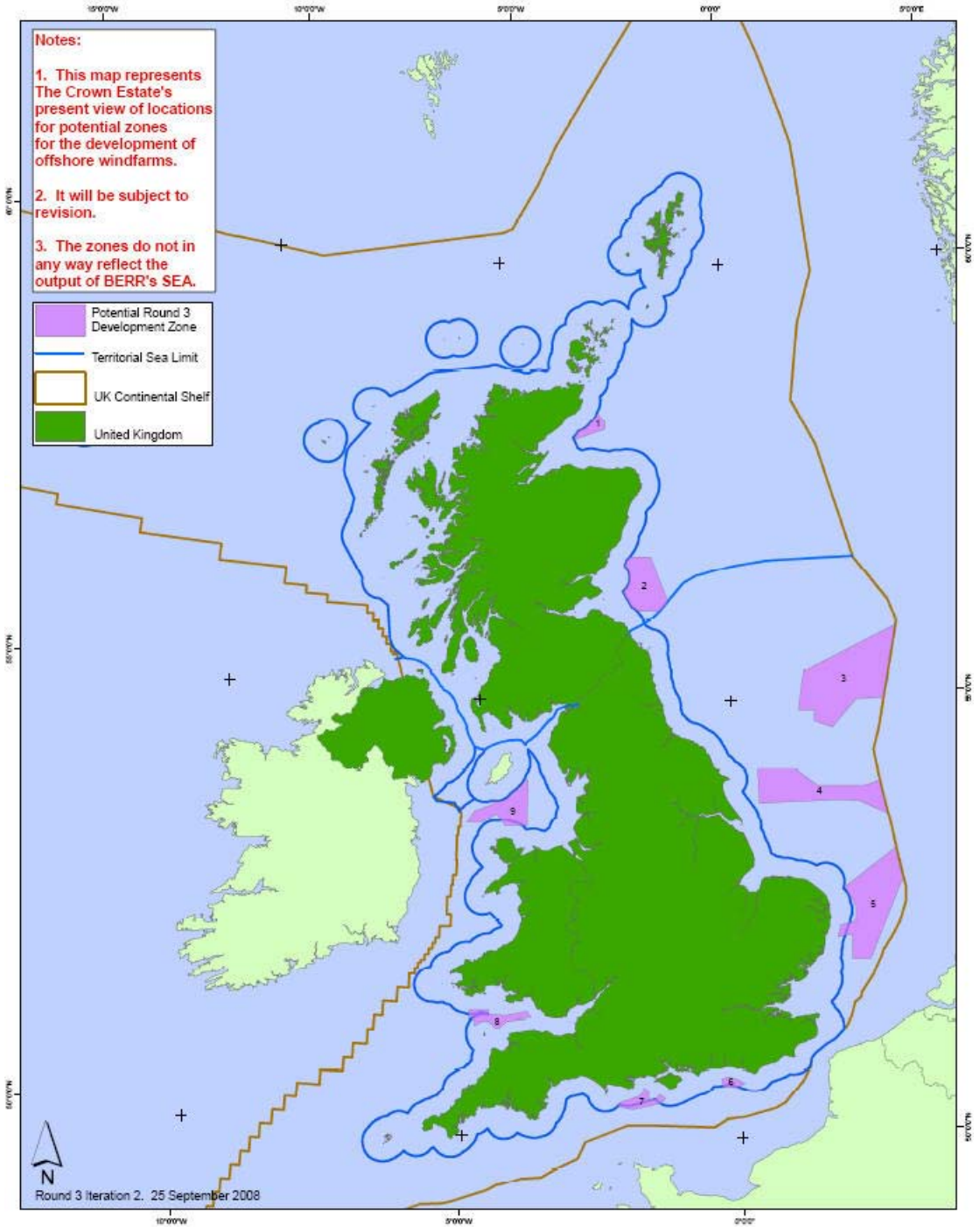

Round 3 offshore wind farm sites [37].

Appendix II

Procedure of Experiment

1. Before the experiment

1.1 Manipulator has to learn the safety information of the laboratory and comply with the rules of laboratory.

1.2 Check all the buttons are off state. In particular, the emergence buttons are off state.

1.3 Check the configuration and circuit connection of experiment and make sure it is ready to do experiment.

2. In the process of experiment

2.1 Turn on the wall switch of converter cabinet.

2.2 Turn on the main switch on the door of the converter cabinet. The indicator light of power converter is on.

2.3 Turn the alarm-safe to off state by the safe key on the door of converter cabinet. Open the door of converter cabinet and turn on the switch of "dSPACE box" (inside, at the bottom of the converter cabinet). Close the door of the converter cabinet. The indicator light of the converter is on.

2.4 Turn on the computer and put into the key. Open the software "dSPACE controldesk" from desktop.

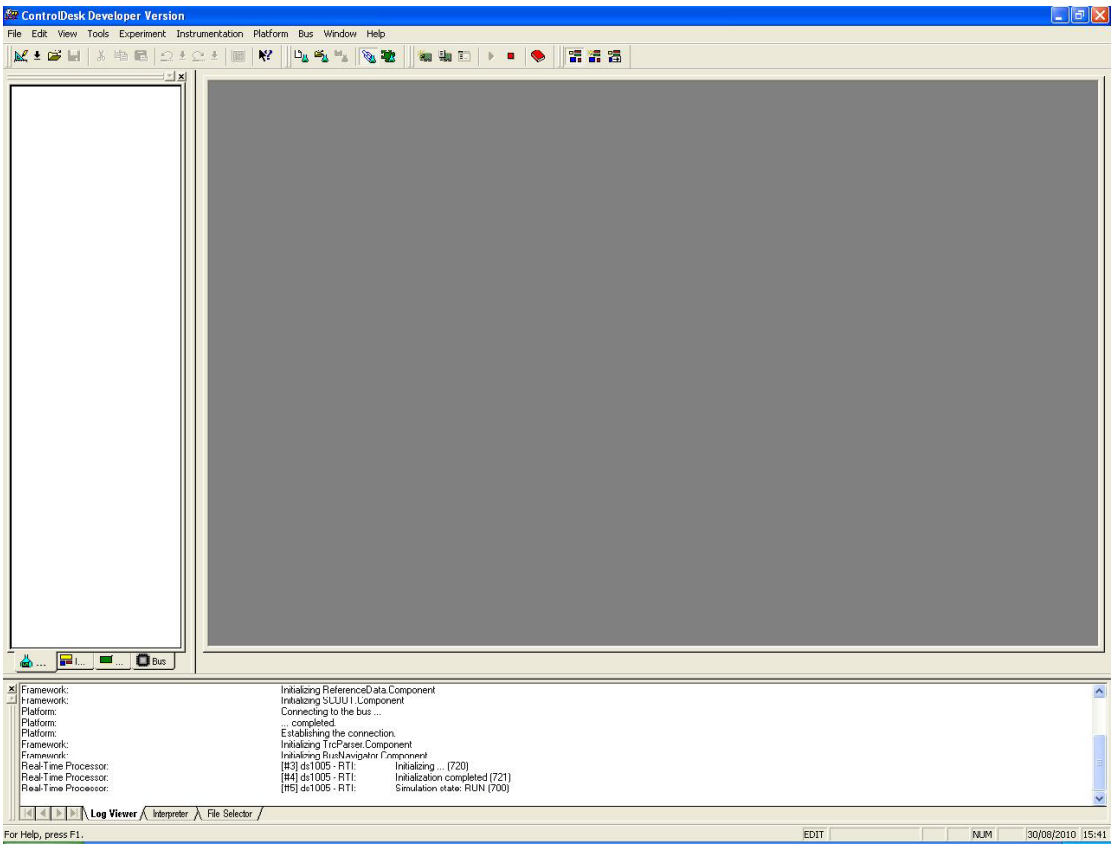

In accordance with the following order, Click File→Open Experiment→C:\dSPACE_R6.5\Work\MT_VSC_HVDC_1G.cdx→Open.

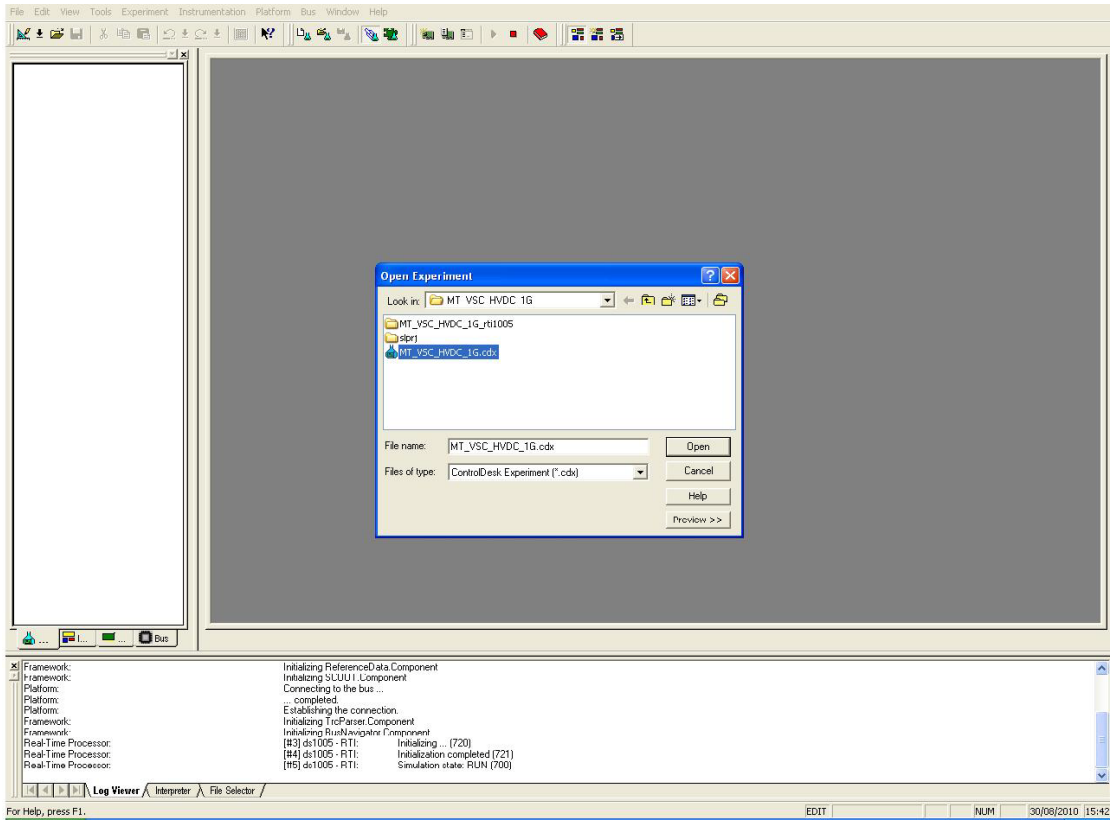

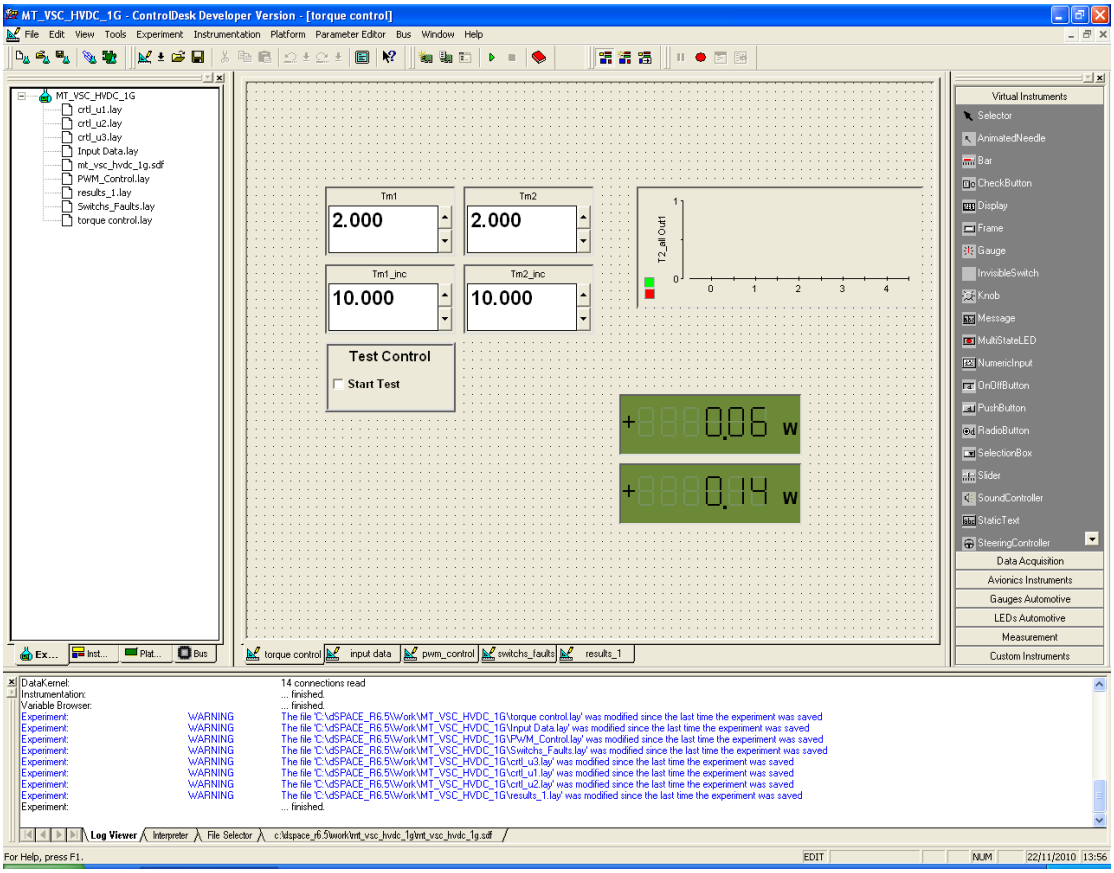

2.5 Click the third tag “Plat…”. Find “MT_VSC_HVDC_1G.mdl” from folder “MT_VSC_HVDC_1G”. Drag “MT_VSC_HVDC_1G.mdl” to the left side

into “Simulink”. Then the Simulink file is shown on the screen. In the interface, we can revise any model of Simulink.

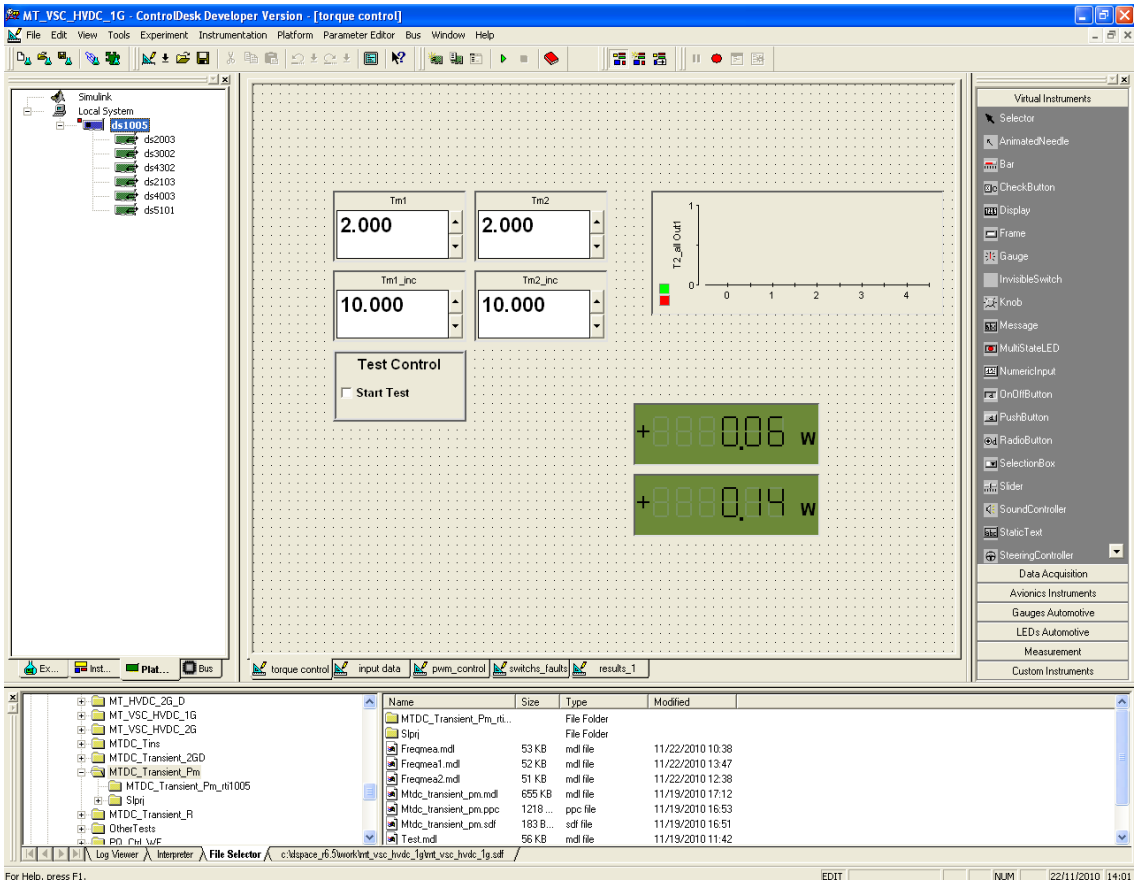

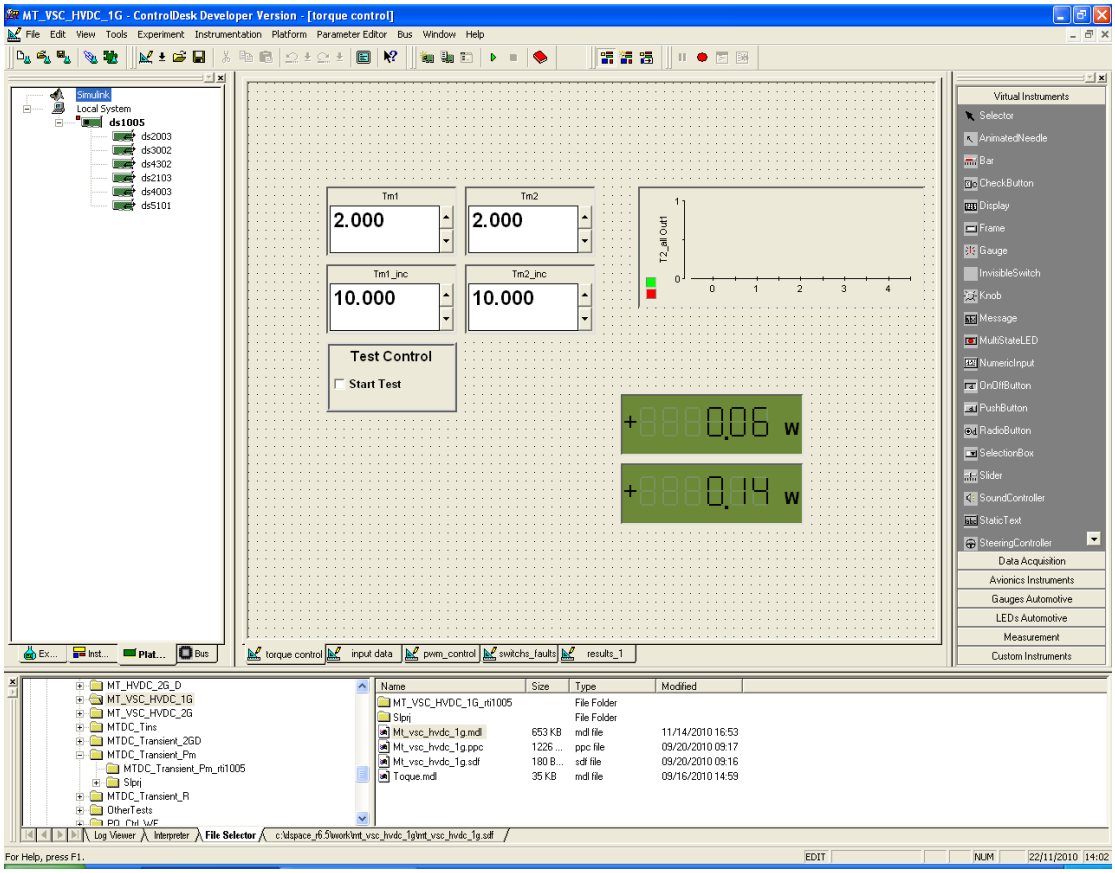

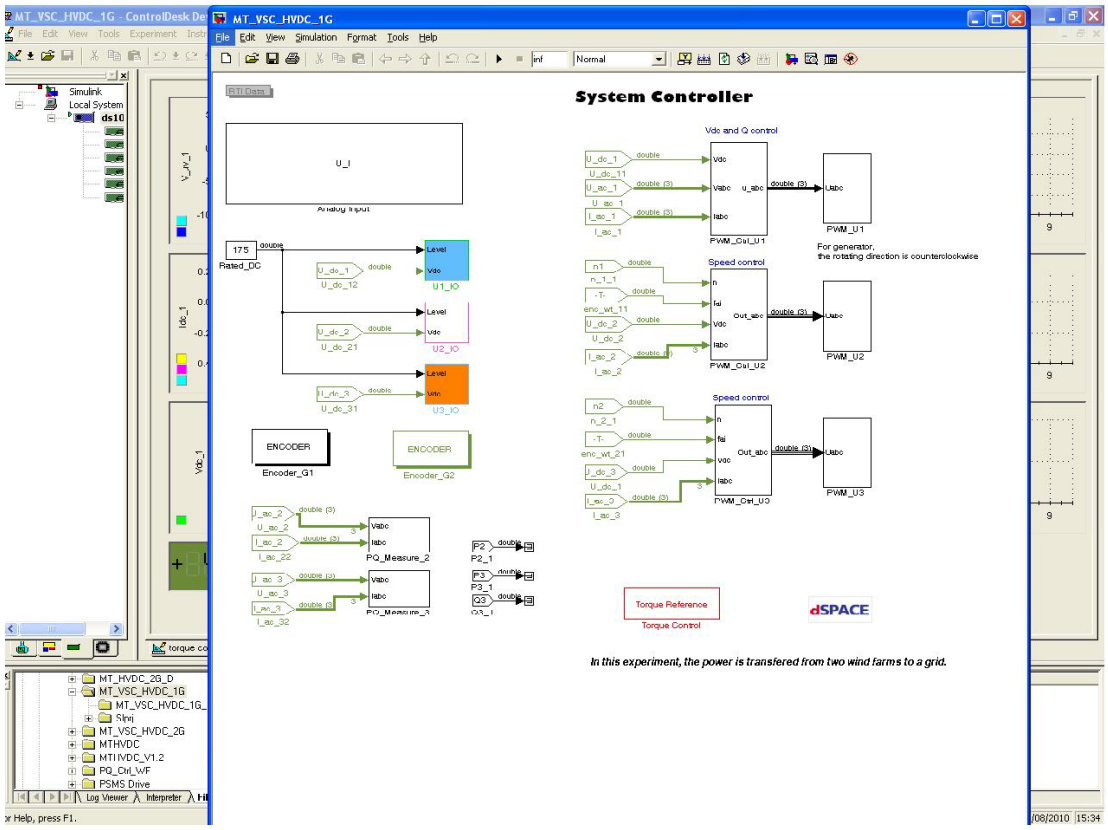

2.6 Build the model. In accordance with the following order, Click Tools→Real-Time Workshop→Build Model.

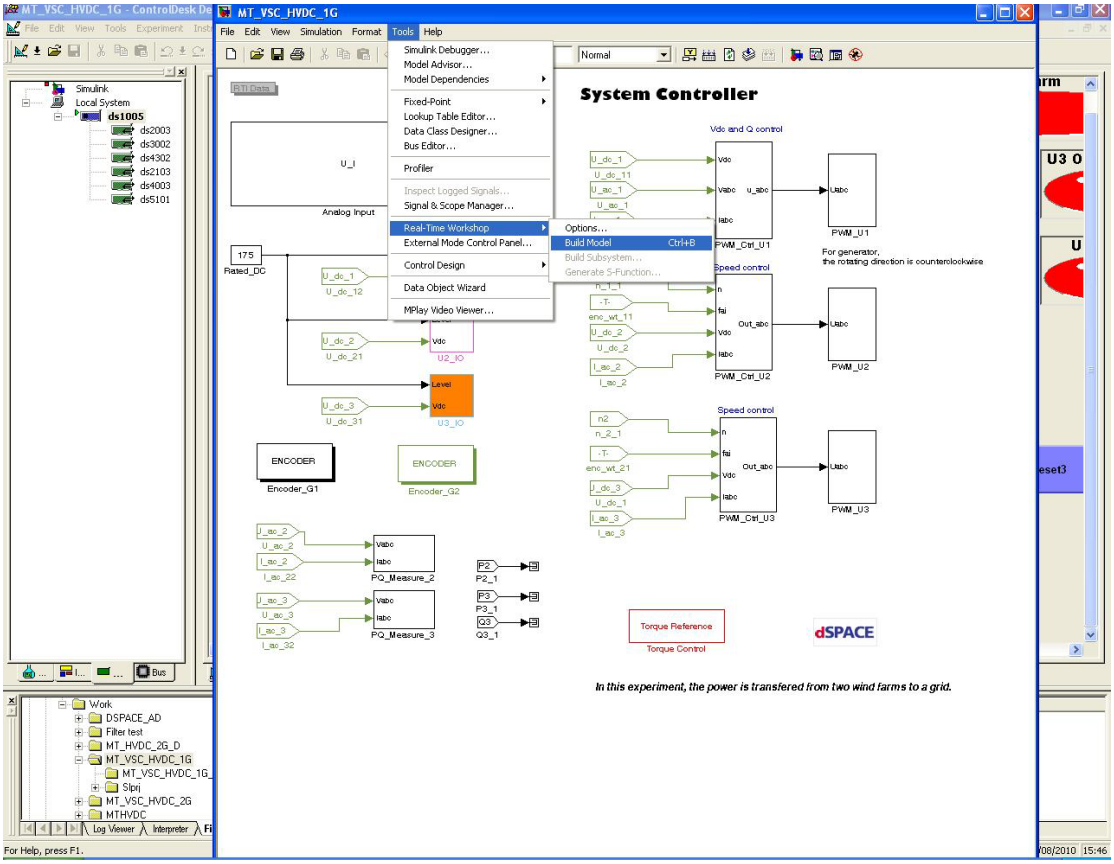
MT_VSC_HVDC_1G
System Controller
Simulink Debugger...
Model Advisor...
Model Dependencies
Fixed-Point
Lookup Table Editor...
Data Class Designer...
Bus Editor...
Profiler
Inspect Logged Signals...
Signal & Scope Manager...
Real-Time Workshop
External Mode Control Panel...
Control Design
Data Object Wizard
MPlay Video Viewer...
Options...
Build Model Ctrl+B
Build Subsystem...
Generate S-Function...
Vdc and Q control
Speed control
PWM_Ctrl_U1
PWM_Ctrl_U2
PWM_Ctrl_U3
PWM_U1
PWM_U2
PWM_U3
For generator, the rotating direction is counterclockwise
ENCODER
Encoder_G1
Encoder_G2
PQ_Measure_2
PQ_Measure_3
Torque Reference
Torque Control
dSPACE
In this experiment, the power is transfered from two wind farms to a grid.

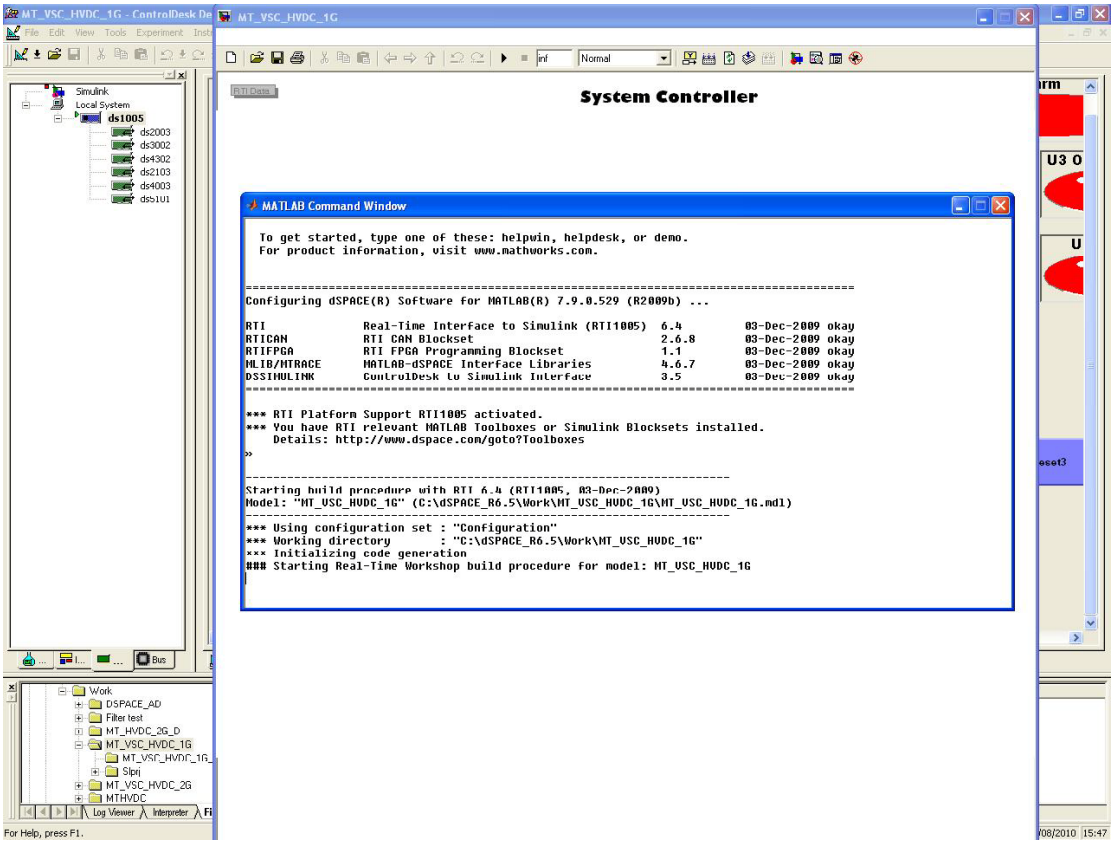
MT_VSC_HVDC_1G
System Controller
MATLAB Command Window
To get started, type one of these: helpwin, helpdesk, or demo.
For product information, visit www.mathworks.com.
Configuring dSPACE(R) Software for MATLAB(R) 7.9.0.529 (R2009b) ...
RTI Real-Time Interface to Simulink (RTI1005) 6.4 03-Dec-2009 okay
RTICAN RTI CAN Blockset 2.6.8 03-Dec-2009 okay
RTIFPGA RTI FPGA Programming Blockset 1.1 03-Dec-2009 okay
MLIB/MTRACE MATLAB-dSPACE Interface Libraries 4.6.7 03-Dec-2009 okay
DSSIMULINK ControlDesk to Simulink Interface 3.5 03-Dec-2009 okay
*** RTI Platform Support RTI1005 activated.
*** You have RTI relevant MATLAB Toolboxes or Simulink Blocksets installed.
Details: http://www.dspace.com/goto?Toolboxes
Starting build procedure with RTI 6.4 (RTI1005, 03-Dec-2009)
Model: "MT_VSC_HVDC_1G" (C:\dSPACE_R6.5\Work\MT_VSC_HVDC_1G\MT_VSC_HVDC_1G.mdl)
*** Using configuration set : "Configuration"
*** Working directory : "C:\dSPACE_R6.5\Work\MT_VSC_HVDC_1G"
*** Initializing code generation
Starting Real-Time Workshop build procedure for model: MT_VSC_HVDC_1G

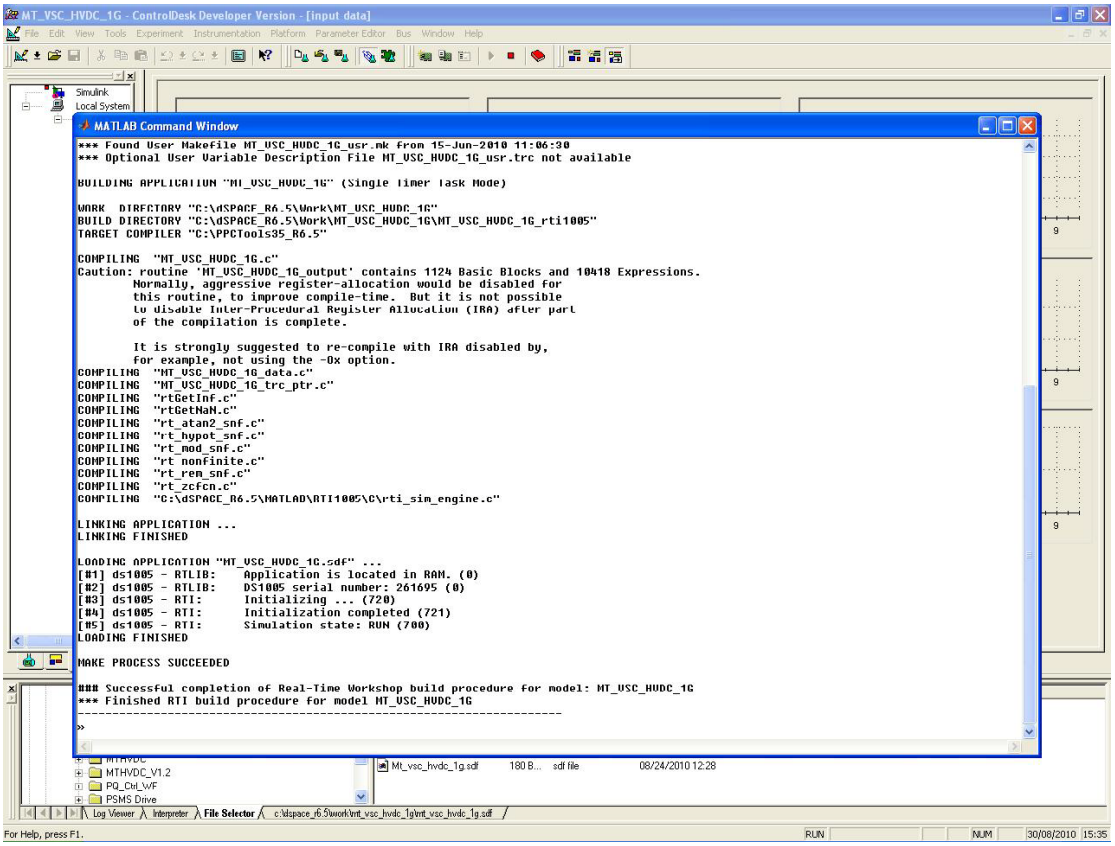

2.7 Find the interface of “Instrumentation”, chose “Animation mode”. It is for reading and writing the real-time data.

2.8 Check the variable transformer set to zero and the state of output breaker is off.

2.9 Turn on the wall switch of the relay. Push the green button of the relay. A crisp sound shows the relay is ready.

2.10 Turn on the output breaker of the variable transformer slowly. A deep sound shows the variable transformer is ready. Adjust the L-L voltage RMS value to 140 V. (the calibration equals to 38 approximately)

2.11 Back to the screen of the computer, and find the interface of “switch-faults”. Left click the “on” button for turning on the “U1_main”.

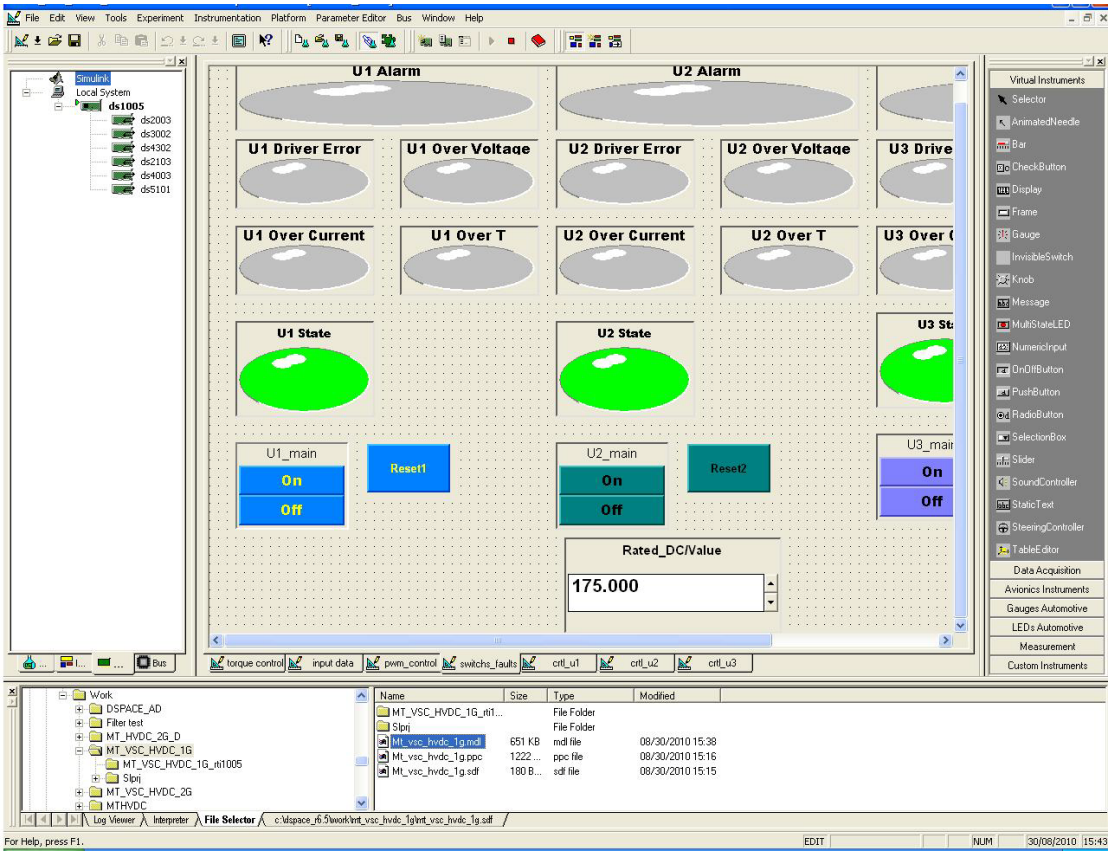

Two sounds can be heard for confirming.

2.12 Repeat the step 2.11 for “U2_main” and “U3_main” of the interface of “switch-fault”.

2.13 Find the interface of “pwm_control”. Tick the “initial” in the “PWM_en_2” (the bottom orange one). After 10 seconds, click the green bottom “Set Index to Zero (G1)” in the mid of the screen. After 10 seconds, also click the purple button “Set Index to Zero (G2)” in the right of the screen. After that, un-tick the “initial” in the “PWM_en_2” (the bottom orange one).

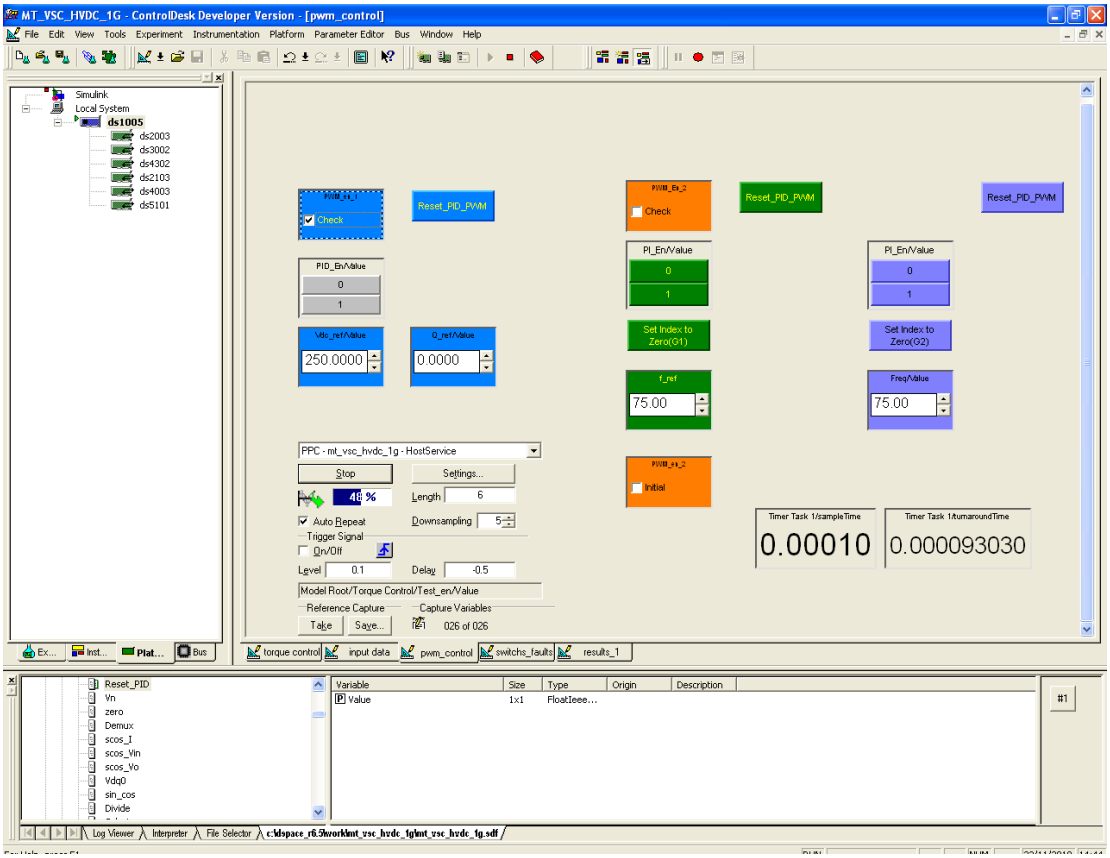

2.14 Turn on the main wall switch of driver cabinet. Turn on the switch in the door of the driver cabinet.

2.15 Find the interface of “pwm_control”. Set the DC voltage “Vdc_ref/Value” equals to 250 V and reactive power “0_ref/Value” equals to 0. Set the frequency of PMSG 1 and PMSG 2 “Freq/Value” equal to 75 Hz. (In this particular case, 75 Hz means 1500 r/m for PMSG due to np=60*f*)

2.16 In the interface of “pwm_control”, tick the check of “PWM_en_1” to enable the converter 1 for gird side. Then find the interface of “switch_faults”, check no error is shown on the screen.

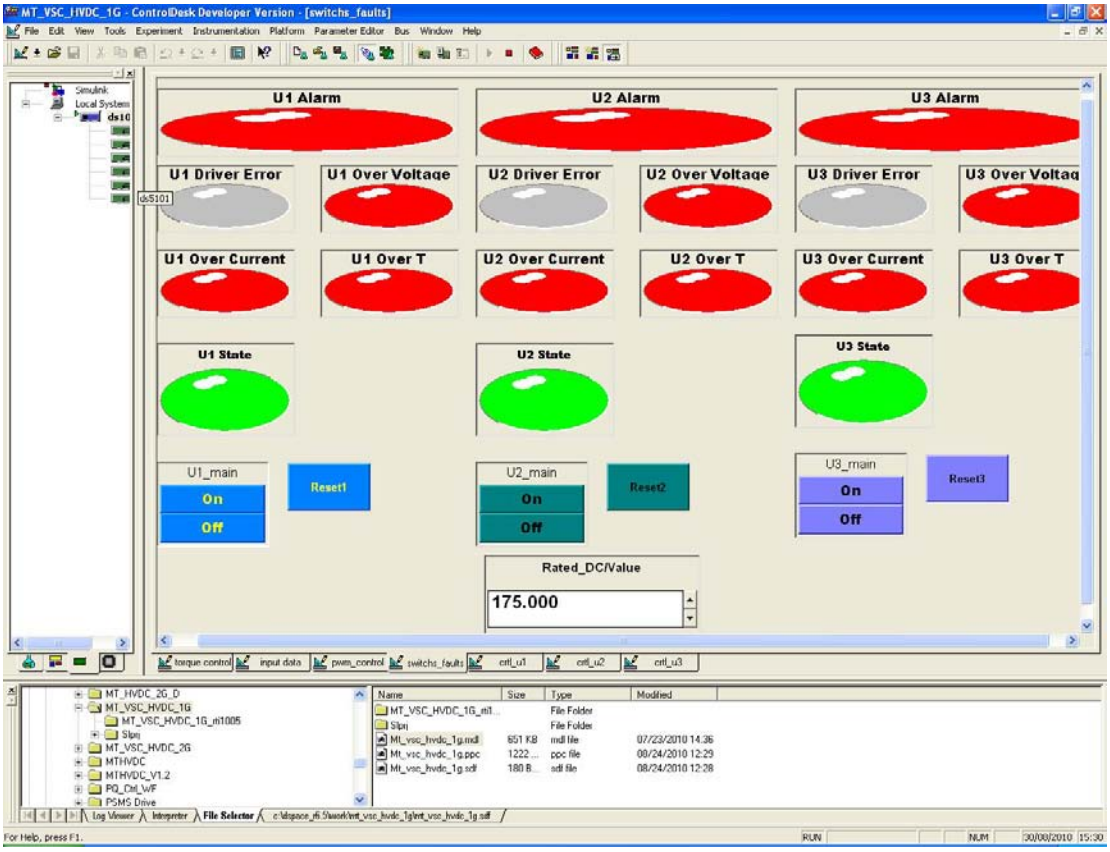

2.17 Find the interface of the "pwm_control". Tick the check of "PWM_en_2" to enable the converter 2&3 for wind farms.

2.18 Find the interface of "torque control". Set the "Tm1" and "Tm2" equal to small numbers (both are 2 in picture) for starting up the PMSGs.

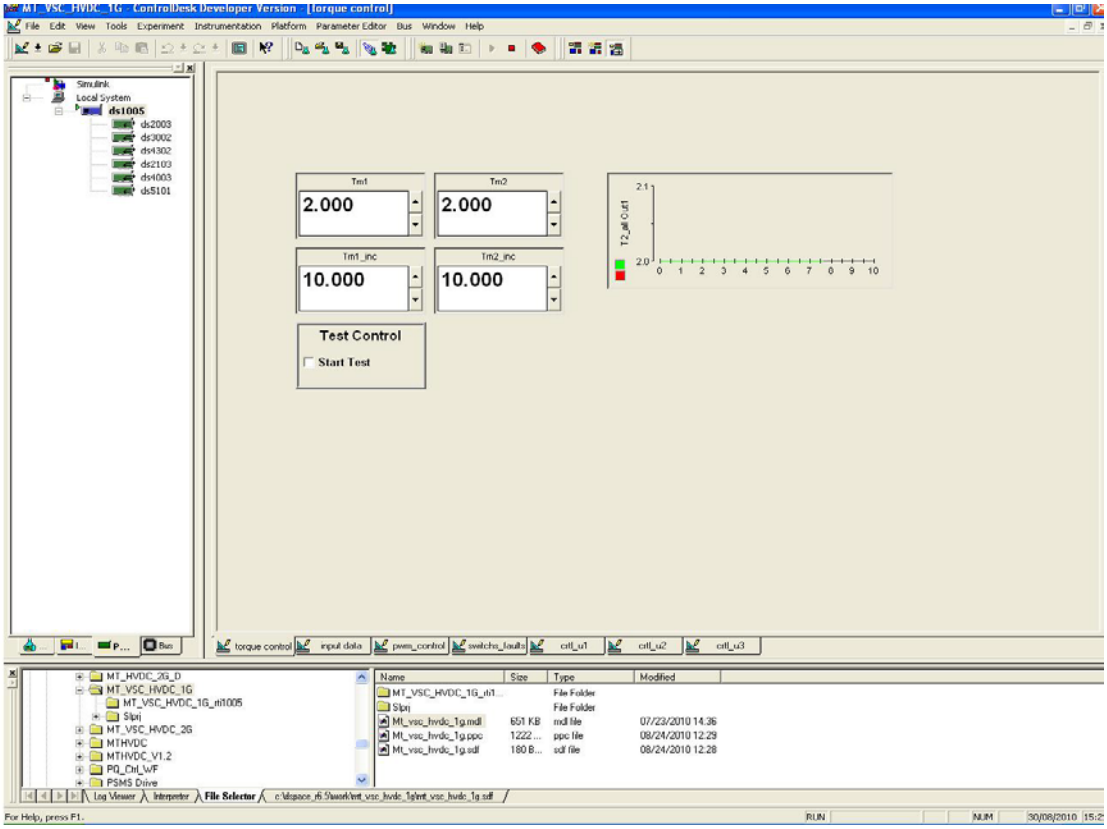

2.19 Find interface of “pwm_control”. Tick the green and purple “1” bottoms of “PI_En/Value” to enable PI controllers.

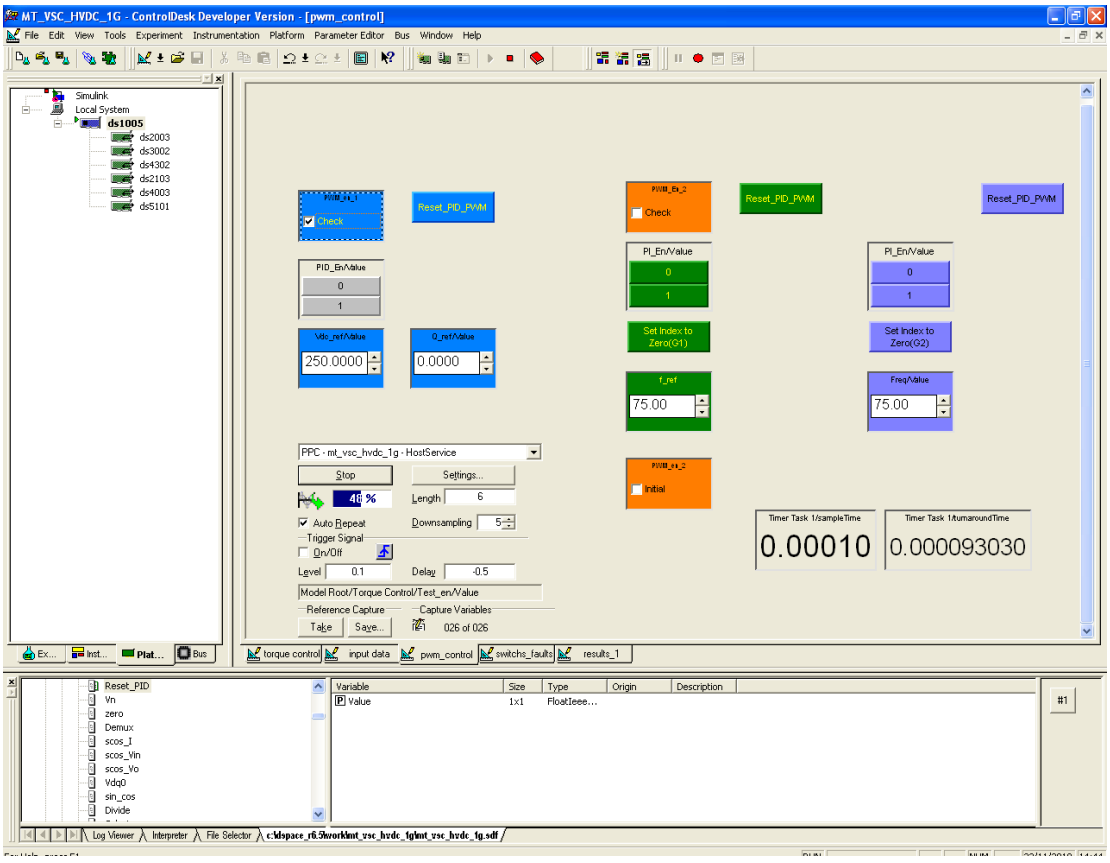

2.20 Turn the model button on the door of driver cabinet from 0 to auto.

2.21 Find the interface of “torque control”. Set the parameters of the experiment. In this specific case, the parameters are as follows, (100% torque equals 1.5 kW)

(a) Experiment 1: Set the ramp change of torque of PMSG 1. It is running 50% torque at 0-5 second and 100% torque at 5.3-10 second. The torque is increasing at 5-5.3 second from 50%-100%. Set PMSG 2 is running 100% torque.

(b) Experiments 2: Set the ramp change of torque of PMSG 1 and PMSG 2. They are both running 50% torque at 0-5 second and 100% torque at 5.3-10 second. The torque is increasing at 5-5.3 second from 50%-100%.

2.22 Experiments results. Find interface of “PWM_control”, click the stop button for capturing the diagrams of results when the bar is 100%. Find the interface of the results, copy as bitmap with hide legend to the word.

3. Stop the experiment.

3.1 Find interface of “torque control”, un-tick the “start test”. Change the parameters of Tm1 and Tm2 to 2.

3.2 Find interface of “pwm_control”, un-tick the check of “PWM_en_2 to stop the converters of wind farm 1 and wind farm 2. Also un-tick the check of “PWM_en_1” to stop the converter of gird side.

3.3 Set the state from auto to 0 on the door of converter cabinet. Turn off the main switch of converter cabinet. Then the white indicator light is off.

3.4 Find interface of “switch_faults”, click off buttons of U1_main, U2_main and U3_main.

3.5 Close the software and pull out the key. Turn off the computer.

3.6 Turn off the dSPACE box inside of the converter cabinet. Turn off the main switch on the door of the converter cabinet. Then the white indicator light is off.

3.7 Turn off the wall switches of driver cabinet and converter cabinet.

3.8 Set the variable transformer to 0. Turn off the output breaker and the relay. Turn off the wall switch of the relay.

3.9 Check all the switches are off states again.

Appendix III

The Table 5 shows multi-terminal LCC-HVDC transmission systems are currently in operation [2, 95],

Name and location	**Year of commissioning**	**Power/ MW**	**Length /km**	**Configuration**
SACOI Italy/France	1967 1986	200 50	406	-Two monopolar terminals -Three monopolar terminals in series (200, 50, 200 MW)
Pacific Intertie USA	1970 1984 1989	1600 400 1100	1360	- Two bipolar terminals 1600 MW - Upgrade of existing terminals to 2000 MW - Four bipolar terminals in parallel Pole 1+2: 2000 MW Pole 3+4: 1100 MW
Hydro Quebec-New England Hydro Canada/USA	1990 1991 1992	1200 800 250	1480	- Two bipolar terminals 1st stage - Two bipolar terminals 2nd stage - Three bipolar terminals in parallel: Radisson 2250 MW Nicolet 2138 MW Sand Pond 1800 MW
Shin-Shinano Japan	1977 1992	300 300	0	Back-to-back Shin-Shinano I : 300 MW at 125 kV DC and 1200 A x 2 Shin-Shinano II : 300 MW at 125 kV DC and 2400 A

Table 5. Applications of MTDC